

FUNCTIONAL AND STRUCTURAL ANALYSIS OF CATALASE-PHENOL
OXIDASE FROM *SCYTALIDIUM THERMOPHILUM*

A THESIS SUBMITTED TO
THE GRADUATE SCHOOL OF NATURAL AND APPLIED SCIENCES
OF
MIDDLE EAST TECHNICAL UNIVERSITY

BY

YONCA YÜZÜGÜLLÜ

IN PARTIAL FULFILLMENT OF THE REQUIREMENTS
FOR
THE DEGREE OF DOCTOR OF PHILOSOPHY
IN
BIOTECHNOLOGY

JANUARY 2010

Approval of the thesis:

**FUNCTIONAL AND STRUCTURAL ANALYSIS OF CATALASE-
PHENOL OXIDASE FROM *SCYTALIDIUM THERMOPHILUM***

submitted by **YONCA YÜZÜGÜLLÜ** in partial fulfilment of the requirements
for the degree of **Doctor of Philosophy in Biotechnology Department, Middle
East Technical University** by,

Prof. Dr. Canan Özgen _____
Dean, Graduate School of **Natural and Applied Sciences**

Prof. Dr. İnci Eroğlu _____
Head of Department, **Biotechnology**

Prof. Dr. Zümrüt B. Ögel _____
Supervisor, **Food Engineering Dept., METU**

Prof. Dr. Michael J. McPherson _____
Co-Supervisor, **Biochemistry Dept., University of Leeds**

Examining Committee Members:

Prof. Dr. Ufuk Bakır _____
Chemical Engineering Dept., METU

Prof. Dr. Zümrüt B. Ögel _____
Food Engineering Dept., METU

Prof. Dr. Gürkan Karakaş _____
Chemical Engineering Dept., METU

Prof. Dr. Erdal Karaöz _____
KOGEM, Kocaeli Univ.

Assoc. Prof. Dr. Nursen Çoruh _____
Chemistry Dept., METU

Date: 07.01.2010

I hereby declare that all information in this document has been obtained and presented in accordance with academic rules and ethical conduct. I also declare that, as required by these rules and conduct, I have fully cited and referenced all material and results that are not original to this work.

Name, Last name: Yonca Yüzügüllü

Signature :

ABSTRACT

FUNCTIONAL AND STRUCTURAL ANALYSIS OF CATALASE-PHENOL OXIDASE FROM *SCYTALIDIUM THERMOPHILUM*

Yüzügüllü, Yonca

Ph.D., Department of Biotechnology

Supervisor: Prof. Dr. Zümrüt B. Ögel

Co-Supervisor: Prof. Dr. Michael J. McPherson

January 2010, 189 pages

Scytalidium thermophilum produces a novel phenol oxidase, which has turned out to be a bifunctional catalase-phenol oxidase (CATPO) during the course of this work, by other researchers of our group. Therefore, in the beginning of the studies, substrate specificity and inhibitor assays were conducted on the crude enzyme, followed by production, purification, cloning, expression, and mutagenesis and crystallography studies for further functional and structural analysis of CATPO. Accordingly, substrate specificity and inhibitory tests applied for crude enzyme characterisation presented the similarity of the phenol oxidase nature of CATPO essentially to catechol oxidase. Production studies were performed to investigate the effects of different factors including induction time, growth temperature, exogenous iron and hydrogen peroxide addition. In view of that, CATPO is constitutively produced in a growth associated manner. However, some phenolic compounds enhance its production. In this study, 15 phenolic compounds were tested for their ability to affect CATPO production. Of the phenolic compounds tested, catechol, resorcinol and vanillic acid caused repression of CATPO production. On the other hand, caffeic acid, myricetin and resveratrol enhanced CATPO production. As a biocatalyst, the efficiency of

CATPO was examined and found to be a good candidate for getting pharmaceutically important drug intermediates. Its dual mechanism was analysed through site-directed mutagenesis. Two conserved residues (His101 and Val142) were mutated to discriminate catalase and phenol oxidase activities. Spectroscopic and mutagenesis studies exhibited the presence of heme *d* centre. Lastly, its structure was analysed by X-ray crystallography and found to have a tetrameric structure.

Keywords: *Scytalidium thermophilum*, catalase, phenol oxidase, functional analysis, X-ray crystallography.

ÖZ

SCYTALIDIUM THERMOPHILUM KATALAZ-FENOL OKSİDAZININ FONKSİYONEL VE YAPISAL ANALİZİ

Yüzügüllü, Yonca

Doktora, Biyoteknoloji Bölümü

Tez Yöneticisi: Prof. Dr. Zümrüt B. Ögel

Ortak Tez Yöneticisi: Prof. Dr. Michael J. McPherson

Ocak 2010, 189 sayfa

Scytalidium thermophilum, grubumuzdaki diğer araştırmacılar tarafından yapılan çalışmalar sırasında aslında çift aktiviteli bir katalaz-fenol oksidaz (CATPO) olduğu keşfedilen özgün bir fenol oksidazı üretmekte olduğu gözlenmiştir. Dolayısıyla, çalışmanın başında saflaştırılmamış enzim kullanılarak gerçekleştirilen substrat seçiciliği ve inhibitör denemelerini, ileriki fonksiyonel ve yapısal analizler için üretim, saflaştırma, klonlama, ekspresyon, mutasyon ve kristallografi çalışmaları izlemiştir. Bu sebeple, enzim karakterizasyonu için gerçekleştirilen substrat seçiciliği ve inhibitör testleri, enzimin (CATPO) fenol oksidaz yapısının daha çok katekol oksidaza benzediğini göstermiştir. İndüklenme zamanı, büyüme sıcaklığı ve dışsal demir ve hidrojen peroksit katkısı gibi etkenlerin enzim üzerine etkisini araştırmak üzere üretim çalışmaları gerçekleştirilmiştir. Bunların sonucunda enzimin (CATPO) büyümeye bağlı olarak konstitütif bir şekilde üretildiği, ancak bazı fenolik bileşiklerin enzim üretimini arttırdığı gözlenmiştir. Bu çalışmada, 15 fenolik madde enzim üretimini etkileyebilme yeterliliklerini araştırmak üzere test edilmiştir. Bu bileşiklerden katekol, resorsinol ve vanilik asidin CATPO üretimini baskıladığı gözlenmiştir. Diğer yandan, kafeik asit, mirisetin ve resveratrolün ise CATPO üretimini

arttırdığı belirlenmiştir. Biyokatalist olarak CATPO enziminin verimliliği araştırılmış ve farmasötik açıdan önemli ilaç ara ürünlerinin eldesinde iyi bir aday olabileceği bulunmuştur. CATPO enziminin çift aktivite mekanizması, mutasyon yoluyla araştırılmıştır. Korunmuş iki amino asit (His101 ve Val142), katalaz ve fenol oksidaz aktivitelerini ayırmak amacıyla mutasyona uğratılmıştır. Spektroskopik ve mutasyon çalışmaları *d* tipi heme grubunun varlığını göstermiştir. Son olarak, enzimin yapısı X-ışını kristallografi ile analiz edilmiş ve tetramerik bir yapıya sahip olduğu bulunmuştur.

Anahtar kelimeler: *Scytalidium thermophilum*, katalaz, fenol oksidaz, fonksiyonel analiz, X-ışını kristallografi.

*To people,
who always believed in me*

ACKNOWLEDGEMENTS

I would like to express my sincere gratitude to Prof. Dr. Zümürüt Begüm Ögel for her valuable guidance, encouragement and understanding throughout the research. She taught me how much important is to question thoughts and create new ideas to become a good scientist.

I want to thank to Prof. Dr. Michael J. McPherson for his great support, advisable guidance and providing such a nice laboratory environment during my study at University of Leeds.

I also wish to express my special thanks to Prof. Dr. Ufuk Bakır for her valuable supervision and help.

My great appreciation is to Prof. Dr. Simon E. Phillips for his useful criticism and valuable guidance.

I wish to extend my thanks to Prof. Dr. Ayhan Sıtkı Demir for making it possible to use BIOCAT laboratory during biocatalysis studies.

I want to thank Assoc. Prof. Dr. Nursen Çoruh for her guidance as a committee member.

My special thanks are due to Dr. Gökhan Duruksu for his endless friendship, Dr. Mark A. Smith, Dr. Chi Trinh, Dr. Arwen R. Pearson and Olcay Mert for sharing their knowledge and experience. I am grateful to Eren Akgül for his deepest support coming from thousands of miles away from Turkey. Loves also go to my dearest friends Canan Y. Tüzün, Nuray Varol, Fulya Saygılı, Çiğdem Kanlıtepe, Gülden Avcı, Betül-Alper Söyler, Esra Uçkun, Abduvali Valiev, Burçak Kocuklu and Nansalmaa Amarsaikhan.

Finally, I want to express my deepest gratitude and love to my parents Seyide-Vedat Yüzügüllü, my beloved sister Bengi Yüzügüllü for their encouragement and great support all through the study.

TABLE OF CONTENTS

ABSTRACT	iv
ÖZ.....	vi
ACKNOWLEDGEMENT	ix
TABLE OF CONTENTS	x
LIST OF TABLES.....	xv
LIST OF FIGURES	xvi
LIST OF ABBREVIATIONS.....	xx

CHAPTERS

1 INTRODUCTION.....	1
1.1 Catalases.....	1
1.1.1 Categorization of Catalases.....	2
1.1.1.1 Monofunctional Catalases.....	2
1.1.1.2 Catalase-Peroxidases.....	6
1.1.1.3 Manganase Catalases	6
1.1.1.4 Minor Catalases	7
1.1.2 Biological Function of Catalase.....	8
1.1.3 Occurance	8
1.1.4 Regulation of Catalase Expression	9
1.1.5 Catalase Cofactors	10
1.1.6 Catalase Catalytic Cycle	12
1.1.6.1 Kinetics.....	14
1.1.6.2 Effect of Inhibitors.....	15
1.1.7 Catalase Production, Purification and Characterisation	15
1.1.7.1 Fungi as Catalase Producers	16
1.1.8 Three Dimensional Structure of Catalase	16
1.1.8.1 Crystallisation Studies	16

1.1.8.2	Overall Structure of Catalases	17
1.1.8.3	Heme Pocket.....	20
1.1.8.3.1	Channels to the Heme Group.....	21
1.2	Phenol Oxidases.....	25
1.2.1	Phenols.....	25
1.2.2	Phenol Oxidase Classification	30
1.2.3	Occurance of Phenol Oxidases in Living Systems	32
1.3	Industrial Usage of Catalases and Phenol Oxidases	32
1.4	Bifunctionality of Catalase and Phenol Oxidase	33
1.5	Oxidative Stress	35
1.5.1	Reactive Oxygen Species.....	36
1.5.2	Defense Mechanisms against ROS	38
1.6	Thermophilic Fungi	39
1.6.1	<i>Scytalidium thermophilum</i>	40
1.6.2	CATPO (Catalase-Phenol Oxidase) of <i>S. thermophilum</i>	40
1.7	Scope of the Study	41
2	MATERIALS AND METHODS	43
2.1	Materials	43
2.1.1	Chemicals, Enzymes and Equipment.....	43
2.1.2	Microorganisms	44
2.1.2.1	Fungal Strains	44
2.1.2.2	Bacterial Strains.....	44
2.1.3	Growth Media, Buffers and Solutions	44
2.1.4	Plasmids and Molecular Size Markers.....	44
2.2	Methods	45
2.2.1	Microbial Cultivations	45
2.2.2	Plasmid DNA Isolation.....	46
2.2.3	Primer Design	47
2.2.4	Polymerase Chain Reaction	47
2.2.5	Visualization and Photography of Nucleic Acids	48
2.2.6	Transformation of <i>E. coli</i> XL-1 Blue.....	48
2.2.6.1	Preparation of Competent Cells	48
2.2.6.2	Transformation of Competent Cells.....	49

2.2.7	Restriction Enzyme Digestion	49
2.2.8	Ligation.....	50
2.2.9	Mutagenesis Studies.....	52
2.2.9.1	Primer Design for Mutagenesis	52
2.2.9.2	Site-Directed Mutagenesis	53
2.2.10	Protein Characterisation.....	56
2.2.10.1	SDS-Polyacrylamide Gel Electrophoresis	56
2.2.10.2	Native-Polyacrylamide Gel Electrophoresis	56
2.2.10.3	UV-Visible Spectral Studies	57
2.2.10.4	Protein Concentration Determination	57
2.2.10.4.1	Absorbance of CATPO at 280 nm	57
2.2.10.4.2	Total Protein Concentration Determination	58
2.2.10.5	Enzyme Assays	58
2.2.11	Statistical Analysis.....	59
2.2.12	Biotransformation of CATPO.....	60
2.2.12.1	Thin Layer Chromatography.....	60
2.2.12.2	High Performance Liquid Chromatography Analysis	60
2.2.12.3	Gas Chromatography Analysis	61
2.2.13	CATPO Purification.....	61
2.2.13.1	Native CATPO Purification.....	61
2.2.13.2	Recombinant CATPO Purification	62
2.2.14	CATPO Crystallisation.....	63
2.2.14.1	Initial Screening Trials.....	63
2.2.14.2	Crystal Optimisation and Cryocooling	64
2.2.14.3	X-Ray Data Collection and Processing.....	66
2.2.14.4	Structure Refinement and Model Building	67
3	RESULTS AND DISCUSSION.....	68
3.1	Characterisation of CATPO in Crude Extracts.....	68
3.1.1	Optimisation of Assay Temperature	69
3.1.2	Oxidation of Phenolic Compounds by CATPO.....	70
3.1.3	Effect of Inhibitors on Phenol Oxidation by CATPO.....	71

3.2	Production of CATPO	73
3.2.1	Time Course of CATPO Production.....	73
3.2.2	Effect of Growth Temperature on CATPO Production	75
3.2.3	Effect of Iron on CATPO Production	76
3.2.4	Effect of Hydrogen Peroxide on CATPO Production.....	77
3.2.5	Effect of Functional Phenolics on CATPO Production	78
3.2.5.1	Diphenolis.....	80
3.2.5.2	Phenolic Acids	83
3.2.5.3	Flavonoids.....	87
3.2.5.4	Resveratrol	91
3.2.5.5	Phenylactic Acid.....	92
3.2.5.6	Evaluation of the Effect of Phenolic Compounds on CATPO Production.....	93
3.3	Biocatalysis using CATPO.....	96
3.3.1	CATPO Biocatalysis with Organic Compounds.....	97
3.3.2	High Performance Liquid Chromatography (HPLC) Results....	100
3.3.3	Gas Chromatography (GC) Results	104
3.4	Molecular Studies	107
3.4.1	Cloning and Expression of <i>S. thermophilum catpo</i> Gene	109
3.4.1.1	PCR Cloning of <i>catpo</i> Gene onto the <i>E. coli</i> Expression Vector	109
3.4.1.2	Isolation of Recombinant Plasmids Containing the <i>catpo</i> Gene	110
3.4.2	Transformation of pETCATPO into <i>E. coli</i> BL21(DE3)star	111
3.4.3	Site-Directed Mutagenesis on <i>catpo</i> Gene of <i>S. thermophilum</i> .	116
3.4.3.1	Primer Design for QuickChange Site-Directed Mutagenesis .	117
3.4.3.2	QuickChange Application to Generate Mutational Variants ..	117
3.5	Purification Results.....	119
3.5.1	Purification of Native CATPO.....	119
3.5.2	Purification of Recombinant CATPO.....	120
3.6	Molecular Weight Determination of CATPO.....	123
3.7	UV-Vis Spectra of Native and Recombinant CATPO.....	124
3.8	Specific Activities of Native, Recombinant Wild Type and Mutant CATPOs.....	127

3.9	Three Dimensional Structure Determination of CATPO.....	129
3.9.1	CATPO Crystallisation.....	130
3.9.1.1	Initial Crystallisation Screening.....	130
3.9.1.2	Optimisation of Crystallisation Conditions.....	131
3.9.2	Crystallisation of CATPO Variants	134
3.9.3	Structure of CATPO	135
4	CONCLUSIONS	140
5	RECOMMENDATIONS.....	142
	REFERENCES	143
	APPENDICES	
A.	GROWTH MEDIA, BUFFERS AND SOLUTIONS PREPARATIONS	162
B.	VECTOR MAP	169
C.	MOLECULAR SIZE MARKERS	172
D.	SDS-PAGE PROTOCOL	174
E.	SIMPLYBLUE SAFESTAIN MICROWAVE PROTOCOL	176
F.	NATIVE-PAGE PROTOCOL	177
G.	BRADFORD ASSAY.....	179
H.	PREPARATION OF TLC PLATES AND SOLVENT SYSTEMS	181
I.	AMMONIUM SULFATE PRECIPITATION PROTOCOL	183
J.	AMINO ACID SEQUENCE OF <i>SCYTALIDIUM THERMOPHILUM</i>	
	CATALASE	184
K.	AMINO ACID SEQUENCE OF pETCATPO	185
L.	SEQUENCE ALIGNMENT OF <i>SCYTALIDIUM THERMOPHILUM</i>	
	CATPO GENE WITH <i>PENICILLIUM VITALE</i> CATALASE GENE.....	186
	CURRICULUM VITAE.....	188

LIST OF TABLES

TABLES

Table 3.1 Phenol oxidation by CATPO and comparison with <i>T. versicolor</i> laccase	72
Table 3.2 Effect of inhibitors on CATPO activity.....	73
Table 3.3 Structure of phenolic compounds tested.....	79
Table 3.4 Dose-dependent effect of phenolic compounds on <i>S. thermophilum</i> CATPO production and biomass generation	96
Table 3.5 TLC results of biotransformation experiments with extracellular CATPO	100
Table 3.6 HPLC results of hydrobenzoin oxidation with <i>S. thermophilum</i> CATPO and <i>T. versicolor</i> laccase.....	104
Table 3.7 Catalase activity measurements under different growth conditions ..	114
Table 3.8 Expression optimisation results of CATPO.....	116
Table 3.9 Absorption spectra data for wild-type and mutant catalase-phenol oxidases produced by <i>E. coli</i> BL21(DE3)star cells	127
Table 3.10 Specific activities of purified catalase-phenol oxidase variants	129
Table 3.11 Relative activities of purified catalase-phenol oxidase variants	129
Table H.1 Thin layer chromatographic systems used in the study	182

LIST OF FIGURES

FIGURES

Figure 1.1 The phylogenetic tree of monofunctional catalases based on the core amino acid sequences	4
Figure 1.2 Multiple sequence alignment of monofunctional catalases in the distal and proximal sides of haem ligand	5
Figure 1.3 Structures of heme <i>b</i> and heme <i>d</i>	11
Figure 1.4 The catalytic cycle of catalases	13
Figure 1.5 Compound I formation	13
Figure 1.6 Schematic drawing of the polypeptide chain and elements of secondary structure in a <i>Neurospora crassa</i> catalase subunit	19
Figure 1.7 Comparison of active site in catalase HP11 and catalase of <i>Proteus mirabilis</i>	20
Figure 1.8 The C ^β -N ^δ bond between His392 and Tyr415	21
Figure 1.9 Channels in CAT-1 of <i>N. crassa</i>	22
Figure 1.10 Main channel of HP11	23
Figure 1.11 Comparison of main and lateral channels of BLC and HP11	24
Figure 1.12 Structures of catechol, resorcinol, and hydroquinone	26
Figure 1.13 Examples of phenolic acids	28
Figure 1.14 The structure of flavonoids	28
Figure 1.15 Structures of different forms of flavonoids	29
Figure 1.16 The structure of two isomers of resveratrol	30
Figure 1.17 The phenol oxidation reaction catalyzed by tyrosinase and catechol oxidase	31
Figure 1.18 Three possible reactions catalyzed by catalase	34
Figure 1.19 Scheme showing formation of oxidative stress	36
Figure 1.20 Generation of reactive oxygen species	37
Figure 1.21 The structure of quercetin as strong antioxidant	39
Figure 2.1 Overview of the QuickChange site-directed mutagenesis method	55

Figure 2.2 Schematic representation of sitting drop vapour diffusion method....	65
Figure 3.1 Effect of temperature on CATPO-phenol oxidase activity of <i>S. thermophilum</i>	69
Figure 3.2 Effect of temperature on CATPO-catalase activity of <i>S. thermophilum</i>	70
Figure 3.3 Time course of <i>S. thermophilum</i> growth and enzyme production on glucose as the carbon source and cultivation at 45°C and 155 rpm	74
Figure 3.4 Effect of growth temperature on catalase production of <i>S. thermophilum</i>	75
Figure 3.5 Effect of adding FeSO ₄ into growth medium on catalase activity in culture supernatants of <i>S. thermophilum</i>	76
Figure 3.6 Effect of adding hydrogen peroxide into the growth medium of <i>S. thermophilum</i> on catalase production and biomass generation	77
Figure 3.7 Catechol effect on <i>S. thermophilum</i> CATPO production and biomass generation	81
Figure 3.8 Hydroquinone effect on <i>S. thermophilum</i> CATPO production and biomass generation	81
Figure 3.9 Resorcinol effect on <i>S. thermophilum</i> CATPO production and biomass generation	82
Figure 3.10 Gallic acid effect on <i>S. thermophilum</i> CATPO production and biomass generation	84
Figure 3.11 Vanillic acid effect on <i>S. thermophilum</i> CATPO production and biomass generation	85
Figure 3.12 Caffeic acid effect on <i>S. thermophilum</i> CATPO production and biomass generation	85
Figure 3.13 Chlorogenic acid effect on <i>S. thermophilum</i> CATPO production and biomass generation	86
Figure 3.14 Coumaric acid effect on <i>S. thermophilum</i> CATPO production and biomass generation	86
Figure 3.15 Kaempferol effect on <i>S. thermophilum</i> CATPO production and biomass generation	88
Figure 3.16 Quercetin effect on <i>S. thermophilum</i> CATPO production and biomass generation	89

Figure 3.17 Myricetin effect on <i>S. thermophilum</i> CATPO production and biomass generation	89
Figure 3.18 Catechin effect on <i>S. thermophilum</i> CATPO production and biomass generation	90
Figure 3.19 Epicatechin effect on <i>S. thermophilum</i> CATPO production and biomass generation	90
Figure 3.20 Resveratrol effect on <i>S. thermophilum</i> CATPO production and biomass generation	92
Figure 3.21 PLA effect on <i>S. thermophilum</i> CATPO production and biomass generation	93
Figure 3.22 Structures of organic compounds used in CATPO biotransformation studies	99
Figure 3.23 Oxidation of hydrobenzoin to benzyl via benzoin formation by <i>S. thermophilum</i> CATPO.....	101
Figure 3.24 Chromatogram of reaction products from the oxidation of hydrobenzoin by <i>S. thermophilum</i> CATPO	102
Figure 3.25 Chromatogram of reaction products from the oxidation of hydrobenzoin by <i>T. versicolor</i> laccase	103
Figure 3.26 Viniferin production from <i>t</i> -resveratrol.....	105
Figure 3.27 GC/MS result of resveratrol	106
Figure 3.28 Experimental strategies for molecular studies on CATPO.....	108
Figure 3.29 The schematic illustration of the location of primers NdeI20 and HindIIIend.....	109
Figure 3.30 Amplification of <i>catpo</i> gene from <i>S. thermophilum</i> using primers NdeI20 and HindIIIend.....	110
Figure 3.31 Isolated plasmids from <i>E. coli</i> pETCATPO transformants	111
Figure 3.32 Expression profile of CATPO at different temperatures and in the presence of IPTG	113
Figure 3.33 Optimisation of CATPO expression.....	115
Figure 3.34 Isolation of plasmid carrying H101N mutation.....	118
Figure 3.35 Isolation of plasmid carrying V142F mutation	118
Figure 3.36 SDS-PAGE analysis of fractions from anion exchange chromatography	119

Figure 3.37 SDS-PAGE analysis of fractions from gel filtration chromatography	120
Figure 3.38 SDS-PAGE analysis of fractions of recombinant CATPO eluted from HiTrap Chelating column	121
Figure 3.39 SDS-PAGE analysis of fractions of H101N eluted from HiTrap Chelating column	122
Figure 3.40 SDS-PAGE analysis of fractions of V142F eluted from HiTrap Chelating column	122
Figure 3.41 Molecular weight determination of CATPO	123
Figure 3.42 UV-Vis spectra of native CATPO	125
Figure 3.43 The comparison of UV-Vis spectra of recombinant wild-type CATPO, H101N and V142F	125
Figure 3.44 Initial small scale CATPO crystal grown at 18°C	131
Figure 3.45 Rod-shaped CATPO crystals	132
Figure 3.46 CATPO crystals in 24 % PEG2000 at 18°C	133
Figure 3.47 The best CATPO crystal in 18 % PEG2000 at pH 6.4, 0.1 M Bis-Tris buffer with 0.1 M Barium chloride crystals in drop and a single crystal used for X-ray data collection	134
Figure 3.48 Single V142F crystal in 10 % PEG4000 at pH 6.0, 0.5 M Sodium cacodylate trihydrate buffer with 0.2 M potassium chloride and 0.01M calcium chloride dehydrate	135
Figure 3.49 Three dimensional CATPO structure	136
Figure 3.50 Structure of CATPO and PVC monomers	137
Figure 3.51 Stereo view of (Fo - Fc) omit map of CATPO heme group	138
Figure 3.52 View of distal and proximal sites in CATPO	139
Figure 3.53 Heme centre in CATPO structure with electron density map	139
Figure B.1 Map of cloning vector, pET28a, Novagen	169
Figure B.2 Map of expression vector, pET-28aHis6TEVCATPO	171
Figure C.1 1 kb DNA Ladder	172
Figure C.2 Low Molecular (NEB) weight-SDS Marker	172
Figure C.3 The NativeMark™ Unstained Protein Standard	173
Figure G.1 Standard curve for Bradford method	180
Figure L.1 Multiple sequence alignment of <i>S. thermophilum</i> CATPO and <i>P. vitale</i> catalases	186

LIST OF ABBREVIATIONS

Å: Angstrom
ABTS: 2,2'-azino-bis-3-ethylbenzthiazoline-6-sulphonic acid
Asn: Asparagine
Asp: Aspartic acid
BLAST: Basic Local Alignment Search Tool
BLC: Bovine liver catalase
BSA : Bovine serum albumin
Ca: Calcium
CAT: Catalase
CATPO: Catalase-phenol oxidase
COOH: Carboxylic acid group
Cpd I: Compound I
CTAB: Cetyl trimethylammonium bromide
Da: Dalton
DEAE: Diethylaminoethyl
DMSO: Dimethylsulfoxide
EC: Enzyme Commission
Enz: Enzyme
EPR: Electron paramagnetic resonance
F: Phenylalanine
GPx: Glutathione peroxidase
H₂O₂: Hydrogen peroxide
HCl: Hydrochloric acid
His: Histidine
HP (I or II): Hydroperoxidase I or II
Ile: Isoleucine
IPTG: Isopropyl β-D-1-thiogalactopyranoside
L-Dopa: 3,4-dihydroxyphenylalanine
Leu: Leucine

Met: Methionine
N: Asparagine
NaCl: Sodium chloride
NH₂: Amino group
NADP: Nicotinamide adenine dinucleotide phosphate
NMR: Nuclear magnetic resonance
Met: Methionine
Mn: Manganese
MPD: 2-methyl-2,4-pentanediol
N: Asparagine
Ni: Nickel
OH : Hydroxyl
OD : Optical density
PAGE: Polyacrylamide gel electrophores
PDB: Protein Data Bank
PEG: Polyethylene glycol
PLA : Phenyllactic acid
PMC : *Proteus mirabilis* catalase
PO : Phenol oxidase
Por : Porphyrin
Pro: Proline
PVC: *Penicillium vitale* catalase
PVP: Polyvinylpyrrolidone
ROS: Reactive oxygen species
SDS: Sodiumdodecyl sulphate
Ser: Serine
SHAM: Salicylhydroxamic acid
SOD: Superoxide dismutase
U: Enzyme activity unit
UV: UltraViolet
TEAC: Trolox equivalent antioxidant capacity
TEV: Tobacco Etch Virus
Tyr: Tyrosine
V: Valine

CHAPTER 1

INTRODUCTION

1.1 Catalases

Catalases are one of the most studied groups of enzymes. The term catalase was first identified by Loew as hydrogen peroxide (H₂O₂) degrading enzyme in 1901 and the protein has been the focus of study for biochemists and molecular biologists ever since (Chelikani *et al.*, 2004). This history of catalases has been well documented by Zámocký and Koller (1999).

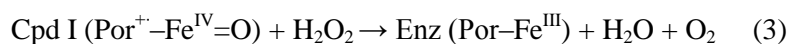
Aerobic organisms are exposed to hydrogen peroxide either internally or externally. Internal production of hydrogen peroxide (H₂O₂) occurs by metabolic redox reactions, as well as the oxidation of thiols, flavins, and ascorbate. External H₂O₂ are generated by abiotic stress or produced by other organisms (Klotz and Loewen, 2003; Loewen, 1997).

The overall reaction for catalase can simply be described as the degradation of two molecules of hydrogen peroxide to water and oxygen (reaction 1).

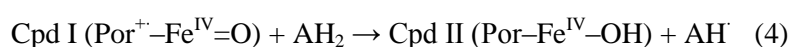


This catalytic reaction occurs in two distinct stages, but what each of the stages includes is mainly based on the kind of catalase (Chelikani *et al.*, 2004). The first stage involves oxidation of the heme using first hydrogen peroxide molecule to form an oxyferryl species in which one oxidation equivalent is taken off from the iron and one from the porphyrin ring to make a porphyrin cation radical (reaction 2). In the second stage, this radical intermediate, known as compound I, is reduced

by a second hydrogen peroxide to regenerate the resting state enzyme, water and oxygen (reaction 3) (Nicholls *et al.*, 2001; Switala and Loewen, 2002).



Catalases can also function as peroxidases, in which suitable organic compound is used as an electron donor (reaction 4).



In general, the peroxidatic reaction of catalases is relatively weak compared to peroxidases. However, this can be significant in the class known as catalase-peroxidases, which will be expressed in detail in section 1.1.1.2.

1.1.1 Categorization of Catalases

Four classes of catalases have been defined depending on the variety of subunit sizes, the number of quaternary structures, the different types of heme prosthetic groups, and the diversity of sequence groups (Mate *et al.*, 2001; Nicholls *et al.*, 2001):

- (a) The classic monofunctional heme containing catalases
- (b) The heme containing catalase-peroxidases
- (c) The non-heme, Manganese containing catalases
- (d) Miscellaneous heme-containing catalases

1.1.1.1 Monofunctional Catalases

These heme-containing catalases (hydrogen peroxide oxidoreductase, E.C. 1.11.1.6) constitute the largest and most extensively studied group of catalases

(Chelikani *et al.*, 2004; Nicholls *et al.*, 2001). They all possess two-step mechanism for dismutation of hydrogen peroxide.

Members of this largest class of catalases can be biochemically subdivided based on having large (75-84 kDa) subunits with heme *d* associated or small (55-69 kDa) subunits with heme *b* associated. All small subunit enzymes so far characterised, unlike larger enzymes, have been found with NADP(H) bound (Chelikani *et al.*, 2004; Klotz and Loewen, 2003). In turn, larger subunit enzymes have been shown to exhibit significantly enhanced stability against high temperatures and proteolysis (Chelikani *et al.*, 2004; Loewen, 1997).

Large and small subunit sized catalases have highly conserved domains, but the former have been reported to have additional 50 residues at the N-terminus and a 150-residue flavodoxin-like domain at the C-terminus. These additional residues may cause larger catalases to become resistant to thermal degradation, denaturants like detergents, organic solvents and salts, and also proteolysis (Chelikani *et al.*, 2003; Díaz *et al.*, 2004). In fact, it has been found that, HPI (from *Escherichia coli*), small subunit sized catalase, is inhibited by incubation at temperatures higher than 50°C, whereas HPII (from *E. coli*), large subunit catalase, retains its activity during incubation up to 70°C (Switala *et al.*, 1999).

Most of monofunctional (typical) catalases characterised in greatest detail have all been confirmed to be active as tetramers, even though dimeric, hexameric enzymes have been reported but never conclusively characterised (Nicholls *et al.*, 2001). There are over 250 known sequences of monofunctional catalases available now and the evolutionary relationships have been discussed in detail (Frugoli *et al.*, 1998; Kim *et al.*, 2000; Klotz *et al.*, 1997; Klotz and Loewen, 2003; Loewen *et al.*, 2000; Mayfield and Duvall, 1996; Scandalios *et al.*, 1997).

All known typical catalases exhibit discrete electronic spectrum with very strong absorbance in the Soret band and R_z (Reinheitszahl) values, indicating heme content of enzyme, were calculated around 1 (i.e. ratio of $A_{406 \text{ nm}}/A_{280 \text{ nm}}$) (Zámocký and Koller, 1999).

Phylogenetic analyses have revealed that monofunctional catalases fall into three member clades, which is presented in Figure 1.1 (Chelikani *et al.*, 2004; Klotz and Loewen, 2003; Nicholls *et al.*, 2001).

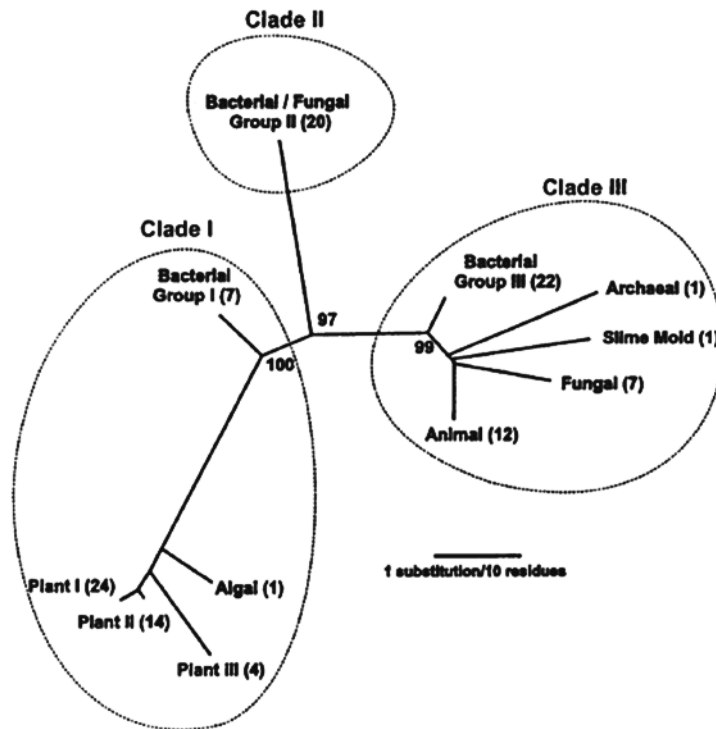


Figure 1.1 The phylogenetic tree of monofunctional catalases based on the core amino acid sequences (Nicholls *et al.*, 2004).

Clade 1 catalases contain predominantly the plant enzymes, one algal representative and one branch of bacterial catalases. Clade 2 enzymes are composed of only large subunit catalases with bacterial and fungal origins (Chelikani *et al.*, 2004; Hara *et al.*, 2007; Nicholls *et al.*, 2001). This clade of catalases exhibits a strong resistance to denaturation by heat and proteolysis (Hara *et al.*, 2007). Clade 3 catalases contain only small subunit enzymes with

bacterial, archaeobacterial, fungal and animal origins. The absence of Clade 3 enzymes in older taxonomic groups suggests that they evolved much later as a result of gene duplication in bacteria that then spread by horizontal and lateral transfers among bacteria to archaeobacteria and eukaryotes (Chelikani *et al.*, 2004; Nicholls *et al.*, 2001). Klotz and Loewen (2003) proposed a model of divergent evolution rather than convergent evolution of the monofunctional catalases based on the phylogeny of the entire monofunctional catalase gene family.

Multiple sequence alignment of typical catalases presented in Figure 1.2 shows that the area around distal histidine, proximal haem and tyrosine are highly conserved (Zámocký and Koller, 1999).

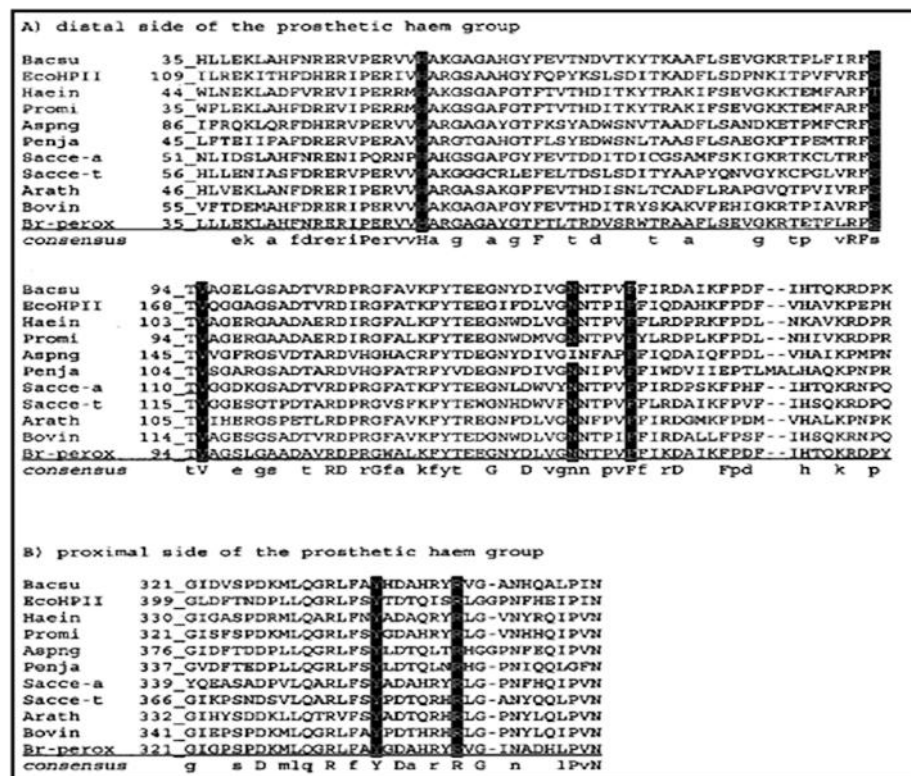


Figure 1.2 Multiple sequence alignment of monofunctional catalases in the distal (a) and proximal (b) sides of haem ligand, correspondingly (Zámocký and Koller, 1999).

1.1.1.2 Catalase-Peroxidases

The next largest class of catalases is known as catalase-peroxidases. Members of this subgroup exhibit significant peroxidatic activity in addition to catalatic activity (Nicholls *et al.*, 2001). They are found in bacteria, archaeobacteria, and fungi. Catalase-peroxidases share sequence similarity with plant peroxidases, which has been approved by the conversion from a predominant catalase activity into a predominant peroxidase activity by a single amino acid change from tryptophan to a phenylalanine, but there is no such similarity to monofunctional catalases (Chelikani *et al.*, 2003; Klotz and Loewen, 2003).

Bifunctional catalase-peroxidases show unusual spectrum with rather low R_z values, which can be explained by nonstoichiometric haem binding. They are more sensitive to high temperatures than monofunctional catalases (Zámocký and Koller, 1999). Furthermore, they show relatively sharp pH dependency unlike typical catalases (Loewen, 1997).

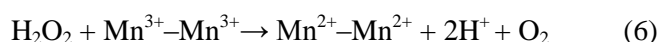
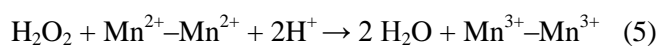
Catalase-peroxidases are active as either dimers or tetramers and contain 0.5 heme *b* per monomer. It has been hypothesized that catalase-peroxidases might have arisen through a gene duplication and fusion (Chelikani *et al.*, 2003; Klotz and Loewen 2003; Nicholls *et al.*, 2001).

1.1.1.3 Manganase Catalases

The nonheme catalases are not as widespread as the heme-containing catalases and there are only three of them so far characterised, one from lactic acid bacteria (*Lactobacillus plantarum*) and two from thermophilic bacteria (*Thermus thermophilus* and *Thermoleophilum album*) (Chelikani *et al.*, 2004; Nicholls *et al.*, 2001). These enzymes are also called pseudo-catalases as their active site contains a manganese-rich reaction instead of heme group (Allgood and Perry 1986; Kono and Fridovich 1983; Whittaker *et al.*, 1999). Crystal structures of two manganese catalases, one from *Thermus thermophilus* and other from

Lactobacillus plantarum, show the presence of dimanganese group in the catalytic centre (Chelikani *et al.*, 2004).

Their catalytic cycle constitutes two stages like heme-containing catalases. The overall reaction requires two-electron redox cycling of the binuclear manganese cluster between the divalent and trivalent states, $\text{Mn}^{2+}\text{-Mn}^{2+} \leftrightarrow \text{Mn}^{3+}\text{-Mn}^{3+}$ (Khangulov *et al.*, 1990a, b, c; Penner-Hahn, 1992; Waldo *et al.*, 1991, 1992; Waldo and Penner-Hahn, 1995). There is no temporal order to the oxidation and reduction stages due to equally stability of the oxidation state of dimanganese cluster. If H_2O_2 encounters $\text{Mn}^{2+}\text{-Mn}^{2+}$, it acts as oxidant (reaction 5) and if $\text{Mn}^{3+}\text{-Mn}^{3+}$ is encountered, the H_2O_2 act as reductant (reaction 6) (Chelikani *et al.*, 2004; Christianson, 1997).



Reaction 5 and 6 are shown as equivalent of reactions 2 and 3 in heme-containing catalases. However, there are two distinctive differences in reaction mechanisms between heme and nonheme catalases. One is that reactive intermediate is not produced during oxidation of reaction centre of nonheme catalases. The second is that both water products are formed in reaction 5, whereas water is produced in each of reactions 2 and 3 in heme catalases (Chelikani *et al.*, 2004). The catalytic mechanism of nonheme catalases is currently under investigation.

1.1.1.4 Minor Catalases

This group of catalases includes heme-containing enzymes, like peroxidases (Arnao *et al.*, 1990), exhibiting low levels of catalytic activity. Chloroperoxidase from *Caldariomyces fumago*, haloperoxidases and bromoperoxidases are examples of minor catalases. Other proteins such as methemoglobin and metmyoglobin have also been observed to have catalytic activity at a very low rate (Mate *et al.*, 2001; Nicholls *et al.*, 2001).

1.1.2 Biological Function of Catalase

Despite catalases play protective role in the removal of reactive oxygen species, particularly those arisen from hydrogen peroxide; they are not essential for cell growth in either *E. coli* (Loewen, 1984) or *Bacillus subtilis* (Loewen and Switala, 1987). However, these enzymes provide selective advantages in a number of environmental situations. For example, it has been seen that cell survival was enhanced in catalase producing cells in the presence of H₂O₂, as compared to catalase-deficient cells (Abril and Pueyo, 1990; McCann *et al.*, 1991; Sammartano *et al.*, 1986; Volkert *et al.*, 1994; Yonei *et al.*, 1987). Catalases also enhance long term survival in stationary phase in aerobic organisms (Loewen, 1999; Mulvey *et al.*, 1990). In addition, it has been suggested that catalase can be an important factor in bacterial virulence. For instance, *Staphylococcus aureus* pathogen requires catalase for intraperitoneal survival in mice (Loewen *et al.*, 2000).

Besides their important roles in the removal of hydrogen peroxide, long term cell survival and virulence, catalases can also function in ethanol and methanol metabolism (Mate *et al.*, 2001; Oshino *et al.*, 1973). Moreover, catalases may play an important role in the compartmentalization of hydrogen peroxide, which has recently gained attention as intra- and intercellular messenger capable of encouraging growth responses in culture at submicromolar levels (Burdon, 1995; Khan and Wilson, 1995; Mueller *et al.*, 1997).

1.1.3 Occurance

Catalase is widely distributed in mammalian and nonmammalian aerobic cells including a cytochrome system and with a few exceptions (*Acetobacter peroxydans* and *Shigella dysenteriae*) only strict anaerobes do not have this enzyme (Deisseroth and Dounce, 1970). In mammalian cells, catalase is found to be in the cytosol, mitochondria, and particularly peroxisomes (Mate *et al.*, 2001).

1.1.4 Regulation of Catalase Expression

The study of the bacterial response to oxidative stress has given insights into how catalase synthesis is controlled in different cells. Studies with *E. coli* and *Salmonella typhimurium* have shown that there are two regulatory pathways available in bacterial catalase expression (Loewen, 1997; Storz and Tartaglia, 1992).

E. coli produces two catalases or hydroperoxidases, the bifunctional catalase-peroxidase HPI and the monofunctional catalase HPII. These two types of catalases are induced independently; HPI synthesis is promoted by H₂O₂ added to medium, and HPII synthesis is induced during growth into stationary phase (Mulvey *et al.*, 1990).

The *katG* gene, encoding HPI, has been found to be regulated by the OxyR regulon which responds to oxidative stress (Loewen, 1997; Mulvey *et al.*, 1990; Storz and Tartaglia, 1992). OxyR protein is a member of LysR family of regulatory proteins that respond to oxidant levels in the cell (Loewen, 1997). OxyR protein undergoes a conformational change during its transition from the reduced (transcriptionally inactive) to the oxidized (transcriptional active) form. This protein directly senses the oxidative stress by becoming oxidized, and that oxidation results in conformational change by which it transduces oxidative stress to RNA polymerase (Storz and Tartaglia, 1992).

The regulatory mechanism of the *katE* gene, encoding HPII, is quite different and requires a functional *katF* gene as a positive effector (Mulvey *et al.*, 1990). HPII levels are expressed at high levels when cells enter stationary phase, are unaffected by hydrogen peroxide and/or anaerobiosis (Loewen, 1997; Mulvey *et al.*, 1990). The most important factor for HPII induction seems to be σ^S , as concluded from studies related with the involvement of additional transcription factors (Meir and Yagil, 1990; Mulvey *et al.*, 1990).

1.1.5 Catalase Cofactors

The prosthetic group of horse liver catalase enzyme was first isolated by Stern in 1935. This non-covalently bound component was identified as protoheme (also called hematin), consisting of an iron atom and a porphyrin ring.

The heme prosthetic group has been found to be buried inside the protein, approximately 20 Å from the surface in almost all heme containing catalases whose structures have been dissolved (Bravo *et al.*, 1995; Fita *et al.*, 1986; Gouet *et al.*, 1995; Murshudov *et al.*, 1992; Vainsthein *et al.*, 1986). Despite the similarities in heme binding pocket, catalases from different sources contain different prosthetic groups (Murshudov *et al.*, 1995). All small subunit size catalases have been shown to include a non-covalently bound iron protoporphyrin IX (heme *b*) as prosthetic group per subunit (Mate *et al.*, 2001; Murshudov *et al.*, 1995). Consecutively, an oxidized form of protoporphyrin IX, heme *d*, has been found in almost all large subunit size catalases (Mate *et al.*, 2001). The heme *d* group characterised in the active sites of crystal structures of two large subunit size catalases, PVC (*Penicillium vitale* catalase) and HPII from *E. coli*, has the structure of the *cis*-hydroxy γ -spirolactone and is rotated 180 degrees about the axis defined by the α - γ -meso carbon atoms, with regard to the orientation found for heme *b* in small subunit size catalases like BVC (bovine liver catalase) (Murshudov *et al.*, 1995). Figure 1.3 shows the structural differences between *b* type and *d* type heme.

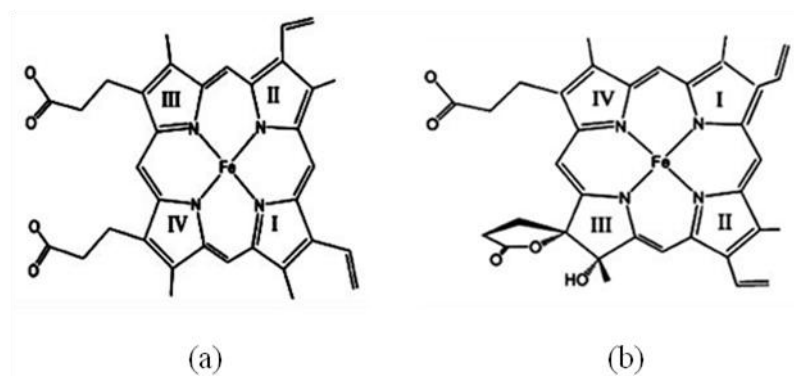


Figure 1.3 Structures of heme *b* (a) and heme *d* (b) (Alfonso-Prieto *et al.*, 2007).

The γ -spirolactone ring and additional hydroxyl group make heme *d* more asymmetric with respect to heme *b*. The conversion of heme *b* to heme *d* has been studied in *E. coli* by many scientists and it is proposed that the oxidation of heme in HP_{II} may be catalyzed by HP_{II} itself (Timkovich and Bondoc, 1990). Loewen and colleagues (1993) also reported this conversion in the presence of hydrogen peroxide. However, the modification takes place on the proximal side of ring III opposite to the essential distal histidine (Bravo *et al.*, 1997; Murshudov *et al.*, 1995). Another possible conversion of protoheme to heme *d* is provided by Diaz *et al.*, 2005. They postulated a mechanism in which singlet oxygen produced catalytically or by photosensitization may hydroxylate C5 and C6 of pyrrole ring III and cause the γ -spirolactone formation in C6 (Diaz *et al.*, 2005).

Heme contacting residues are rather found to be different for heme *d* and protoheme enzymes. Such residues for PVC involve Ile41, Val209, Pro291, and Leu342 and for HP_{II} contain Ile114, Ile279, Pro356, and Leu407, while analogous residues for BLC are Met60, Ser216, Leu298 and Met349. These differences may determine heme orientation (Maj *et al.*, 1998; Murshudov *et al.*, 1995).

Small subunit size catalases have the ability to bind NADP(H) cofactor which is not essential for the activity of catalase (Kirkman and Gaetani, 1984); but it is believed to have role in protecting the enzyme from formation of catalytically inactive intermediate (compound II) by promoting its reduction to resting state (Fe^{3+}) during catalytic cycle (Cattani and Ferri, 1994; Hillar and Nicholls, 1992). According to this hypothesis, large subunit enzymes, whose catalytic cycle lacks compound II formation, do not require to bind NADP(H) (Hillar and Nicholls, 1992). It has also been found that NADP(H) is essential for the dismutation of small peroxides, other than hydrogen peroxide (Cattani and Ferri, 1994). Instead, large subunit size catalases possess the extra C-terminal domain with a flavodoxin-like topology (Mate *et al.*, 2001; Murshudov *et al.*, 1995). Despite this difference, residues defining the NADPH pocket in the bovine liver catalase appear to be well preserved in HPII. Only two residues that interact ionically with NADP(H) in the bovine catalase (Asp212 and His304) differ in HPII (Glu270 and Glu362), but it has been proven that their mutation to the bovine sequence does not promote nucleotide binding (Sevinc *et al.*, 1999).

1.1.6 Catalase Catalytic Cycle

As described in previous sections, catalytic reaction occurs in two steps (Chelikani *et al.*, 2004; Nicholls *et al.*, 2001; Switala and Loewen, 2002). First phase of catalytic cycle involves reaction of ferric enzyme and hydrogen peroxide molecule to generate compound I and water. In the second stage, compound I combines with a second molecule of hydrogen peroxide molecule to regenerate the ferric enzyme, molecular oxygen and water (Nicholls *et al.*, 2001). Figure 1.4 shows the reaction steps in catalase cycle (Zámocký *et al.*, 2001).

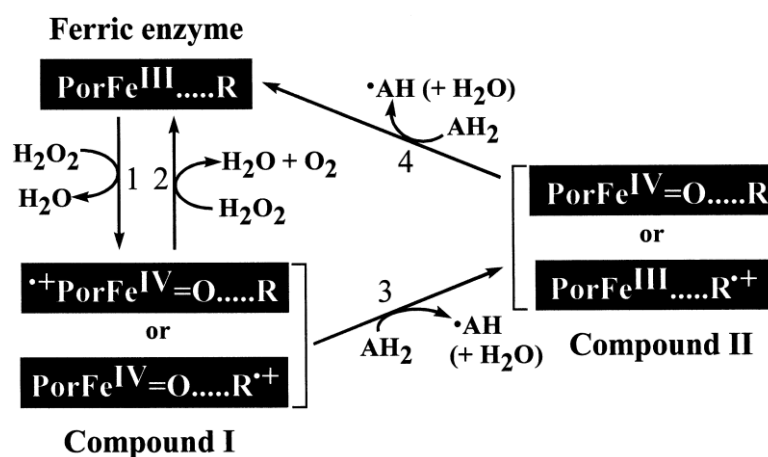


Figure 1.4 The catalytic cycle of catalases (Zámocký *et al.*, 2001).

Paulos and Kraut firstly proposed the formation of compound I using crystal structure of cytochrome c peroxidase in 1980 (Figure 1.5). According to this mechanism, proton transfer takes place from hydrogen peroxide to distal imidazole group and iron-oxygen bond is generated (Jones and Dunford, 2005).

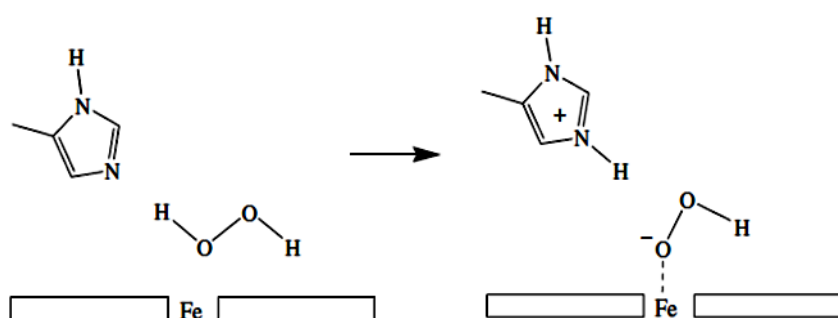


Figure 1.5 Compound I formation (Jones and Dunford, 2005; Paulos and Kraut, 1980).

The studies of water release or rebinding to the coproduct formation site have shown that compound I intermediate might exist in two forms either a wet form in which a water molecule is present at or near the site of coproduct water formation, or dry form where the coproduct water formation site is dry. It is assumed that the presence of water may play significant role in both substrate selectivity and the variety of redox pathways available in the donor oxidation phase of the catalytic cycles (Jones, 2001; Jones and Dunford, 2005).

Compound I intermediate is also perceived in the presence of organic peroxides as substrate and the reaction rate of compound I production decreases with an increase in the molecular size of the leaving group such as $\text{H}^- > \text{CH}_3^- > \text{HOCH}_2^- > \text{CH}_3\text{CH}_2^- > \text{CH}_3\text{C(=O)}^- > \text{CH}_3(\text{CH}_2)_2^- > \text{CH}_3(\text{CH}_2)_3\text{OOH}^-$ (Hara *et al.*, 2007). At low hydrogen peroxide concentrations and in the presence of suitable organic electron donors, compound I can be reduced by one-electron addition leading to formation of compound II (a formal Fe^{4+} state) which can cause enzyme inactivation. In this reaction, the porphyrin accepts one electron, therefore losing its radical character (Alfonso-Prieto *et al.*, 2007; Mate *et al.*, 1999).

1.1.6.1 Kinetics

The proposed BCT (Bonnichsen *et al.*, 1947) mechanism supports that catalase enzyme is never saturated with its substrate, H_2O_2 , and that turnover of enzyme increases indefinitely as substrate concentration increases (Nicholls *et al.*, 2001). Apparently, catalases has been recognized with a rapid turnover rate and the maximum observed velocities ranging between 54,000-833,000 reactions per second (Switala *et al.*, 2002).

The classical kinetic parameters, V_{max} , k_{cat} and K_{m} , cannot be directly applied to the observed data as catalases do not follow Michaelis-Menten kinetics except at very low substrate concentrations. However, at concentrations below 200 mM, all small subunit size catalases show Michaelis-Menten-like dependence of velocity. At concentrations above 300-500 mM, most small subunit size catalases suffer

inactivation. Conversely, large subunit size catalases begin to suffer inhibition above 3 M hydrogen peroxide concentrations (Chelikani *et al.*, 2004; Switala *et al.*, 2002).

1.1.6.2 Effect of Inhibitors

Catalases are sensitive to various compounds interacting with the active-site heme. Such compounds include cyanide, azide, hydroxylamine, aminotriazole and mercaptoethanol (Switala *et al.*, 2002).

1.1.7 Catalase Production, Purification and Characterisation

Catalases are ubiquitous enzymes present in almost all aerobic prokaryotic and eukaryotic organisms (Bravo *et al.*, 1995). Among those, the biochemistry of *E. coli* catalases, HPI (catalase-peroxidase) and HPII (monofunctional catalase), have been extensively studied. These two enzymes give response to metabolic changes differently from each other. For example, HPI was induced by eight fold when cells of *E. coli* were grown at ascorbate concentrations 0.57-5.7 mM in aerated medium (Loewen *et al.*, 1985; Richter and Loewen, 1982). In turn, any carbon source derived from tricarboxylic acid cycle caused a five to ten fold increase in HPII levels during logarithmic growth (Loewen *et al.*, 1985).

For production of two types of catalases in *E. coli*, cultures were grown with forced aeration overnight at 37°C. Crude extracts were fractionated with ammonium sulfate and fractions were then applied to DEAE (Diethylaminoethyl) cellulose column for purification (Loewen and Switala, 1986; Mate *et al.*, 2001).

The absorption spectra of catalases have been well documented (Mate *et al.*, 2001). Protoheme containing catalases have a Soret band at 405 nm and smaller bands at 500, 540 and 622 nm. Heme *d* containing enzymes exhibits an almost identical Soret band and three banded region is shifted to 590, 630 and 715 nm, respectively (Maj *et al.*, 1998).

1.1.7.1 Fungi as Catalase Producers

Fungi are reported to be high producers of catalases and contain distinct genes encoding different types of catalases that are differently regulated according to conditions (Hisada *et al.*, 2005; Isobe *et al.*, 2006).

Different types of catalases have been isolated from a number of fungi including *Alternaria alternata* (Caridis *et al.*, 1991), *Aspergillus fumigatus* (Hearn *et al.*, 1992; Paris *et al.*, 2003; Takasaka *et al.*, 1999), *Aspergillus nidulans* (Calera *et al.*, 2000; Kawasaki and Aguirre, 2001; Navarro *et al.*, 1996), *Aspergillus niger* (Meyer *et al.*, 1997), *Aspergillus oryzae* (Hisada *et al.*, 2005), *Blakeslea trispora* (Gessler, 2002), *Cladosporium fulvum* (Bussink and Oliver, 2001), *Neurospora crassa* (Gessler, 2002; Kamel and Tahany, 1973), *Penicillium simplicissimum* (Fraaije *et al.*, 1996), *Penicillium vitale* (Vainshtein *et al.*, 1981 and 1986), *Phanerochaete chrysosporium* (Kwon and Anderson, 2001), *Saccharomyces cerevisiae* (Hortner *et al.* 1976; Ruis and Koller, 1997; Zámocký *et al.*, 1995), *Septoria tritici* (Levy *et al.*, 1992), and *Thermoascus aurantiacus* (Wang *et al.*, 1998).

1.1.8 Three Dimensional Structure of Catalase

1.1.8.1 Crystallisation Studies

Catalase was one of the first enzymes to be crystallised (Sumner and Dounce, 1937). The first X-ray structure of catalase obtained from the fungus *P. vitale* was first determined by Vainshtein *et al.* (1981) at 3.5 Å resolution. This structure was then refined to 2.0 Å resolution by Vainshtein *et al.* (1986). Fita and coworkers also reported the refined three dimensional structure of bovine liver catalase using 2.5 Å resolution data leading to compare the structures of BLC and PVC (Fita *et al.*, 1986; Melik-Adamyán *et al.*, 1986).

The crystallisation of catalase HP11 from *E. coli* was first reported by Tormo *et al.* (1990). Crystals were obtained using hanging drop vapour diffusion method at 4°C using polyethylene glycol (PEG) as precipitant (Tormo *et al.*, 1990). Later, better crystals were obtained when catalase HP11 enzyme was crystallised at 22°C with a protein concentration of 15 mg/mL using the hanging drop vapour diffusion method in the presence of PEG 3350 (Bravo *et al.*, 1999) and crystals diffracted at 1.8 Å resolution (Mate *et al.*, 2001).

The crystal structures of eleven monofunctional heme containing catalases from different sources have been reported including those from, bovine liver (Fita *et al.*, 1986; Murthy *et al.*, 1981), *Enterococcus faecalis* (Hakansson *et al.*, 2004), *Escherichia coli* (Bravo *et al.*, 1995; Bravo *et al.*, 1999), *Helicobacter pylori* (Loewen *et al.*, 2004), human erythrocytes (Ko *et al.*, 1999; Putnam *et al.*, 2000), *Micrococcus lysodeikticus* (Murshudov *et al.*, 1992), *Neurospora crassa* (Díaz *et al.*, 2004), *Penicillium vitale* (Vainshtein *et al.*, 1981; Vainshtein *et al.*, 1986), *Proteus mirabilis* (Gouet *et al.*, 1995), *Pseudomonas syringae* (Carpena *et al.*, 2003), and *Saccharomyces cerevisiae* (Mate *et al.*, 1999).

1.1.8.2 Overall Structure of Catalases

All catalases, whose structure have been dissolved, exhibit highly conserved β -barrel core structure (Chelikani *et al.*, 2003). Their structure is composed of four domains (Bravo *et al.*, 1999; Fita and Rossmann, 1985; Mate *et al.*, 2001; Melik-Adamyan *et al.*, 1986; Vainshtein *et al.*, 1986):

- a) an amino terminal arm
- b) an anti-parallel eight stranded β -barrel domain
- c) wrapping domain
- d) α -helical domain

The amino-terminal domain is an extended arm and is quite variable in length ranging from 53 residues in *Proteus mirabilis* catalase (PMC) to 127 in HP11 (Mate *et al.*, 2001; Melik-Adamyan *et al.*, 1986). This domain is involved in

extensive intersubunit interactions and residues from this region contribute to define the heme pocket of a symmetry related subunit. The extent of the intersubunit interactions increases with the length of domain showing the molecular stability of catalases (Mate *et al.*, 2001).

The second domain, referred to as β -barrel domain, is the central feature of catalase. The first half of the β -barrel provides most of the residues involved in forming the cavity on the heme's distal side. The second half of the β -barrel contributes to the NADP(H) binding pocket in small subunit catalases. This domain also includes at least six helices located along the polypeptide chain in two long insertions between β -strands (Fita and Rossmann, 1985; Mate *et al.*, 2001; Melik-Adamyanyan *et al.*, 1986).

The wrapping loop is an extended region of almost 110 residues that connects the β -barrel and α -helical regions. This region lacks the secondary structure in long stretch of polypeptide chain between residues 366-420, but it contains the essential helix (α_9) defining the heme proximal side including tyrosine residue. This portion of polypeptide chain participates in various interdomain and intersubunit interactions particularly with residues from the amino terminal arm region from another subunit (Fita and Rossmann, 1985; Mate *et al.*, 2001; Melik-Adamyanyan *et al.*, 1986).

The α -helical region contains four anti-parallel helices that are close to some of the helices from the β -barrel domain (Mate *et al.*, 2001; Melik-Adamyanyan *et al.*, 1986).

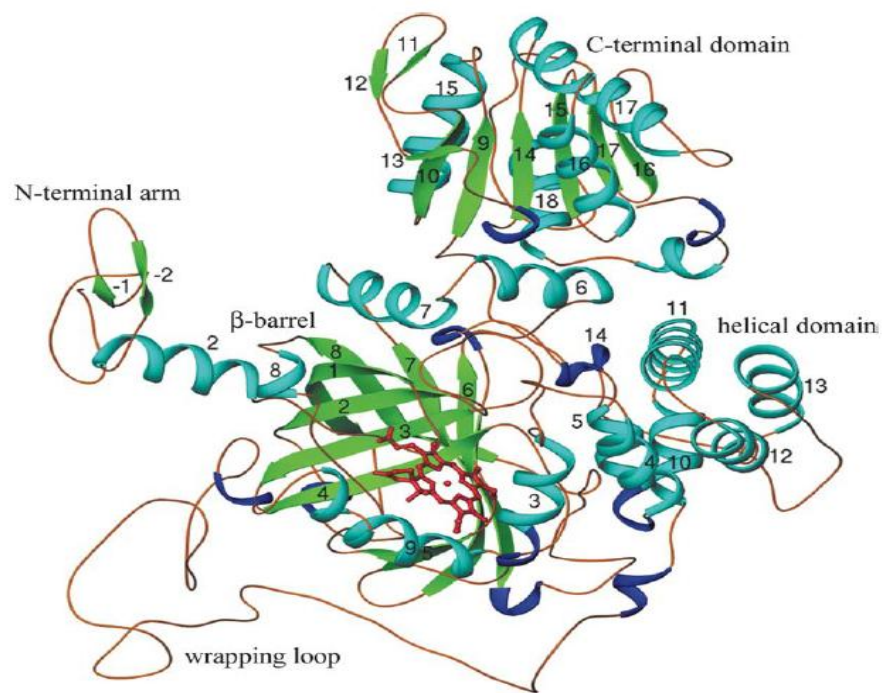


Figure 1.6 Schematic drawing of the polypeptide chain and elements of secondary structure in a *Neurospora crassa* catalase subunit (Díaz *et al.*, 2004).

Unlike BLC, the structures of PVC and HP11 present an extra carboxy-terminal domain including roughly 150 residues with a high content of secondary structure elements organized with a “flavodoxin-like” topology (Bravo *et al.*, 1999; Mate *et al.*, 2001; Melik-Adamyán *et al.*, 1986). The possible role of this extra domain in PVC remains unknown (Mate *et al.*, 2001). In BLC, prior to the flavodoxin-like domain is occupied by an NADP(H) molecule (Fita and Rossmann, 1985).

Although PVC and HP11 share common structural similarities, HP11 differs in the existence of 60 residues at N-terminal end that increase the contact area between subunits (Bravo *et al.*, 1995).

1.1.8.3 Heme Pocket

In all catalases, the heme group is deeply buried in the core structure and its distance from the nearest part of the molecular surface is about 20 Å (Loewen, 1997; Mate *et al.*, 2001).

Three residues, tyrosine on the proximal side of the heme (Tyr415 in HP11) and histidine and asparagine on the distal side (His128 and Asn201 in HP11), are believed to be essential for catalysis (Mate *et al.*, 2001). The oxygen of the phenolic hydroxyl group of tyrosine is the proximal ligand of the heme iron and is most likely deprotonated having negative charge so that can contribute to the stabilization of the high oxidation states of iron. The imidazole ring of distal histidine is placed almost parallel to the heme at a mean distance of about 3.5 Å above either pyrrole ring III in PMC or pyrrole ring IV in PVC and HP11 (Figure 1.7). The histidine and asparagine residues on the distal side of the heme make the environment strongly hydrophobic (Mate *et al.*, 2001).

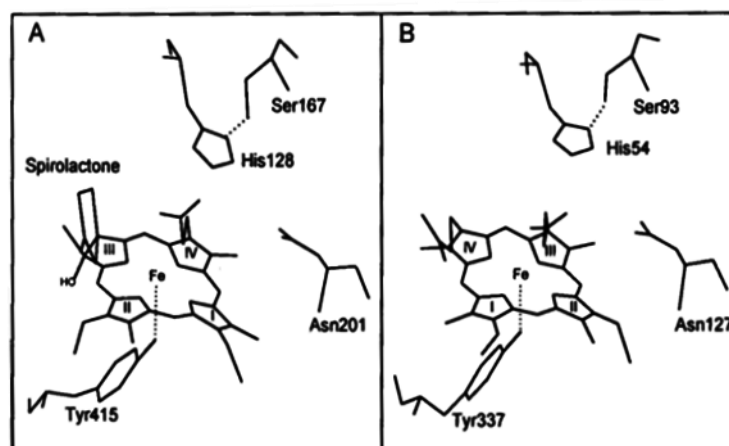


Figure 1.7 Comparison of active site in catalase HP11 (A) and catalase of *Proteus mirabilis* (B) (Loewen, 1997).

A conserved serine residue (Ser167 in HPII) is also found to be hydrogen bonded to the N^δ of the essential histidine and might facilitate the enzymatic mechanism (Bravo *et al.*, 1999).

Despite possessing the same type of heme in active site, PVC and HPII differ in the presence of covalent bond between tyrosine and histidine residues. As shown in Figure 1.8, HPII contains a novel type of covalent bond joining the C^β of the essential Tyr415 and the N^δ of His392 but not in PVC (Bravo *et al.*, 1997; Bravo *et al.*, 1999; Mate *et al.*, 1999; Melik-Adamyan *et al.*, 2001).

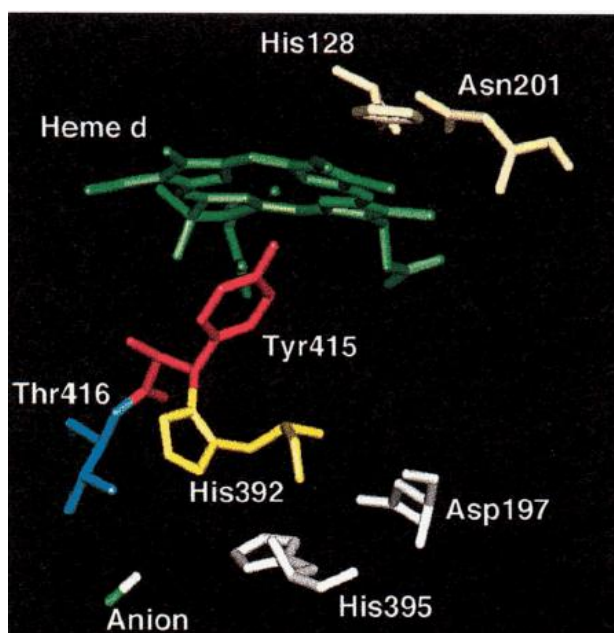


Figure 1.8 The C^β-N^δ bond between His392 and Tyr415 (Bravo *et al.*, 1997).

1.1.8.3.1 Channels to the Heme Group

The limited accessibility to heme grouping catalases requires the presence of channels (Mate *et al.*, 2001). Three channels, the main channel oriented perpendicular to the plane of heme, the lateral channel approaching in the plane

of heme and the central channel leading from the distal side of the heme to the central cavity, connect the active site to the exterior of enzyme (Chelikani *et al.*, 2003; Díaz *et al.*, 2004).

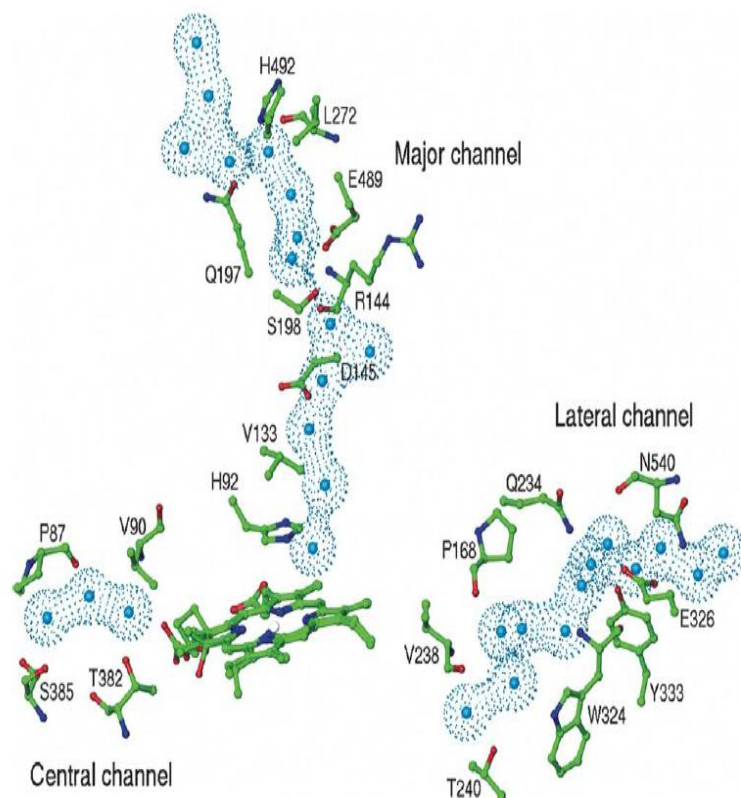
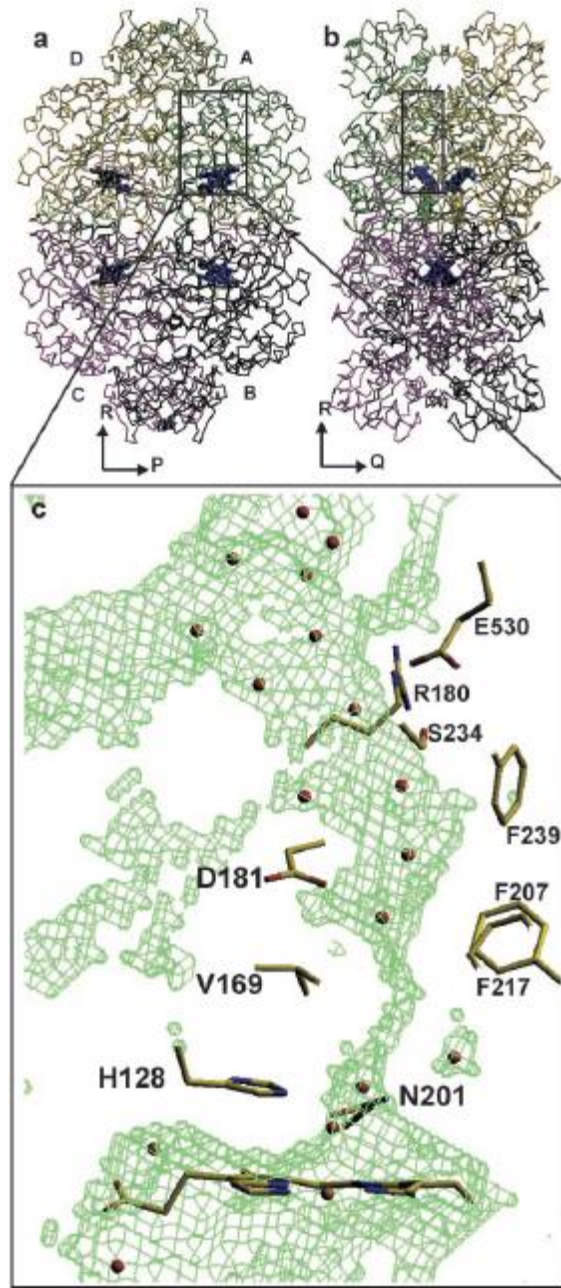


Figure 1.9 Channels in CAT-1 of *N. crassa* (Díaz *et al.*, 2004).



The main channel is considered to be the primary route for substrate movement to the active site (Chelikani *et al.*, 2003; Switala and Loewen, 2002). It is funnel-shaped with 30 Å long in small catalases (Fita and Rossmann, 1985; Mate *et al.*, 2001), while in large catalases that channel is replaced by an elongated, constricted, and possibly bifurcated channel that includes the C-terminal domain of adjacent subunit (Mate *et al.*, 2001; Switala and Loewen, 2002).

Figure 1.10 Main channel of HP11 (Chelikani *et al.*, 2003).

The conserved residues in the main channel are shown in Figure 1.10 including the essential histidine, a valine and an aspartate, (His128, Val169, and Asp181 in

HPH) situated 4, 8 and 12 Å from the heme, respectively (Chelikani *et al.*, 2003). The histidine residue is essential for catalysis in HPH and the side chain of valine residue makes the channel narrower to a diameter of about 3 Å that prevents any molecule larger than H₂O and H₂O₂ from gaining access to the active site. The role of aspartate has not been investigated in any catalase, but the presence of negatively charged side chain has been found to be critical for catalysis (Chelikani *et al.*, 2003).

The lateral, or minor channel approaches heme above and below the essential asparagine and emerges in the molecular surface at location corresponding to the NADP(H) binding pocket in catalases that bind a cofactor (Figure 1.11, Mate *et al.*, 2001). The function of this channel remains unknown (Díaz *et al.*, 2004). Molecular dynamics analysis indicates that water can exit the protein through this channel (Sevinc *et al.*, 1999).

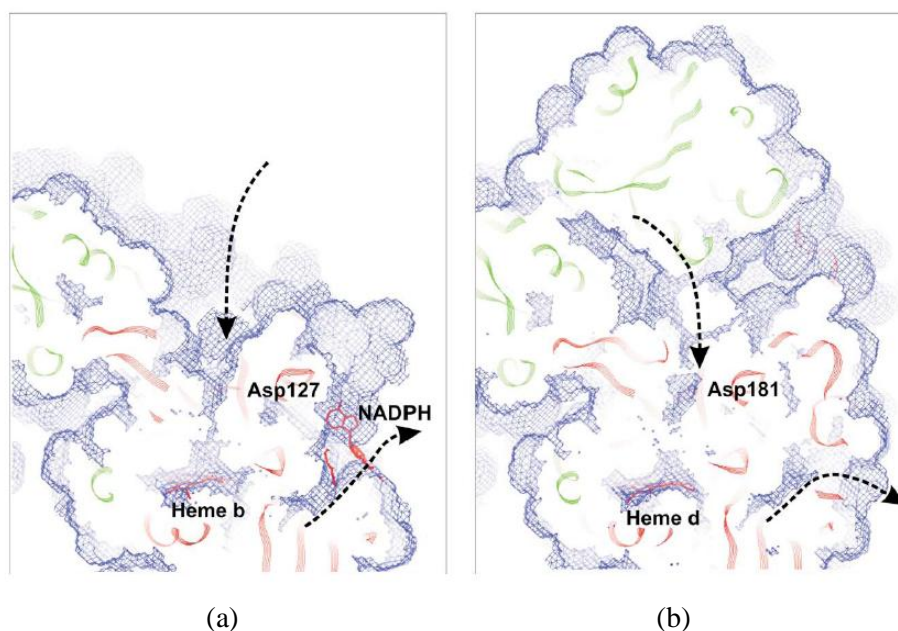


Figure 1.11 Comparison of main and lateral channels of BLC (a) and HPH (b) (Switala and Loewen, 2002).

The main channel is preferred route for substrate entry, but it might be too long and narrow for the release of reaction products (water and molecular oxygen). As the central channel is mainly hydrophilic and leads to the central cavity that is contiguous to the bulk water, this could be a way out for O₂. However, substitutions of amino acid residues extending the major channel in large catalases might allow the exit of oxygen through main channel. In fact, oxygen preferentially exits through main channel instead of central one in all catalases having *b* type heme in the active site. Thus, the presence of minor channels might be alternative mechanism for a fast release of products under condition of high H₂O₂ stress. These results indicate that O₂ can exit the enzyme through different channels; although the main exit in large catalases might be through the central channel and in small catalases through the major channel (Díaz *et al.*, 2004; Kalko *et al.*, 2001).

1.2 Phenol Oxidases

Phenol oxidases consist of a group of enzymes capable of oxidizing a number of aromatic compounds by molecular oxygen (Ögel *et al.*, 2006; Sanchez-Amat and Solano, 1997). These enzymes are involved in secondary metabolic activities such as melanin synthesis (Griffith, 1994). The polymerization reactions of phenol oxidases are related to the changes in cell wall permeability, intercellular locations and the removal of toxic metabolites (Mayer, 1987; Mayer and Harel, 1979).

1.2.1 Phenols

The word “phenol” is used to refer any organic compound that contains a six-membered aromatic ring (benzene), bonded directly to a hydroxyl group (–OH). Phenols are bifunctional compounds; hydroxyl group and aromatic ring inreact strongly leading to novel properties of phenols (Kaptan, 2004).

Phenolic compounds are secondary metabolites of plants that are involved in defense against radiation or aggression by pathogens. They are effective free radical scavengers and metal chelators which are mediated by the presence of *para*-hydroxyl groups. Phenolics are different in size ranging from simple phenols like catechol, hydroquinone and resorcinol to large polymers like tannins (Ferguson, 2001; Manach *et al.*, 2004; Rahman *et al.*, 2006; Tomás-Barberán and Espín, 2001).

Phenolics can be classified into different groups as a function of the number of phenolic rings and of the structural elements that bind these rings to one another (Manach *et al.*, 2004): Simple phenols, Phenolic acids, Flavonoids, Stilbenes and Lignans.

Two-hydroxy phenols are representatives of simple phenols (Figure 1.12). The three dihydroxy derivatives of benzene as simple phenolics are 1,2- (catechol), 1,3- (resorcinol), and 1,4-benzenediol (hydroquinone) (Kaptan, 2004).

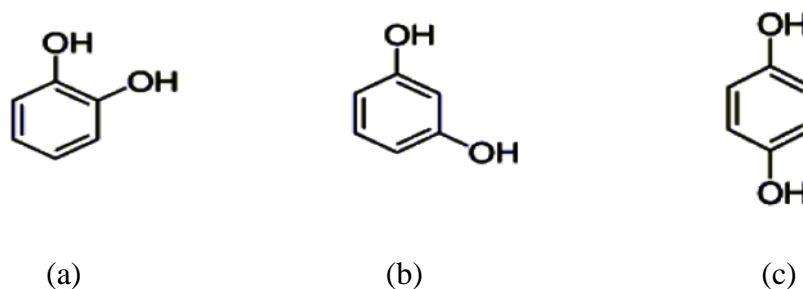


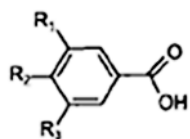
Figure 1.12 Structures of catechol (a), resorcinol (b), and hydroquinone (c).

The free radical scavenging ability of two-hydroxy phenols has been studied and it has been observed that *ortho*-structured phenols like catechol have the greatest scavenging ability. Kinetic experiments have also shown that catechol had the largest rate coefficient among the two-OH phenols at all temperatures and in all

solvents, followed by hydroquinone and resorcinol, which denoted the contribution of *ortho* position to effective scavenging of free radicals (Thavasi *et al.*, 2009). In contrast to the beneficial scavenging ability of catechol, its cytotoxic effects on different cells have been observed as well. Catechol and hydroquinone have been found to be significantly more toxic than resorcinol due to the fact that resorcinol is less oxidized under the conditions existing in the culture medium and therefore not producing sufficient levels of oxygen radicals (Miura *et al.*, 2000; Passi *et al.*, 1987).

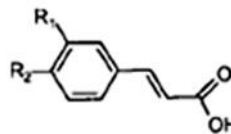
Phenolic acids can be divided into two classes, namely derivatives of benzoic acid and derivatives of cinnamic acid (Figure 1.13). Gallic acid is the most representative compound of first group of phenolic acids. It is generally present in tea, red fruits, black radish and onions (Manach *et al.*, 2004). Sakaguchi and coworkers (1998) found that gallic acid induces cell death in cancer cells with higher sensitivity than normal cells. Tannic acid and vanillic acid are also involved in this class. The second groups of compounds are more common and *p*-coumaric acid, caffeic acid and ferulic acid are the examples of that group. These acids are generally found in making esters with quinic acid, shikimic acid, and tartaric acid. Caffeic and quinic acid combine to form chlorogenic acid, which is found in high concentrations in coffee (Manach *et al.*, 2004). Caffeic and chlorogenic acid increase the plasma antioxidant capacity, the concentrations of endogenous antioxidants like vitamin E and *ex vivo* resistance of lipoproteins to oxidation (Lafay *et al.*, 2005; Lafay *et al.*, 2006; Nardini *et al.*, 1997; Natella *et al.*, 2002). Chlorogenic acid can also reverse the pro-oxidant effects of drugs like paraquat (Lafay *et al.*, 2006; Tsuchiya *et al.*, 1996).

Hydroxybenzoic acids



$R_1 = R_2 = \text{OH}, R_3 = \text{H}$: Protocatechuic acid
 $R_1 = R_2 = R_3 = \text{OH}$: Gallic acid

Hydroxycinnamic acids



$R_1 = \text{OH}$: Coumaric acid
 $R_1 = R_2 = \text{OH}$: Caffeic acid
 $R_1 = \text{OCH}_3, R_2 = \text{OH}$: Ferulic acid

Figure 1.13 Examples of phenolic acids (Manach *et al.*, 2004).

Flavonoids are benzo- γ -pyrone derivatives composed of phenolic and pyrane rings (Figure 1.14). They are classified according to the oxidation level of the C-ring including flavonols, flavones, isoflavones, flavanones, anthocyanidins and flavanols (Heim *et al.*, 2002; Manach *et al.*, 2004; Pourcel *et al.*, 2006; Rice-Evans, 2001).

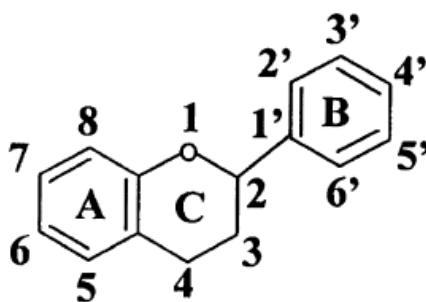


Figure 1.14 The structure of flavonoids (Heim *et al.*, 2002).

Flavonols are the most ubiquitous flavonoids in foods, and quercetin and kaempferol are involved in this class of flavonoids. Quercetin and kaempferol have been shown to possess antioxidant activities. Flavones are much less common than flavonols. Flavones are found in tomatoes and certain aromatic plants. Isoflavones are structurally similar to estrogens. Flavonols exist in both monomer form (catechin) and polymer form (proanthocyanidins). Anthocyanins are natural pigments and exist in different forms, both colored and uncoloured, depending on pH (Manach *et al.*, 2004).

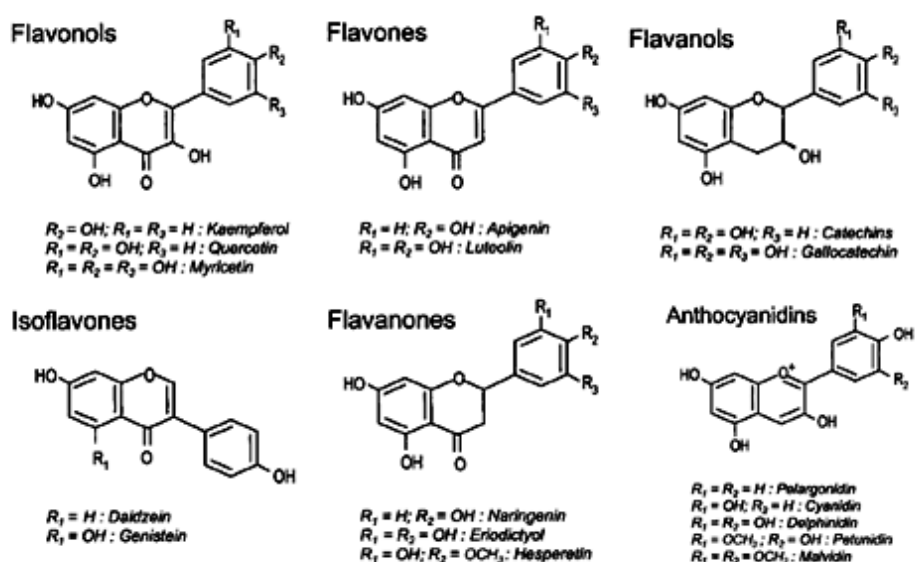


Figure 1.15 Structures of different forms of flavonoids (Manach *et al.*, 2004).

Flavonoids have many protective roles in biological systems including their capacity to transfer electrons free radicals, metal chelating activity, antioxidant enzyme activation, alpha-tocopherol radical reduction, and oxidase inhibition (Heim *et al.*, 2002). Among those flavonoids described above, *ortho*-diphenols

can be oxidized to their corresponding semiquinones and quinones by phenol oxidases in a mechanism called browning (Pourcel *et al.*, 2006).

Stilbenes are found in low quantities in the human diet and have antifungal activities against pathogens (Jeandet *et al.*, 2002; Manach *et al.*, 2004). Resveratrol is 3,4',5-trihydroxystilbene that presents especially in red wines. It is composed of two phenolic rings connected by a double bond (Figure 1.16, Rahman *et al.*, 2006). Two isoforms of resveratrol are possible; but *trans* form is more stable than *cis* form (Trela and Waterhouse, 1996). It plays important role in the prevention of carcinogenesis (Nicotra *et al.*, 2004; Stopper *et al.*, 2005). Resveratrol has also been shown to exhibit estrogenic activity (Ashby *et al.*, 1999; Bowers *et al.*, 2000; Gehm *et al.*, 1997). Oligomers of resveratrol called viniferin are reported to have antimicrobial, anti-HIV, anti-inflammatory activities (Nicotra *et al.*, 2004).

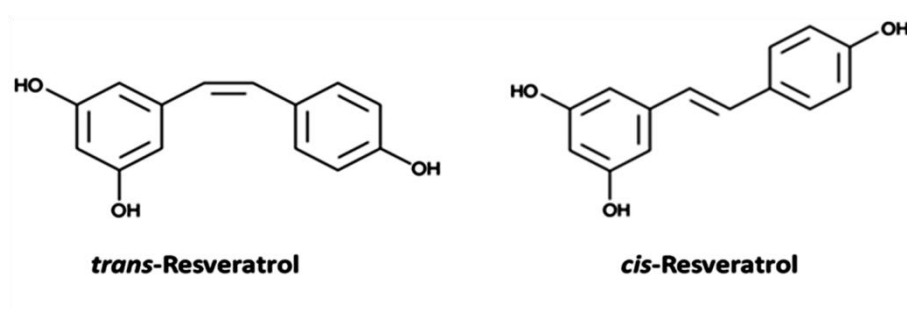


Figure 1.16 The structure of two isomers of resveratrol (Rahman *et al.*, 2006).

1.2.2 Phenol Oxidase Classification

Phenol oxidases are a group of copper containing enzymes responsible for hydroxylation of monophenols to *o*-diphenols and oxidation of *o*-diphenols to *o*-diquinones (Mazzafera and Robinson, 2000). Three classes of phenol oxidases are tyrosinase, catechol oxidase and laccase.

Tyrosinases (monophenol monooxygenase; E.C. 1.14.18.1) catalyze hydroxylation of monophenols (cresolase activity) and subsequent oxidation of *o*-diphenols to corresponding *o*-quinones (catechol oxidase activity). These quinones self-polymerize or react with other substances to form high molecular weight black/brown pigments such as melanins (Marusek *et al.*, 2006).

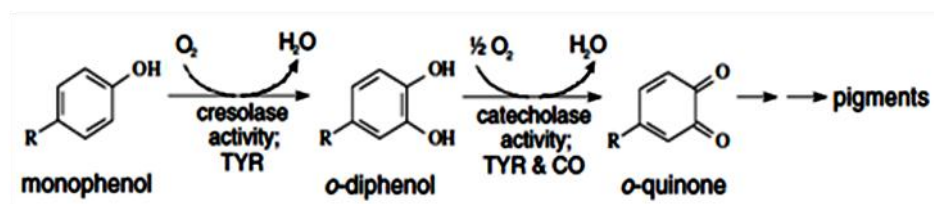


Figure 1.17 The phenol oxidation reaction catalyzed by tyrosinase and catechol oxidase (Marusek *et al.*, 2006).

Catechol oxidases (*o*-diphenol oxidoreductase; EC 1.10.3.1) are key enzymes in melanin pathway and they are only active on *o*-diphenols (Rompel *et al.*, 1999; Sanchez-Amat and Solano, 1997). The substrate specificity of catechol oxidases investigation shows high activity with catechol, 4-methylcatechol and caffeic acid (Gerdemann *et al.*, 2002) and inhibition with substrates containing –COOH group (Rompel *et al.*, 1999).

Laccases (*p*-benzendiol: oxygen oxidoreductase; E.C. 1.10.3.2) are member of multicopper oxidases as they have three spectroscopically different copper centres (type 1, 2 and 3). These enzymes oxidize a wide range of *p*- and *o*-diphenolic compounds, showing more affinity for the first group (Sanchez-Amat and Solano, 1997).

1.2.3 Occurance of Phenol Oxidases in Living Systems

Phenol oxidases are widely distributed through all the phylogenetic scale, from bacteria to mammals (Sanchez-Amat and Solano, 1997). Tyrosinases have been characterised from different sources including bacteria, fungi, plants and mammals (Halaoui *et al.*, 2006a; Marusek *et al.*, 2006; Mayer, 2006; van Gelder *et al.*, 1997) The best characterised tyrosinases are from *Streptomyces glaucescens* (Lerch and Ettliger, 1972) and the fungi *Agaricus bisporus* (Wichers *et al.*, 1996) and *Neurospora crassa* (Lerch, 1976). Catechol oxidases have been studied in details from different organisms such as *Ipomoea batatas* (sweet potatoes, Eicken *et al.*, 1998), *Lycopus europaeus* (Krebs, 1995). Laccases are not present in animals (Sanchez-Amat and Solano, 1997); their presence has been reported in many plants including *Rhus vernicifera* (Durante *et al.*, 2004), some bacteria (Claus, 2003) and insects (Nakamura and Go, 2005). Examples of fungal laccases are *Agaricus bisporus* (edible mushroom, Morozova *et al.*, 2007), *Lentinula edodes* (rice mushroom, Silva *et al.*, 2004), *Pleurotus ostreatus* (oyster mushroom, Morozova *et al.*, 2007), *Pycnoporus sanguineus* (Eugenio *et al.*, 2009), *Scytalidium thermophilum* (Xu , 2001), and *Trametes versicolor* (Pazarlıoğlu *et al.*, 2004).

1.3 Industrial Usage of Catalases and Phenol Oxidases

Catalases are commonly used in any industry where hydrogen peroxide is desired to be removed from a system that is pasteurization or bleaching. One such example is the use of catalase in the textile industry for the removal of H₂O₂ from cotton fabrics. Catalases are also used in the food industry for disposing of hydrogen peroxide used in milk pasteurization (Amorim *et al.*, 2002; Chu *et al.*, 1975; United States Patent, No. 5646025).

Phenol oxidases have a wide range of industrial applications including waste water treatment (Durán and Esposito, 2000), biomaterial synthesis (Mikolasch and Schauer, 2009), applications in the alcoholic and non-alcoholic beverage industry for selective removal of phenol derivatives (Minussi *et al.*, 2002),

decolouration of dyes in textile industry (Claus *et al.*, 2002), applications in pulp and paper industries (Bajpai, 1999; Leonowicz *et al.*, 2001), improvement of taste and color of tobacco shreds in tobacco industry (Shi *et al.*, 2001) and treatment in Parkinson's disease (Ates *et al.*, 2007; Carvalho *et al.*, 2000).

1.4 Bifunctionality of Catalase and Phenol Oxidase

There are numbers of reports available showing that catalase and phenol oxidase activities somehow overlap in such a way that catalases possess additional oxidase activity and phenol oxidases exhibit further catalase activity. This relationship might be clarified by the release of hydrogen peroxide as a result of polyphenol oxidation (Akagawa *et al.*, 2003). Hydrogen peroxide generation by phenol oxidation was also reported by Aoshima and Ayebe (2007). They observed high concentrations of H₂O₂ in beverages like tea or coffee immediately after opening caps due to oxygen.

Mushroom tyrosinase exhibiting catalase activity in the presence of hydrogen peroxide was first introduced by Jolley *et al.*, 1974. Later, this bifunctional activity of tyrosinase was also investigated by Garcia-Molina *et al.*, 2005 and Yamazaki *et al.*, 2004. Besides this novel tyrosinase, one isozyme of catechol oxidase from sweet potatoes (*Ipomoea batatas*) was found to have catalase-like activity (Gerdemann *et al.*, 2001).

In literature, the single known catalase with oxidase activity is mammalian catalase. This enzyme has been reported to present oxidase activity when hydrogen peroxide is absent or levels of H₂O₂ is low (Kirkman and Gaetani, 2006; Vetrano *et al.*, 2005). Vetrano *et al.* described the possible reaction mechanisms of catalases as shown in Figure 1.18.

As mentioned in previous sections, the main function of catalase is the decomposition of hydrogen peroxide into water and oxygen (catalatic activity). Moreover, it is known that catalases can oxidize low molecular weight alcohols in the presence of low concentrations of H₂O₂ (peroxidatic activity). The catalatic

mechanism of catalases is a two-step process in which catalase heme Fe^{3+} reduces one hydrogen peroxide molecule to water and generate a porhyrin cation radical called compound I, which is then oxidized by a second hydrogen peroxide to give molecular oxygen and water. The peroxidatic activity stems from the oxidation of alcohols by compound I through single electron transfer. Vetrano *et al.* expressed a novel oxidase activity in the absence of hydrogen peroxide. This oxidase reaction involves the interaction of catalase heme with a strong reducing agent like Benzidine (HB) and molecular oxygen leading to the formation of a compound II-like intermediate. The subsequent electron transfer causes substrate oxidation and regeneration of resting enzyme. An incomplete reaction may result in the formation of radical centred intermediates and the production of superoxide.

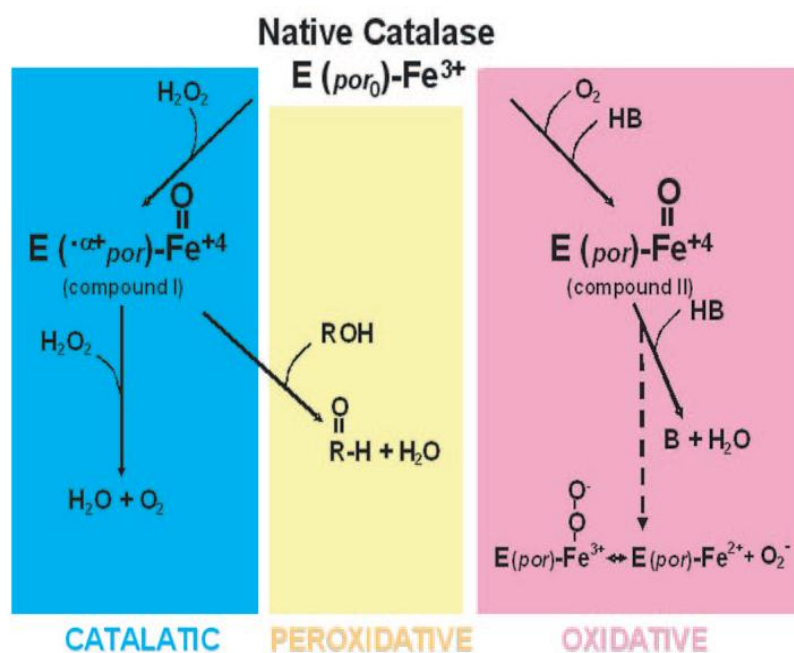


Figure 1.18 Three possible reactions catalyzed by catalase (Vetrano *et al.*, 2005).

Recently, catalase from the thermophilic fungus *Scytalidium thermophilum* has been reported to possess additional phenol oxidase activity (Kocabas *et al.*, 2008). This enzyme, named as CATPO, is the first bifunctional catalase-phenol oxidase in the literature that is characterised in detail.

1.5 Oxidative Stress

Aerobic organisms use molecular oxygen for respiration and energy supply. During these metabolic processes, free radicals and reactive oxygen species (ROS) are formed. Highly reactive oxidants are neutralized by antioxidant defense system involving enzymes such as catalase, superoxide dismutase, glutathione peroxidase, and various non-enzymatic antioxidants like vitamins (A, E and C), glutathione, ubiquinone, and flavonoids (Angelova *et al.*, 2005; Urso and Clarkson, 2003).

Oxidative stress occurs when antioxidants are depleted and/or if the increase in ROS generation is greater than the ability of the defences to cope (Figure 1.19). Therefore, oxidative stress can be defined as imbalance between oxidants and antioxidants in favour of the oxidants, leading to cellular damage (Scandalios, 2005; Sies, 1997). There are many natural sources of oxidative stress, for example exposure to herbicides, UV-radiation, extreme temperatures, toxins like aflatoxin, air pollutants, heavy metals and xenobiotics.

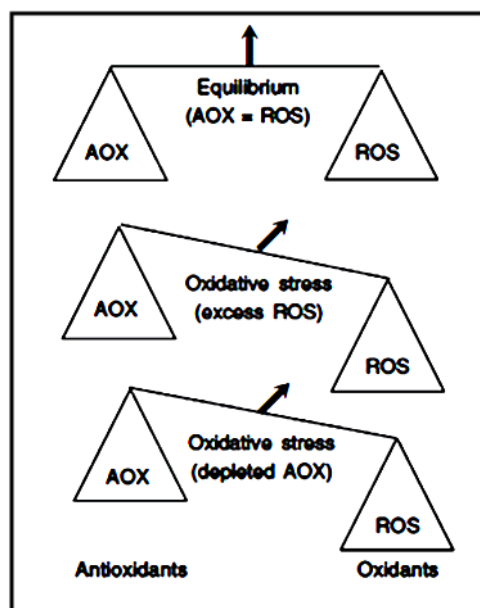


Figure 1.19 Scheme showing formation of oxidative stress (Scandalios, 2005).

Oxidative stress has been reported to be related with several diseases including atherosclerosis, hypertension, inflammation, cystic fibrosis, cancer, type-2 diabetes, or neurodegenerative diseases such as Parkinson's or Alzheimer's disease. In addition, it has been linked to aging. Accumulated free radicals cause severe cellular damage through interaction with DNA, proteins, and lipids. Incomplete repair of such damage leads to the age-related deterioration (Scandalios, 2005; Schrader and Fahimi, 2006).

1.5.1 Reactive Oxygen Species

Molecular oxygen is relatively unreactive in its ground state (O_2). However, this molecule can cause the formation of highly reactive excited states like free radicals and derivatives (Scandalios, 2005).

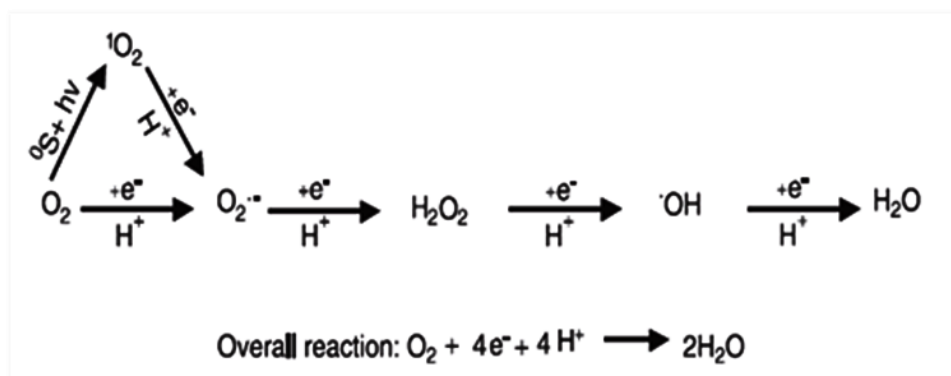


Figure 1.20 Generation of reactive oxygen species (Scandalios, 2005).

ROS are produced by partial reduction of molecular oxygen to water (Aguirre *et al.*, 2005). These include superoxide radical ($O_2^{\cdot-}$), hydrogen peroxide (H_2O_2), and hydroxyl radical ($\cdot OH$). Superoxide radical is formed through one-electron reduction of molecular oxygen ($O_2 + e^- \rightarrow O_2^{\cdot-}$). Hydrogen peroxide can also be generated by dismutation of $O_2^{\cdot-}$, which is catalyzed by superoxide dismutase via hydroperoxyl radical ($O_2^{\cdot-} + H^+ \rightarrow HO_2^{\cdot}$; $2HO_2^{\cdot} \rightarrow H_2O_2 + O_2$). Hydroxyl radical is probably the most highly reactive and toxic form of oxygen and it can be formed by the metal ion (e.g., iron or copper)-catalyzed decomposition of hydrogen peroxide ($H_2O_2 + O_2^{\cdot-} \rightarrow O_2 + OH^- + \cdot OH$) (Scandalios, 2005; Schrader and Fahimi, 2006).

Besides their harmful role, reactive oxygen species perform important functions during different cellular processes when tightly regulated (Scandalios, 2005). For example, hydrogen peroxide and superoxide radical act as intracellular signalling molecules by modulating the activity of transcription factors. Some of the other functions of ROS involve regulation of antioxidant gene expression, induction of apoptosis or necrosis, cell differentiation, antimicrobial activity, ion transport, pathogen-related gene activation and calcium ion (Ca^{2+}) mobilization (Belozerskaya and Gessler, 2006; Scandalios, 2005).

Consequently, the steady-state level of reactive oxygen species within the cells is significant (Scandalios, 2005). At low concentrations, they play critical roles in cellular processes; but their continuous production leads to uncontrollable cellular damage and finally cell death in virtually all aerobes.

1.5.2 Defense Mechanisms against ROS

All cells contain several enzymes and low-molecular weight compounds to keep ROS concentration at a level favorable for cell development (Belozerskaya and Gessler, 2006). Enzyme systems acting as antioxidants are represented by superoxide dismutase (SOD), catalase (CAT), and glutathione peroxidase (GPx). Non-enzymatic defense systems include thiol-containing compounds like glutathione and thioredoxin, carotenoids, ascorbic acid, vitamin E and flavonoids (Belozerskaya and Gessler, 2006; Valko *et al.*, 2007).

Enzymatic defences protect cells from free radicals by converting them to less reactive species. SOD catalyzes dismutation of superoxide radical to hydrogen peroxide which is substrate of catalase. GPx catalyzes destruction of H₂O₂ with concomitant conversion of reduced glutathione (GSH) to glutathione disulfide (Scandalios, 1995; Schrader and Fahimi, 2006).

Phenolic derivatives are one of the groups of antioxidants that have been studied by many research groups. The major structural characteristic responsible for antioxidative and free radical scavenging activity is the phenolic hydroxyl group. Phenols have the ability to donate the hydrogen atom of the phenolic hydroxyl group to the free radicals, therefore stopping the propagation chain during oxidation. The second hydroxyl group at the *ortho*-position (catechol ring) also reduces the O–H bond dissociation enthalpy and increases the rate of H-atom transfer to peroxy radicals. The presence of a third hydroxyl group increases the antioxidant capacity further (Torres de Pinedo *et al.*, 2006).

Flavonoids have antioxidant activity which is totally dependent on the presence of a catechol structure in the B-ring, an unsaturated 2,3 double bond in

conjugation with a 4-oxo function and a 3-hydroxyl group in the C ring (Figure 1.21). Among structurally homologous flavones and flavanones, peroxy and hydroxyl scavenging increase linearly according to the total number of hydroxyl groups (Heim *et al.*, 2006; Rice-Evans, 2001).

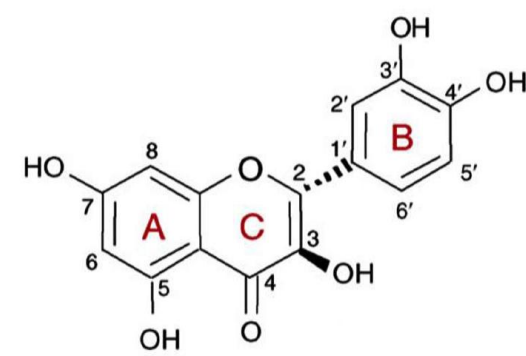


Figure 1.21 The structure of quercetin as strong antioxidant (Pourcel *et al.*, 2006).

Another structural feature that might increase the antioxidant capacity includes alkyl chain containing the primary hydroxyl group or phenolic ring and the presence of carboxylic or alcohol group in phenolic derivatives. This may cause stabilization of radical produced during oxidation, but its contribution to antioxidant capacity remains unclear (Torres de Pinedo *et al.*, 2006).

1.6 Thermophilic Fungi

The thermophilic fungi have a growth temperature minimum at or above 20°C and growth temperature maximum at or above 50°C, and the thermotolerant forms have a temperature range of growth from below 20 to ~55°C (Maheshwari

et al., 2000). They are highly resistant at elevated temperatures which are essential for degradation of lignin during composting (Tuomela *et al.*, 2000).

Thermophilic fungi have become an attractive target for many scientists due to the efficiency of thermostable enzymes in industrial applications (Ögel *et al.*, 2001).

1.6.1 *Scytalidium thermophilum*

Scytalidium thermophilum, also known as *Humicola grisea* var. *thermoidea*, *Humicola insolens*, and *Torula thermophila*, is an important thermophilic fungus in the production of mushroom compost (Straatsma *et al.*, 1994; Wiegant, 1992). *S. thermophilum* grows optimally at temperatures around 45 to 50°C and it is believed that this thermophilic fungus in mushroom compost significantly promotes the growth of edible mushroom *Agaricus bisporus*. This growth-inducing effect of *S. thermophilum* on mushroom mycelium can be described at three levels. Firstly, this thermophilic fungus leads to a reduction in ammonia concentration so that mushroom mycelium keeps growing. Secondly, it immobilizes nutrients in a form that they become available for mushroom mycelium. Lastly, it has a growth-promoting effect on mycelium which has also been revealed for a number of other thermophilic fungi (Wiegant *et al.*, 1992).

1.6.2 CATPO (Catalase-Phenol Oxidase) of *S. thermophilum*

S. thermophilum catalase-phenol oxidase (CATPO) was found to be a tetrameric, heme containing protein with a total molecular weight of 320 kDa. Catalase and phenol oxidase activities were stable at pH 7 and isoelectric point (pI) was reported to be 5 (Kocabas *et al.*, 2008; Ögel *et al.*, 2006).

This enzyme was purified by anion exchange chromatography followed by gel filtration. The pure CATPO was shown to be highly active on catechol (Kocabas *et al.*, 2008; Ögel *et al.*, 2006).

S. thermophilum CATPO is a bifunctional enzyme. Besides its major hydrogen peroxide degrading activity, it also catalyzes phenol oxidation. In order to see the structural basis of this dual functionality, purified enzyme was crystallised by hanging-drop vapour-diffusion method and diffraction data were collected at 2.8 Å (Kocabas *et al.*, 2009).

1.7 Scope of the Study

The primary aim of this study was to analyse the production and activity of CATPO from *Scytalidium thermophilum*, to solve its three dimensional structure, to establish a recombinant expression system, and to examine the mechanism of its phenol oxidase activity.

Towards this aim, a series of complementary studies were carried out. Biochemical studies involved the enhancement of CATPO production of *S. thermophilum* with potential inducers, the investigation of the production and biocatalytic activity in the presence of phenolic compounds, selected according to different chemistry and functionality, substrate specificity and inhibitor assays and the utilization of enzyme in bioorganic transformations with several organic compounds.

To determine the three dimensional structure, *S. thermophilum* CATPO was purified by two chromatography systems including anion exchange and gel filtration, crystallised by sitting-drop vapour diffusion method. X-ray diffraction data of good quality crystals were collected at Diamond Light Source (The United Kingdom). The crystal structure of *S. thermophilum* CATPO was determined using previous crystallographically determined *Penicillium vitale* catalase (PVC; PDB code: 2IUF) as a model.

For recombinant expression system, the synthetic codon optimised *Scytalidium catpo* gene was cloned into pET_{eca0} containing 6xHis, TEV site and Δ19aa. Then, this gene was expressed in *E. coli* BL21(DE3)star cells and optimisation of expression system was performed by playing with different parameters like

temperature, shaking rate, time of incubation, IPTG (Isopropyl β -D-1-thiogalactopyranoside) concentration and aeration volume.

To clarify the dual mechanism of *S. thermophilum* CATPO, two mutations including H101N for catalase activity inhibition and V142F for investigation of phenol oxidase activity were performed. Mutational variants were purified by Ni-affinity chromatography and characterised in terms of optical spectrum and kinetic behaviour. Crystals of variants were also obtained by sitting-drop vapour diffusion method.

CHAPTER 2

MATERIALS AND METHODS

2.1 Materials

2.1.1 Chemicals, Enzymes and Equipment

All chemicals, molecular size markers and enzymes used in this study were supplied from Sigma-Aldrich (Germany), AppliChem (Germany), Fluka (Switzerland), Merck (Germany), Invitrogen (UK), Amersham Bio-Sciences (USA), Interchim (France), Epicentre Biotechnologies (UK) and Fermentas (Lithuania). QIAprep Spin Miniprep Kit for plasmid DNA isolation and QIAquick PCR Purification Kit were from Qiagen (UK). Pre-Cast protein gels (Invitrogen, UK) were used for protein separation at neutral pH environment. Centrifugal concentrators (Amicon, USA; Microcon, USA and Microsep, USA) were used to concentrate proteins. Membranes (Millipore, USA and Minisart, Germany) were utilized for filter sterilization of buffers in purification and of other solutions. FPLC purification systems (GradiFrac and ÄKTAPrime) and its columns were purchased from GE Healthcare Bio-Sciences (Amersham, USA). Slide-A-Lyzer Dialysis Cassettes were used for dialysis of protein solution before purification was supplied from Pierce (USA). Temperature-controlled spectrophotometer used to measure enzyme activities was supplied from Shimadzu (UV 1700). Crystallisation equipments, chemicals and solutions were from Hampton research (USA).

2.1.2 Microorganisms

2.1.2.1 Fungal Strains

Scytalidium thermophilum (type culture *Humicola insolens*) was kindly provided by Dr. Mehmet BATUM from ORBA Inc.

2.1.2.2 Bacterial Strains

Escherichia coli XL-1 Blue and BL21(DE3)star cells were used for amplification of the plasmid carrying codon optimised *catpo* gene and for high-level heterologous expression, respectively.

2.1.3 Growth Media, Buffers and Solutions

The composition of the growth media, buffers, and solutions are given in Appendix A.

2.1.4 Plasmids and Molecular Size Markers

His tagged pET28a vector (Appendix B) including TEV cleavage site replacing the native thrombin site was a generous gift from Prof. R.E. Sockett and made by Dr. John Taylor, University of Nottingham.

Molecular size markers for DNA and protein are given in Appendix C.

2.2 Methods

2.2.1 Microbial Cultivations

Scytalidium thermophilum was inoculated onto YpSs agar plates as described in Appendix A (Cooney and Emerson, 1964) and incubated at 45°C for 4-5 days until complete sporulation. These agar plates can be stored at 20°C for maximum 2 months. Spores from these stock cultures were inoculated into 10 mL liquid preculture media, known as YpSs broth (Appendix A), containing glucose instead of starch as carbon source. After 24 hours of incubation at 45°C, the preculture was transferred into the main culture supplemented with copper sulfate. Preculture volume was 2 % of the main culture volume. Cultures were incubated in a shaker incubator at 45°C with 155 rpm shaking rate. On 5th day of their growth, cell biomass was separated from liquid medium containing protein of interest by filtration through a Whatmann No.1 filter paper and separated cell biomass was dried overnight at 60°C for growth curve measurements. The filtrate was centrifuged at 10,000 rpm for 10 min. The supernatant was either used as crude enzyme solution for assay experiments or exposed to ammonium sulfate fractionation, followed by dialysis overnight against 50 mM Tris-HCl, pH 8. The dialysed suspension was then filtered through 0.2 µm filters to remove any precipitate before purification.

Stock cultures of *Escherichia coli* XL-1 Blue were grown on LB Kanamycin agar plates (Appendix A) at 37°C and stored at 4°C up to 3 weeks. For the preparation of competent cells, *E. coli* XL-1 Blue was inoculated in 2.5 mL Luria-Bertani's (LB) medium (Appendix A) and incubated at 37°C and 200 rpm overnight. Then, 250 mL of LB medium supplemented with 20 mM MgSO₄ was inoculated with the entire 2.5 mL overnight culture of *E. coli* XL-1 Blue and incubated at 37°C until the absorbance at 600 nm reached 0.4-0.6.

A fresh single colony of *Escherichia coli* BL21(DE3)star was inoculated into 10 mL of LB medium in the presence of 50 µg/mL kanamycin and incubated overnight at 37°C with shaking (200 rpm). The culture was then transferred into

1 L fresh LB with antibiotics (50 µg/mL kanamycin) in 2.4 L conical flask and cultured at 37°C (200 rpm) until OD₆₀₀ is approximately equal to 0.6-0.8. 0.1 mM IPTG was added to induce the cells of *E. coli* BL21(DE3)star cells including recombinant plasmid and cells were grown at 30°C (120 rpm) for 24 hours. The cells were then harvested for 10 min at 6,000 rpm and the pellets were frozen at -80°C. 2 hours later, frozen cells were lysed using 100 mL lysis buffer (Appendix A). The lysed cells were then centrifuged for 30 min at 10,000 rpm. The supernatant (100 mL) was then used as crude enzyme solution and dialyzed overnight against 20 mM Phosphate buffer (pH 7.4), including 0.5 M NaCl. The dialysed periplasmic fraction was then filtered through 0.2 µm filters to remove any precipitate before purification.

2.2.2 Plasmid DNA Isolation

The plasmids were purified according to the instructions given in the QIAprep Spin Miniprep Kit (Qiagen).

E. coli XL1 Blue cells containing recombinant plasmid (pET-28a TEV) were incubated overnight in 5 mL LB broth with kanamycin at a concentration of 50 µg/mL. The cells were centrifuged at 8,000 rpm for 10 min and the supernatant was discarded. The bacterial pellet was resuspended in 250 µL of Buffer P1 (resuspension buffer) (Appendix A) and transferred into a microcentrifuge tube. Then, 250 µL of Buffer P2 (lysis buffer) (Appendix A) were added and mixed thoroughly by inverting the tube 4-6 times. After adding 350 µL of Buffer N3, the tube was mixed immediately by inverting the tube 4-6 times. The mixture was centrifuged at 13,000 rpm for 10 min in a table-top microcentrifuge. The supernatant was removed and passed through the QIAprep spin column by pipetting. The column including supernatant was then centrifuged for 30-60 s and the flow-through was discarded. The column was then washed with equilibration buffer by adding 750 µL of Buffer PE and centrifuged for 30-60 s. After centrifuging, the flow-through was discarded and the column was centrifuged again for an additional 1 min to remove residual wash buffer. To elute DNA, the QIAprep column was placed in a clean 1.5 mL microcentrifuge tube and 50 µL

of Buffer EB (elution buffer) (Appendix A) was added to the centre of each QIAprep spin column. Then, the column was kept for 1 min and then centrifuged for 1 min at 13,000 rpm.

2.2.3 Primer Design

E. coli codon optimised intronless *catpo* gene was synthesized by Genscript. For the amplification of this *catpo* gene from a pUC57 clone, the following two primers were designed:

NdeI20:

5'-GGAATTCCATATGACCTGCCCGTTCGCTGACCCG-3'

HindIIIend:

5'-CAAGCTTGGGTAAAGAGTCCAGAGCGAAACGGTC-3'

The oligonucleotide primers shown above were designed to amplify a product which removed the N-terminal 19 amino acids corresponding to the signal peptide.

2.2.4 Polymerase Chain Reaction

A 50 μ L reaction mixture contained:

- Sterile double distilled water to give a final volume of 50 μ L
- 5 μ L Reaction buffer (10X) or KOD buffer
- 2 μ L MgSO₄ (25 mM)
- 5 μ L dNTP mix (0.2 mM)
- 1.5 μ L Forward primer (5 μ M)
- 1.5 μ L Reverse primer (5 μ M)
- 1 μ L Plasmid DNA (5 ng/ μ L)
- 1 μ L Tag DNA polymerase or KOD Hot start DNA polymerase

Amplifications were performed according to the following cycle:

95°C	2 min	
<hr/>		
95°C	30 s	} X 30
52-72°C	30 s	
72°C	2.5 min	
<hr/>		
72°C	10 min	
4°C	18-20 h	

2.2.5 Visualization and Photography of Nucleic Acids

For visualization and analysis of plasmids and PCR products, 0.8 % (w/v) agarose gel (Appendix A) in 1X TAE Buffer (Appendix A) was used. The gel was melted and cooled to 50°C for 20 min. After the addition of DNA gel stain (Ethidium bromide) at a concentration of 1 µg/mL, the gel was poured into a mould and allowed to solidify. Then it was placed into the tank of horizontal electrophoresis apparatus and covered with 1X TAE buffer.

Samples were mixed with a loading dye 6:1 and gently loaded to the wells. Electrophoresis was carried out at 90 V for 40 min. Then, the gel was visualized on a UV transilluminator and photographed by a Gel Documentation System (BioRad).

2.2.6 Transformation of *E. coli* XL1 Blue

2.2.6.1 Preparation of Competent Cells

E. coli XL-1 Blue cells were cultivated as mentioned in section 2.2.1. After the optical density at 600 nm reached 0.4-0.6, cells were pelleted by centrifugation at

5,000 x g for 10 min and gently resuspended in 100 mL ice-cold TFB1 solution (Appendix A) and incubated on ice for 5 min. Then, cells were again pelleted by centrifugation at 5,000 x g for 5 min and supernatant was discarded. After cells were gently resuspended in 10 mL TFB2 (Appendix A), which contains glycerol, cells were incubated on ice for 60 min. Aliquots of 200 μ L were transferred to eppendorf tubes and flash-frozen in liquid nitrogen before storage at -80°C.

2.2.6.2 Transformation of Competent Cells

20 μ L of plasmid DNA was added to 100 μ L of competent cells and gently mixed by swirling the pipette tip and incubated on ice for 30 min. Cells were heat-shocked by incubating at 42°C for 1 min and cooled on ice for 2 min. Then, 1 mL LB medium supplemented with 20 mM MgSO₄ (Appendix A) was added and kept at 37°C plus shaking for 45 min. 100 μ L aliquots were finally spread on LB kanamycin agar plates (Appendix A) and incubated overnight at 37°C.

2.2.7 Restriction Enzyme Digestion

Restriction enzyme reaction was set up as follows:

- Sterile double distilled water to give a final volume of 60 μ L
- 10X NE Buffer to give a final concentration of 1X
- 45-47 μ L DNA obtained from plasmid isolation
- 2.5 μ L NdeI
- 2.5 μ L HindIII
- 0.6 μ L BSA (from stock 100X)

The reaction mixture was incubated at 37°C for minimum 2 hours to overnight.

2.2.8 Ligation

The PCR fragment was digested with appropriate restriction enzyme as explained in section 2.2.7. The plasmid was then dephosphorylated with alkaline phosphatase. The reaction mixture for the dephosphorylation of plasmid DNA was prepared as follows:

- Sterile double distilled water to give a final volume of 20 μL
- 10X Alkaline phosphatase buffer (2 μL) to give a final concentration of 1X
- 1 μL Alkaline phosphatase
- Solution of DNA (1 to 20 pmol)

The reaction mixture was incubated at 37°C for minimum 1-2 hours to overnight. Then, digested plasmid DNA was cleaned using QIAquick Spin Kit. According to the protocol, 5 volumes of Buffer PBI (Binding buffer) was added to 1 volume of the PCR reaction mixture and mixed gently. After placing a QIAquick column in a provided 2 mL collection tube, the sample was applied to column and centrifuged for 30-60 s. The flow-through was discarded and the QIAquick column was placed into the same tube. Then, 750 μL Buffer PE (wash buffer) was added to column and centrifuged again for 30-60 s. The flow-through was discarded once again and the QIAquick column was placed into the same tube. The column was then centrifuged in a 2 mL collection tube provided for 1 min and later each QIAquick column was placed in a clean 1.5 mL centrifuge tube. To elute DNA, 50 μL Buffer EB (10 mM Tris-Cl, pH 8.5) was added to the centre of the QIAquick membrane and centrifuged for 1 min.

Cleaned PCR product was then ligated into the vector (pET-28a TEV) which was also digested with same restriction endonucleases with the one used for digestion of PCR product according to the procedure explained in section 2.2.7. A 20 μL ligation mixture in a microfuge tube contained:

- Sterile double distilled water to give a final volume of 20 μL
- 1 μL Vector (pET-28a TEV)
- 13 μL Insert
- 2 μL T4 DNA Ligase
- 4 μL 5X T4 DNA Ligase Buffer

A control reaction was set up, including all the reagents listed above except the insert. The ligation mixture was incubated at 16°C overnight. The entire 20 µL ligation mixture was transformed to competent *E. coli* XL-1 Blue cells according to the transformation procedure explained in section 2.2.6.2. The transformed cultures were plated on LB agar containing kanamycin and plates were incubated at 37°C overnight.

Colony PCR method was used to quickly screen plasmid inserts directly from *E. coli* XL-1 Blue cells. The reaction mixture of 50 µL was set up as follows:

- 25 µL DNA
- 5 µL Buffer (10X)
- 5 µL dNTPs
- 2 µL MgSO₄
- 1.5 µL Forward primer
- 1.5 µL Reverse primer
- 1 µL Taq DNA polymerase
- Sterile double distilled water to give a final volume of 50 µL

95°C	2 min			
95°C	30 s			X 30
55°C	30 s			
72°C	2.5 min			
72°C	10 min			
4°C	18-20 h			

Positive colonies containing insert of interest were picked and then plasmid DNA was isolated from these colonies (section 2.2.2) and finally expressed in *E. coli* BL21(DE3)star cells (section 2.2.6.2).

2.2.9 Mutagenesis Studies

A modified Stratagene's QuikChange site-directed mutagenesis procedure using KOD Hot start DNA polymerase (Novagen) was used to introduce point mutations into the codon optimised synthetic *catpo* gene.

2.2.9.1 Primer Design for Mutagenesis

The oligonucleotide primers shown below were designed including desired mutations and ordered from Invitrogen. Primers were between 28 and 39 bases in length with a melting temperature (T_m) of 80°C or higher. The desired mutation was in the middle of primer with ~10-15 bases of correct sequence on both sides. Primers contained a minimum GC content of 40 % and terminated in GC bases.

For His101N replacements, the sequence CAC was changed to AAC and for Val142F replacements, the sequence GTT was changed to TTC.

Primer 1 (forward and reverse)

H101Nf: 5'-CGGAACGTGCTGTTAACGCTCGTGGTGC-3'

H101Nr: 5'-GCACCACGAGCGTTAACAGCACGTTCCG-3'

Primer 2 (forward and reverse)

V142Ff:

5'-CGTTCGTTTCTCTACCTTCGCTGGTTCTCGTGGTTCTGC-3'

V142Fr:

5'-GCAGAACCACGAGAACCAGCGAAGGTAGAGAAACGAACG-3'

2.2.9.2 Site-Directed Mutagenesis

QuickChange site-directed mutagenesis kit is used to make point mutations, switch amino acids, and delete or insert single or multiple amino acids. This method is performed using KOD Hot Start DNA Polymerase and a temperature cycler. The basic procedure utilizes a supercoiled double stranded DNA (dsDNA) vector with an insert of interest and two synthetic oligonucleotide primers containing the desired mutations (Figure 2.1).

The oligonucleotide primers, each complementary to opposite strands of the vector, were extended during temperature cycling by using KOD Hot Start DNA polymerase from Stratagene. Incorporation of the primers generated a mutated strand containing staggered nicks, resulting in a linear amplification of the template. The product was then treated with *DpnI*, an endonuclease specific for methylated and hemimethylated DNA. Since DNA isolated from almost all *E. coli* strains is methylated, *DpnI* treatment resulted in the digestion of the parental DNA, leaving only the mutation-containing newly synthesized DNA that was then transformed, into *E. coli* XL-1 Blue competent cells.

The reaction mixture was set up included:

- 5 μL of 10X reaction buffer
- 2 μL (10 ng) of plasmid DNA (5 ng/ μL)
- 1.25 μL of oligonucleotide forward primer (100 ng/ μL)
- 1.25 μL of oligonucleotide reverse primer (100 ng/ μL)
- 1 μL of dNTP mix (0.2 mM)
- 39.5 μL of sterile double distilled water to a final volume of 50 μL
- 1 μL of KOD Hot Start DNA polymerase (1 U/ μL)

Temperature cycling was carried out as follows:

95°C	2 min	
<hr/>		
95°C	30 s	} X 30
52-72°C	30 s	
72°C	7 min 30 s	
<hr/>		
72°C	10 min	
4°C	18-20 h	

The presence of linear amplification products was checked by electrophoresis of a 4 µL sample through a 0.8 % agarose gel (section 2.2.5).

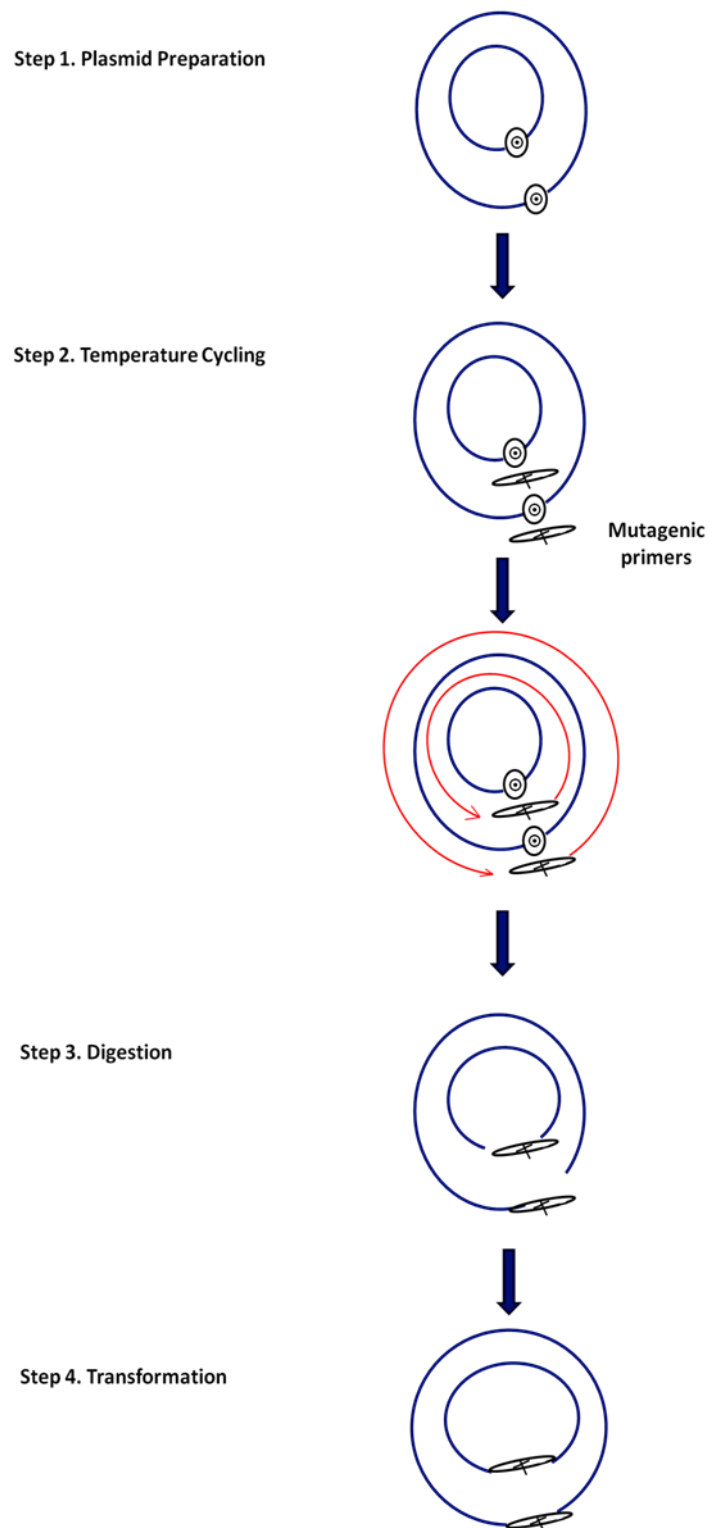


Figure 2.1 Overview of the QuickChange site-directed mutagenesis method (Stratagene).

Digestion of amplification products:

1 μL of *DpnI* restriction enzyme (10 U/ μL) was directly added to amplification reaction below the mineral oil overlay by using a small, pointed pipet tip. Then, reaction mixture was gently and thoroughly mixed by pipetting the solution up and down several times. Finally, reaction mixture was spun down in the microcentrifuge for 1 min and immediately incubated at 37°C for 1 h to digest the parental (*i.e.*, the nonmutated) supercoiled dsDNA.

2.2.10 Protein Characterisation

2.2.10.1 SDS-Polyacrylamide Gel Electrophoresis

The NuPAGE[®] System (Invitrogen) was used to separate proteins on the basis of their molecular size as described in Appendix D. The gel system consists of pre-cast Tris-HCl buffered (pH 6.4) polyacrylamide gels, with a separating gel that operates at pH 7. Samples were separated through gels containing 10 % acrylamide in the presence of either MES buffer (for 35 min at 200 V), or MOPS buffer (for 50 min at 200 V). The gels were stained according to the SimplyBlue SafeStain Microwave protocol (Appendix E). The low molecular weight-SDS Marker kit (Amersham Biosciences) was used as size standards (Appendix C).

2.2.10.2 Native-Polyacrylamide Gel Electrophoresis

Native-PAGE was carried out on precast NativePAGE Novex 4-16 % Bis-Tris gel (Invitrogen, UK) as described in Appendix F. This gel system operates at pH 7.5 during electrophoresis providing better band resolution. The NativeMark[™] Unstained Protein Standard (Invitrogen, UK) was used for molecular weight estimation of proteins and composed of 8 standard proteins in a range of 20-1200 kDa, including IgM hexamer (1236 kDa), IgM pentamer (1048 kDa), apoferritin band 1 (720 kDa), apoferritin band 2 (480 kDa), B-phycoerythrin (242 kDa),

lactate dehydrogenase (146 kDa), BSA (66 kDa), soybean trypsin inhibitor (20 kDa).

2.2.10.3 UV-Visible Spectral Studies

All studies including spectroscopic measurements were performed on 2401 PC UV/Vis spectrophotometer (Shimadzu) at room temperature. Absorption spectra of purified wild type and mutant variants were recorded in 1 cm quartz cuvette between 200-900 nm.

2.2.10.4 Protein Concentration Determination

2.2.10.4.1 Absorbance of CATPO at 280 nm

The protein concentration was routinely determined from the absorbance at 280 nm. The readings were taken at room temperature in a 1 mL quartz cuvette using the 2401 PC UV/Vis spectrophotometer (Shimadzu). The concentration was deduced from the absorbance value using the Beer-Lambert law (Equation 2.1):

$$A = \epsilon cl \quad (2.1)$$

Where ϵ is the molar extinction coefficient ($M^{-1} cm^{-1}$), A is the absorbance of the peak or shoulder, c is the concentration ($mol L^{-1}$), l is the path length (cm). The extinction coefficient of CATPO at 280 nm was determined as $80455 M^{-1} cm^{-1}$ and its molecular mass was 78624.7 Da (both estimated from Expasy). Therefore, the conversion factor can be calculated by dividing molecular mass to extinction coefficient, 0.977. The A_{280} value was multiplied by this conversion factor of 0.977 to obtain CATPO concentration in mg/mL.

2.2.10.4.2 Total Protein Concentration Determination

Total protein concentration was determined according to the Bio-Rad Protein Assay (Bio-Rad) based on the method of Bradford (Bradford, 1976). This method is based on dye-binding assay in which a differential shift of absorbance of the Coomassie Brilliant Blue G-250 dye (from 465 nm to 595 nm) occurs in response to protein concentration. BSA (Bovine serum albumin) is used as standard in this assay.

1000 μL of the Bio-Rad Dye reagent was added to 20 μL of BSA solutions (2.4 to 20 $\mu\text{g}/\text{mL}$) and protein solutions. After incubation for 5-10 min at room temperature, the absorbance at 595 nm was measured for all samples. The standard curve was plotted (Appendix G) and protein concentration was determined using this standard plot.

2.2.10.5 Enzyme Assays

Catalase and phenol oxidase assays were determined spectrophotometrically. Catalase activity was measured using a method described by Beers and Sizer (1952) where the disappearance of hydrogen peroxide was followed at 240 nm. The assay mixture was composed of 10 mM Hydrogen peroxide solution, 100 mM Sodium Phosphate Buffer (pH 7), and suitably diluted enzyme in a total volume of 2 mL. Before addition of enzyme, substrate solution was incubated in the spectrophotometer for 4-5 min to achieve temperature equilibration. Enzyme activity was determined using the initial rate of the reaction and the extinction coefficient for H_2O_2 was taken as $39.4 \text{ M}^{-1} \text{ cm}^{-1}$ (Merle *et al.*, 2007). One enzyme unit was defined as the amount of enzyme that catalyzes the decomposition of 1 μmol H_2O_2 per minute and was calculated by the following formula (Equation 2.2):

$$\text{U/mL} = (\Delta\text{OD}/\Delta t) \times (1/\epsilon) \times (1000) \times (V_s^*/V_s) \times (\text{DF}) \quad (2.2)$$

Where ΔOD is the change in optical density, Δt is the change in time (min), ϵ is the molar extinction coefficient ($M^{-1}cm^{-1}$), V_s^* is total volume of solution in cuvette (mL), V_s is the total volume of supernatant in cuvette (mL), and DF is the dilution factor if dilution is possible. The coefficient 1000 in the formula is used to adjust the extinction coefficient from $1/(\text{mole } L^{-1})$ to $1/(\mu\text{mole } mL^{-1})$.

Phenol oxidase activity was measured by following the increase in absorbance at 420 nm. The substrate solution (100 mM catechol in 100 mM sodium phosphate buffer, pH 7) was prepared freshly just before use, due to rapid autooxidation of catechol with molecular oxygen in air. Both buffer and enzyme solutions were preincubated for 5 min at 60°C in waterbath. Phenol oxidase activity measurements were performed using both enzyme blank (no substrate, only supernatant) and substrate blank (buffer and catechol, no culture supernatant) to obtain more accurate results. The reaction mixture consists of 0.5 mL 100 mM catechol solution in 100 mM phosphate buffer (pH 7) as substrate, 0.5 mL enzyme solution at different dilution rates and 1 mL 100 mM phosphate buffer at pH 7. Enzyme activity was determined using the initial rate of the reaction and the extinction coefficient as $3450 M^{-1}cm^{-1}$ for catechol (Ögel *et al.*, 2006) and one enzyme unit was defined as the amount of enzyme required for the formation of one nanomole of product per min and was calculated using the same formula described above.

All reactions were carried out using 1 mL disposable plastic cuvettes. A minimum of three measurements was recorded for each sample.

2.2.11 Statistical Analysis

One-way analysis of variance (ANOVA) was used to test the effect of phenolic compounds on fungal growth and CATPO production. All statistical analyses were performed with MINTAB 15. Confidence level was established as 95 %.

2.2.12 Biotransformation of CATPO

Biotransformation products of various organic compounds were investigated by setting up reactions in either DMSO or ethanol. Each substrate was utilised at 10 mg/mL concentration and reaction temperature was adjusted to 60°C.

2.2.12.1 Thin Layer Chromatography

Thin layer chromatography was performed to screen product formation at every 24 hours. Samples were spotted onto TLC silica plates purchased from Sigma-Aldrich at suitable size by capillary tubes. Seven different mobile phases were selected according to their polarity. The running solvents according to the type of substrate are given in Appendix H. The plates were developed at room temperature in a vertical separating chamber. The spots were detected under short UV light. When product formation was detected, the reaction was stopped by addition of solvent. Then, the product was extracted into organic phase (ethyl acetate) and immediately analyzed by high performance liquid chromatography (HPLC) or gas chromatography (GC).

2.2.12.2 High Performance Liquid Chromatography Analysis

The conversion of hydrobenzoin to benzil was studied by HPLC from Thermo separation with P2000 vacuum pump and UV1000 detector. Chromquest was the controller program for retention time, peak width, and peak area. Detection was performed at 254 nm. OD chiral column was used to analyse all fractions and the solvent system consisted of 10 % of isopropanol and 90 % of hexane at HPLC grade.

2.2.12.3 Gas Chromatography Analysis

Resveratrol biocatalysis product was analyzed by GC, Thermo Separation Product. Samples were injected into autosampler from which the samples were then passed through 50 m capillary column in the oven at 250°C.

HPLC and GC analyses were carried out by Olcay Mert in the Department of Chemistry, BIOCAT lab of Prof. Dr. Ayhan Sıtkı Demir.

2.2.13 CATPO Purification

2.2.13.1 Native CATPO Purification

Separation of *S. thermophilum* CATPO from other proteins in culture supernatant was achieved by a two-step procedure including anion exchange and gel filtration chromatography. Q Sepharose High Performance (Amersham Biosciences, USA) is a strong ion exchanger, based on rigid, highly cross-linked, beaded agarose structure. The bound exchanger is $-N^+(CH_3)_3$ which has a maximum binding capacity of 70 mg/mL. The medium was packed into a XK 16/20 column (Amersham Biosciences), which was connected to an ÄKTA PRIME (Amersham-Pharmacia). All subsequent steps were conducted at a flow rate of 1 mL/min and all solutions were filtered through a 0.45 µm filter before use. The column media was washed with 10 volumes of buffer A (50 mM Tris-HCl, pH 8), and then charged with 10 volumes of buffer B (1 M NaCl in 50 mM Tris-HCl, pH 8), and then equilibrated with 10 volumes of buffer A.

Crude CATPO was prepared by centrifugation of culture at 10,000 rpm for 10 min, followed by ammonium sulfate fractionation (50 % and 80 %) (Appendix H) and dialysed overnight against 50 mM Tris-HCl, pH 8.0. After filtering supernatant through 0.20 µm filter, sample was loaded onto column. The bound CATPO was then washed with 10 volumes of same buffer. A gradient of increasing salt concentration was used to elude the protein (from 0 % to 100 % of

buffer B), which was collected in 3 mL fractions. The presence of CATPO was checked by running a SDS-PAGE gel. The fractions containing CATPO were pooled and dialyzed overnight against 50 mM Tris-HCl, pH 8. The dialyate was then concentrated to 2 mL for the subsequent purification.

Gel filtration chromatography was performed using a prepacked HiPrep 26/60 Sephacryl S-200 high resolution column (Amersham Biosciences, USA). Column was equilibrated with 50 mM Tris-HCl, pH 8 and operated at a flow rate of 1 mL/min by collecting 1 mL fractions in 150 mL elution volume. Similar to anion exchange, the presence of CATPO was checked by running SDS-PAGE gel. The purest fractions including CATPO were pooled together and then transferred to Microsep 10K tubes (USA) and centrifuged at 13,000 rpm until a concentration between 6 and 9 mg/mL was reached. The concentration was determined from either the absorbance at 280 nm or Bradford assay (section 2.2.10.4).

The concentrated protein was either used immediately for crystallisation trials, or stored at 4°C for subsequent spectrophotometric and kinetic characterisation.

2.2.13.2 Recombinant CATPO Purification

Recombinant wild-type and variants were purified by affinity chromatography using HiTrap Chelating HP (1 mL) column (GE Healthcare, USA). This column, when charged with Ni²⁺ ions, selectively retains proteins if complex-forming amino acid residues, in particular histidine, are exposed on the surface of protein. Histidine-tagged proteins can be eluted from HiTrap Chelating HP with buffers including imidazole.

After connecting the column to GradiFrac (GE Healthcare, USA), it was washed with distilled water 2 or 3 times. Column was then charged with 10 volumes of 0.1 M NiSO₄ and washed with water to remove excessive metal. Later, it was equilibrated with 10 volumes of binding buffer (20 mM NaPhosphate, 0.5 M NaCl, 20 mM Imidazole, pH 7.4). The periplasmic fraction was loaded onto column at a flow rate of 1 mL/min. The bound His-tagged recombinant CATPO

was washed with binding buffer including 100 mM Imidazole, pH 7.4. A gradient of increasing imidazole concentration was used to elute protein (from 20 % to 100 % elution buffer, 20 mM NaPhosphate, 0.5 M NaCl, 0.5 M Imidazole, pH 7.4), which was collected in 1 mL fractions. Each fraction was tested for protein purity by running SDS-PAGE gel. All buffers and liquids used in purification were filtered through 0.45 µm filter, and flow rate was 1 mL/min.

Fractions containing purest protein were pooled together and dialyzed overnight first against 20 mM NaPhosphate, 0.5 M NaCl, pH 7.4 to remove imidazole and second against 20 mM NaPhosphate, pH 7.4 to remove remaining salt from protein solution. The soluble protein was then transferred to Microsep 10K tubes (USA) and centrifuged at 13,000 rpm until a concentration between 6 and 12 mg/mL was reached. The concentration was determined from either the absorbance at 280 nm or Bradford assay (section 2.2.10.4).

The concentrated protein was either used immediately for crystallisation trials, or stored at 4°C for subsequent spectrophotometric characterisation studies.

2.2.14 CATPO Crystallisation

CATPO was crystallised in a slow, controlled precipitation procedure from aqueous solution under conditions that did not denature protein. Several steps were involved during crystallisation and each step was optimized to give high quality CATPO crystal.

2.2.14.1 Initial Screening Trials

Screening tests were performed to find ‘hits’ or ‘leads’ that point to conditions that may be conducive to crystallisation. For this purpose, CATPO was exposed to a variety of agents.

96 well crystallisation plates (Greiner) and 8 different screening kits (Hampton Research, USA), including different buffers, salts and precipitants, were used. The crystal screen solution of 60 μL was pipetted manually into each well. Purified enzyme of 0.5 μL was mixed with 0.5 μL of the well solution by a liquid handling robot Oryx4 (Douglas Instruments, USA). Plates were incubated at 18°C for any crystal growth.

Drops were checked under light microscope and possible crystals were tested for being salt crystal or not by coomassie staining. About 1 μL of coomassie dye was added to the drop and incubated for couple hours. Protein crystals would become dark blue after staining, whereas salt crystals would remain their colour.

2.2.14.2 Crystal Optimisation and Cryocooling

Initial screening helps to determine the conditions of crystal growth only roughly. Therefore, new crystallisation trays were set up to get bigger and good quality crystals around the conditions observed from these initial trials.

Finding the exact conditions to produce good crystals requires optimisation studies by changing various parameters affecting crystal growth. These parameters include protein concentration, buffer type, pH, precipitant type and concentration, additive type and concentration.

The sitting drop was used for generating crystals (Figure 2.2). Classically, 2-4 μL of protein sample (between 3 and 9 mg/mL) was gently mixed with the same volume of mother liquor in a microbridge insert (Crystal Microsystems). The microbridges were placed in Linbro tissue culture plates (24 well) containing 1 mL of mother liquor per well and sealed with adhesive cover slip.

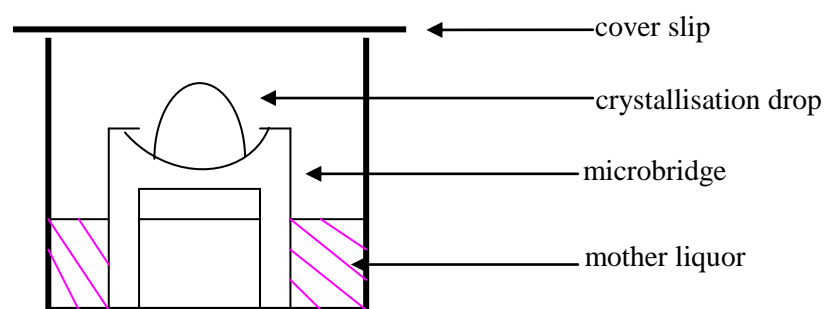


Figure 2.2 Schematic representation of sitting drop vapour diffusion method.

Distilled water, all buffers and solutions used for setting up trays were filtered through 0.2 μm filters. The trays were stored at 18°C and checked everyday for the presence of crystals.

Most macromolecular crystals held at room temperature during data collection lose their order after only a few seconds in an unattenuated third generation synchrotron source X-ray beam. For a crystal held at 100K (-173°C), a much longer total X-ray exposure can be tolerated without severely affecting the diffraction quality, so usually one or more complete data sets can be collected from a single crystal. Since cryocooling can reduce the damaging effects of radiation, many crystallographers collect their data at 100K (-173°C) (Garman and Owen, 2006).

The basic principle of cryocooling is based on the prevention of crystalline ice formation within the sample during cooling. This can be achieved by replacing water with a suitable cryoprotectant. Various cryoprotectant solutions like MPD (2-methyl-2,4-pentandiol), glycerol, ethylene glycol, and different PEGs (polyethylene glycols) were used here to prevent any abrupt variations of the crystal environment that might damage it during cooling. Cryoprotectants were added to drop either directly or indirectly in diffusion controlled system. The second method is a much longer process, but reduces the damage greatly in crystal structure.

Stable crystals were then picked up in an appropriately sized nylon loop (Hampton research) and then plunged into liquid nitrogen.

2.2.14.3 X-Ray Data Collection and Processing

The diffraction data used to solve the three dimensional structures of CATPO variants were collected at Diamond Light Source (Oxford, UK). The stability of crystals in cryoprotectant solvents was tested for their X-ray diffraction quality in University of Leeds (UK) by single exposures of the crystal to the X-ray source under a nitrogen stream at 100K (-173°C), before being taken to Diamond Light Source. Good quality frozen crystals were stored under liquid nitrogen for data collection at Diamond.

Collected data was processed using software from the CCP4 suite of programs (Collaborative Computational Project, 1994), MOSFLM, and SCALA. MOSFLM program uses a set of diffraction images to generate a set of indices (*hkl*s) with their associated intensities (and estimates of their uncertainties), together with an accurate estimate of the crystal unit-cell parameters. The process can be conveniently divided into three stages. The first (autoindexing) determines the unit-cell parameters and the orientation of the crystal. The second step is to refine the initial estimate of the unit-cell parameters and also the crystal mosaicity using a procedure known as post-refinement. The third step is to integrate the images, which consists of predicting the positions of the Bragg reflections on each image and obtaining an estimate of the intensity of each reflection and its uncertainty (Leslie, 2006). MOSFLM generates mtz file, format used for storage of reflection data.

SCALA reads a sorted mtz file and measures the quality of data and achievement of collection strategy. The various factors affecting measured intensity include crystal deterioration, variations in incident beam volume or intensity, timing/rotation errors, poor shutter synchronisation. This program calculates R_{merge} (measure of internal consistency), completeness, multiplicity, scale and B-factor (function of time) to measure any radiation damage (Evans, 2005).

TRUNCATE calculates the structure factor amplitudes from merged intensities. This requires knowledge of the average relationship between resolution and measured intensity.

2.2.14.4 Structure Refinement and Model Building

The crystal structure of CATPO was determined using the structure of *P. vitale* catalase, available in protein data bank (2IUJ), as a model to obtain phases. With this phase information it was possible to calculate an electron density map by Fourier transform of calculated and measured structure factors. Calculation of Fo-Fc and 2Fo-Fc electron density, visualised using the program *COOT* (Emsley and Cowtan, 2004), facilitated empirical assessment of how closely the model fitted the observed data. The program *REFMAC5* was used to carry out rigid body and restrained refinement of the models against the data. The dictionary stores information about monomers which represent the constitutive building blocks of biological macromolecules (amino acids, nucleic acids and saccharides) and about numerous organic/inorganic compounds commonly found in macromolecular crystallography. It also describes the modifications the building blocks undergo as a result of chemical reactions and the links required for polymer formation (Vagin *et al.*, 2004).

CHAPTER 3

RESULTS AND DISCUSSION

Scytalidium thermophilum is a thermophilic fungus that survives mainly in compost environment. It is also known as an inducer of *Agaricus bisporus* (edible mushroom) growth and mushroom production (Straatsma *et al.*, 1994). *S. thermophilum* produces large amounts of melanin (Lyons and Sharma, 1998) that requires the activity of phenol oxidases. In our laboratory, the phenol oxidases of *S. thermophilum* were, therefore, of interest.

An extracellular phenol oxidase of *S. thermophilum* was thereby discovered and named as STEP (*S. thermophilum* phenol oxidase) (Ögel *et al.*, 2006). For that reason, in the early stages of this study, enzyme activity measurements were performed using catechol as the substrate for phenol oxidase activity. Two years later, this enzyme was found to be a catalase having additional oxidase activity after a series of purification and sequencing experiments (Kocabas *et al.*, 2008). This bifunctional enzyme was then called as catalase-phenol oxidase (CATPO). As a result of that observation, later activity tests were carried out using both catechol and hydrogen peroxide as substrates.

3.1 Characterisation of CATPO in Crude Extracts

Characterisation studies included the optimisation of assay temperature for catalase and phenol oxidase activities and substrate specificity and inhibitor assay of phenol oxidase enzyme as well. According to the optimisation of assay conditions studied by Mete (2003), Kaptan (2004) and Sutay (2007), characterisation experiments were carried out at pH 7.

3.1.1 Optimisation of Assay Temperature

Phenol oxidase activity of CATPO was determined at different temperatures varying from 45 to 65°C. The optimum temperature was found to be 60°C for *S. thermophilum* phenol oxidase as illustrated in Figure 3.1. Relative activity was over 80 % at 65°C, but below 55 % at 45°C. This shows that phenol oxidase activity was sensitive to temperatures below 60°C.

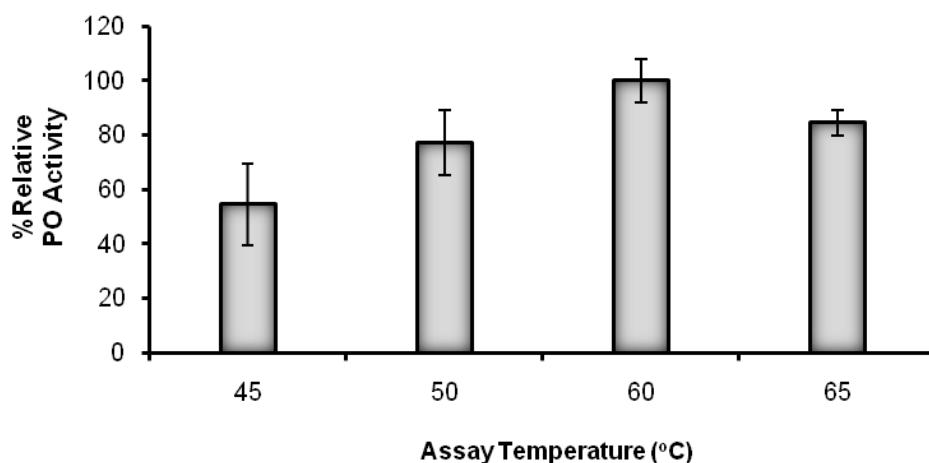


Figure 3.1 Effect of temperature on CATPO-phenol oxidase activity of *S. thermophilum*.

For the catalase activity of CATPO, an interval of 25-70°C was analysed for the determination of optimum catalase assay temperature.

Relative activities were over 60 % between 25-70°C (Figure 3.2). The optimum temperature for catalase activity tests was 60°C, similar to phenol oxidase activity. However, catalase activity did not appear to be as sensitive to temperature as the phenol oxidase activity.

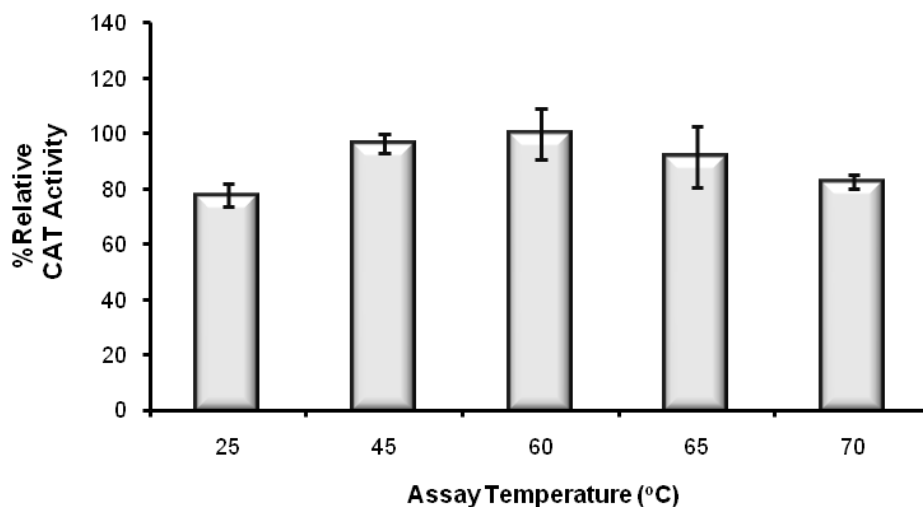


Figure 3.2 Effect of temperature on CATPO-catalase activity of *S. thermophilum*.

3.1.2 Oxidation of Phenolic Compounds by CATPO

In this study, a number of different substrates such as catechol, *p*-hydroquinone, ABTS, guaiacol, L-dopa, tyrosine, caffeic acid, gallic acid and tannic acid were used to analyze the catalytic properties of CATPO-phenol oxidase activity. Comparison of relative activities was also made with *Trametes versicolor* laccase (Sigma). According to the results shown in Table 3.1, higher activities were observed with catechol, L-dopa, and caffeic acid, but tyrosine hydroxylation was not detected. This result exhibited the lack of cresolase activity. CATPO oxidised neither ABTS nor guaiacol, which are known as laccase-specific substrates (Burton, 2003). There was low catalytic activity observed on the *p*-diphenolic compound, hydroquinone. These findings demonstrated that the phenol oxidation nature of CATPO resembled catechol oxidases.

The results were consistent with the previous study reported by Sutay (2007). The author stated that purified CATPO exhibited catechol oxidase activity but no laccase-like activity. Additionally, there was low relative activity of the pure

enzyme on *p*-hydroquinone which is supported by HPLC analysis (Avci, unpublished). Oxidation of *p*-hydroquinone is observed mainly by laccases, rather than catechol oxidases (Table 3.1).

3.1.3 Effect of Inhibitors on Phenol Oxidation by CATPO

The effect of various phenol oxidase inhibitors on the phenol oxidation activity of CATPO was analysed with catechol as the substrate. Inhibitors were chosen according to the information in the literature (Rescigno *et al.* 2002; Walker and McCallion 1980). As presented in Table 3.2, in the presence of salicylhydroxamic (SHAM) and *p*-coumaric acid, typical catechol oxidase and tyrosinase inhibitors (Lim *et al.* 1999; Rescigno *et al.* 2002), CATPO activity was shown to be inhibited. However, it is noted that *p*-coumaric acid did not completely inhibited the phenol oxidase activity. This compound is commercially used to prevent enzymatic browning (Walker, 1995; Walker and Ferrar, 1998).

SHAM is known by its ability to scavenge iron and copper of enzymes (Lim *et al.* 1999; Rescigno *et al.* 2002); therefore it was not surprising to see an inhibition with this metal-chelating compound due to the presence of heme *d* prosthetic group in the active site of CATPO.

p-Coumaric acid (4-hydroxycinnamic acid) has been reported as a competitive inhibitor for phenol oxidases (Lim *et al.*, 1999; Mayer and Harel, 1979). Due to having an electron-withdrawing group, –COOH, it tends to behave as an inhibitor rather than a substrate for phenol oxidases (Rescigno *et al.*, 2002).

The phenol oxidase activity of CATPO activity was found to be enhanced both by the non-ionic detergent cetyltrimethylammonium bromide (CTAB), known as an inhibitor of laccase, and polyvinylpyrrolidone (PVP), and known as an inhibitor of *o*-diphenol oxidase (Walker and McCallion 1980).

PVP has been documented to make complex with phenols in an attempt to prevent their oxidation by phenol oxidases (Walter and Purcell, 1980). On the

other hand, the low-amounts of PVP were indicated to enhance oxidase activity (Ceni *et al.*, 2008). Due to the complex nature of culture media including gallic acid, addition of PVP at low concentrations might avoid loss of enzymatic activity through binding to the compounds in liquid medium.

Carbon monoxide, reported as inhibitor of tyrosinase, was shown not to inhibit the phenol oxidase activity. This result was not surprising since CATPO was shown not to have monophenolase activity.

Table 3.1 Phenol oxidation by CATPO and comparison with *T. versicolor* laccase

Substrate	<u>CATPO-PO</u> % Relative Activity	<u>T.versicolor laccase</u> % Relative Activity
100 mM Catechol	100	7.4
L-DOPA	36.7	Nd
L-DOPA + 0.01% SDS	7.5	Nd
L-Tyrosine	Nsa	Nd
L-Tyrosine + 0.02% SDS	Nsa	Nd
<i>p</i> -Hydroquinone	26	92
ABTS *	Nsa	3858
ABTS **	Nsa	35056
Guaiacol*	Nsa	258
Guaiacol**	Nsa	21597
Caffeic acid	27.5	Nd
Gallic acid	70.8	Nd
Tannic acid	24	Nd
ABTS + CTAB**	Nd	1744

* *In phosphate buffer*, ** *In acetate buffer*, Nsa; *No significant activity*, Nd; *Not determined*

Table 3.2 Effect of inhibitors on CATPO activity

Substrate + Inhibitor	% Relative Activity
Catechol (no inhibitor)	100
+ 25 mM SHAM	40.1
+ 50 mM SHAM	30.7
+ 25 mM CTAB	117.8
+ 50 mM CTAB	123.2
+ 20 mM PVP	99
+ 30 mM PVP	113.1
+ 30 mM <i>p</i> -coumaric acid	68.5
+ 40 mM <i>p</i> -coumaric acid	63.3
+ 50 mM <i>p</i> -coumaric acid	58.8

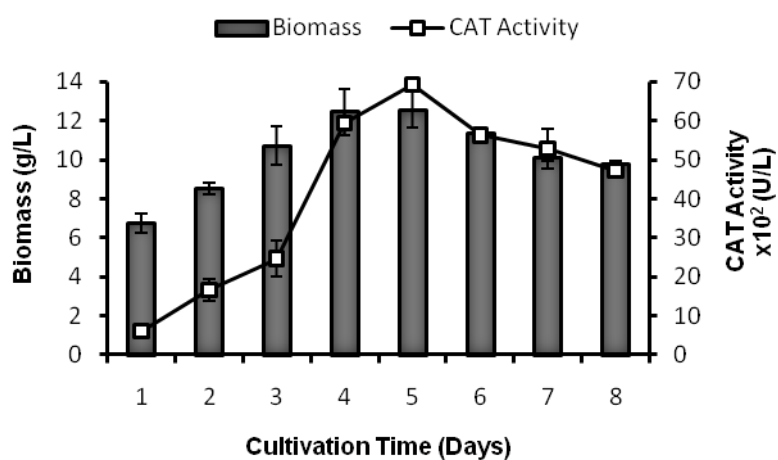
3.2 Production of CATPO

Production studies involved the analysis of the effect of factors like induction time, growth temperature, exogenous iron and hydrogen peroxide addition on the growth of *Scytalidium thermophilum*, and CATPO production. Previous studies on the optimisation of enzyme activity has shown an optimum assay temperature for both catalase and phenol oxidase enzyme as 60°C. Accordingly, throughout the production experiments, 60°C assay temperature was used.

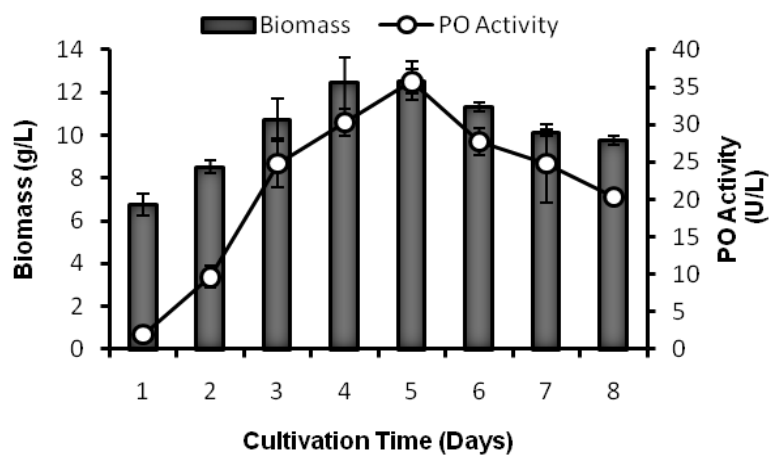
3.2.1 Time Course of CATPO Production

Scytalidium thermophilum extracellular CATPO production and fungal biomass generation, over 8 days of cultivation on 4 % glucose-containing modified YpSs medium (Appendix A), in batch culture, is presented in Figure 3.3a & b. The best glucose concentration for enzyme production was determined by Kaptan (2004).

The exponential phase lasted up to day four, followed by stationary phase until day six. Maximum enzyme production was observable at day 5, whereas no significant difference was detected between day 4 & 5. CATPO production was constitutive and simultaneous to microbial growth, indicating growth-associated production of the enzyme, rather than being a secondary metabolite.



(a)



(b)

Figure 3.3 (a) Time course of *S. thermophilum* growth and catalase production; (b) Time course of *S. thermophilum* growth and phenol oxidase production on glucose as the carbon source and cultivation at 45°C and 155 rpm.

3.2.2 Effect of Growth Temperature on CATPO Production

S. thermophilum was grown at different temperatures varying from 30 to 55°C. The culture supernatant was used in enzyme activity measurements.

As shown in Figure 3.4, the optimum growth temperature for CATPO production, based on catalase activity, was 45°C.

The temperature profile of *S. thermophilum* catalase activity can be regarded as reasonably high within the range determined by other fungal catalases. Except *Thermoascus auranticus* having optimum growth temperature of 43°C (Wang *et al.*, 1998), most catalase producing fungi grow optimally between 25 and 30°C (Isobe *et al.*, 2006).

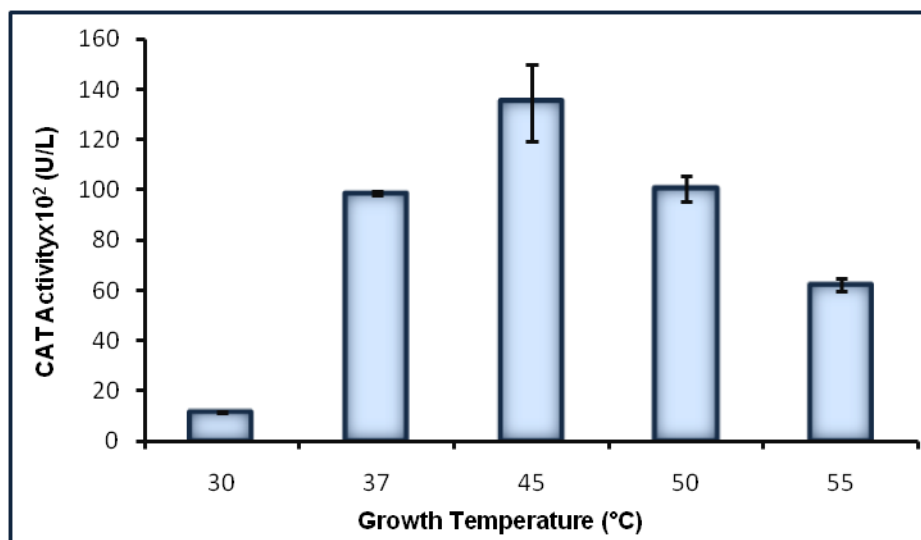


Figure 3.4 Effect of growth temperature on catalase production of *S. thermophilum*.

3.2.3 Effect of Iron on CATPO Production

Catalases are heme-containing enzymes. Adding iron into the growth medium may enhance CATPO activity by overcoming iron limitations, if any.

Effect of adding FeSO₄ on catalase activity in culture supernatants was analysed at 0.001-0.015 % (w/v). As shown in Figure 3.5, the highest catalase activity was observed at 0.004 % FeSO₄ concentration. Using higher amounts of FeSO₄ up to 0.015 % enhanced catalase activity during the exponential growth phase of *S. thermophilum*. However, the observed difference was not significant as compared to the control. This suggests that a significant iron limitation of activity does not exist, or the iron limitation of activity is irrespective of medium iron concentration.

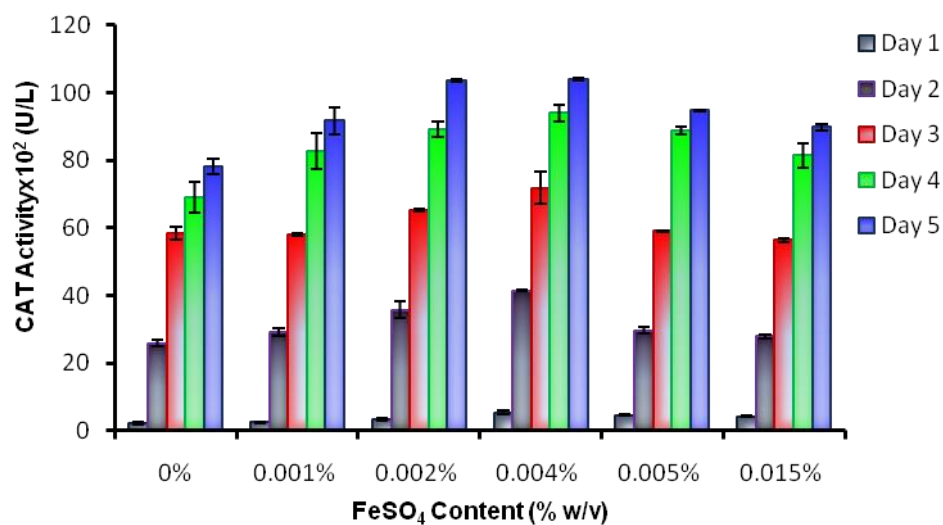


Figure 3.5 Effect of adding FeSO₄ into growth medium on catalase activity in culture supernatants of *S. thermophilum*.

3.2.4 Effect of Hydrogen Peroxide on CATPO Production

Catalase production is induced either by H₂O₂ addition or during the stationary phase of microorganisms (Mulvey *et al.*, 1990). Monofunctional catalase synthesis is promoted when cells enter stationary phase and unaffected by hydrogen peroxide. On the other hand, catalase-peroxidase synthesis increases in response to oxidative stress. In order to study the effect of hydrogen peroxide for its ability to enhance *S. thermophilum* catalase production, hydrogen peroxide was added to the growth medium in a concentration range of 0.1-2 mM.

Figure 3.6 indicates that the highest catalase activity was observed at 0.1 mM. However, this effect was not significantly high with respect to the control, without hydrogen peroxide.

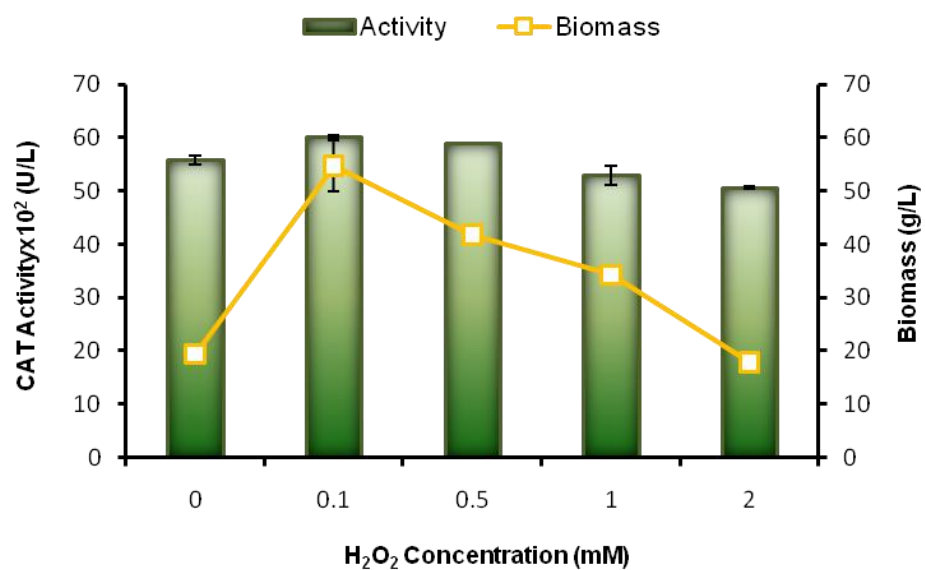


Figure 3.6 Effect of adding hydrogen peroxide into the growth medium of *S. thermophilum* on catalase production and biomass generation.

3.2.5 Effect of Functional Phenolics on CATPO Production

Effect of functional phenolics on *S. thermophilum* CATPO production was performed using 15 phenolic compounds selected according to their different chemistry and functionality. The molecular formula of compounds is given in Table 3.3. All experiments were performed at 5th day of cultivation.

All the phenolic compounds tested here are plant derived antioxidants even though these antioxidants may turn out to be pro-oxidants leading to oxidative stress, thus, becoming the cause of ROS generation in some cases (Heim *et al.* 2002).

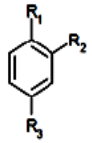
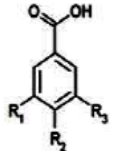
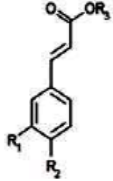
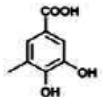
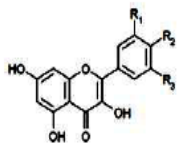
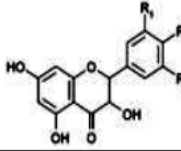
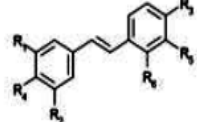
The pro-oxidant activity is thought to be directly proportional to the total number of hydroxyl groups. In a study reported by Won Lee and Joo Lee (2006), gallic acid containing multiple hydroxyl groups, particularly in their B-rings, was found to increase the production of free radicals.

The oxidized forms of phenolics, such as the semiquinone radical or benzoquinone, can also be documented as a source of ROS. They were shown to undergo reduction by nicotinamide adenine dinucleotide (NADH) nonenzymatically, resulting in the formation of a redox cycle to produce abundant ROS (Oikawa *et al.*, 2003).

Several studies have reported that these phenolic compounds of plant origin have antimicrobial and antiviral activity besides their antioxidant potential. The *o*-quinones, the products of phenol oxidation, have been shown to possess antimicrobial activity (Lule and Xia, 2005). Hydroxycinnamates exhibit a considerable antimicrobial effect under appropriate conditions. Gallic, *p*-hydroxybenzoic acid and related phenolics have been found to retard or partially inhibit the growth and toxin production of *Clostridium botulinum* (Pierson and Reddy, 1982). Conversely, some phenolic acids like caffeic, gallic acid and flavon-3-ols (kaempferol and quercetin) were observed to have no inhibitory effect on *Aspergillus niger* and the yeasts *Saccharomyces cerevisiae* and *Candida*

albicans (Rauha *et al.* 2000). There is no information available in the literature on the action of phenolic compounds on thermophilic fungi.

Table 3.3 Structure of phenolic compounds tested

Group	Compound	R ₁	R ₂	R ₃
Simple phenols				
	Catechol	OH	OH	H
	Hydroquinone	OH	H	OH
	Resorcinol	H	OH	OH
Hydroxybenzoic acids				
	Gallic acid	OH	OH	OH
	Vanillic acid	H	OH	OCH ₃
Hydroxycinnamic acids				
	Caffeic acid	OH	OH	
	Coumaric acid	OH	H	
	Chlorogenic acid	H	H	
Flavonols				
	Kaempferol	H	OH	H
	Quercetin	OH	OH	H
	Myricetin	OH	OH	OH
Flavanols				
	Catechin	OH	OH	H
	Epicatechin	OH	OH	H
Stilbene				
	Resveratrol	OH	OH	OH

3.2.5.1 Diphenolics

Preliminary experiments with diphenolics were performed to determine the concentration range of phenolic compounds, which exhibited a strong inhibition at concentrations above 2 mM and enhancement around 0.5 mM on fungal growth. Considering this, catechol, hydroquinone and resorcinol were added to the growth medium of *S. thermophilum* at 0.1-2 mM. Figure 3.7, 3.8 & 3.9 indicate their concentration effect on CATPO production and biomass generation.

As shown in Figure 3.7, low catechol concentration (0.1 mM) resulted in 19 % increase in biomass generation but higher amounts (>0.1 mM) caused significant ($P<0.001$) inhibition (47 %) in growth with respect to the control. In terms of activity, catalase and phenol oxidase activities were initially increased by 20 and 7 %, respectively. This was then followed by a gradual decrease in CATPO production in a dose-dependent manner.

Hydroquinone exerted a slight inhibitory effect on the growth of *S. thermophilum* (Figure 3.8). At 2 mM, the reduction in biomass production was found to be 32 % compared to the control. Unlike catechol, no initial increase was observed at low doses. Regarding CATPO production, this *p*-diphenol enhanced CATPO production at low concentrations (<0.5 mM), whereas at higher amounts (1-2 mM) catalase and phenol oxidase activities were 23 % and 12 % inhibited, respectively.

In contrast to hydroquinone and catechol, resorcinol caused 41 % increase in fungal growth, which was noticeable ($P<0.05$) (Figure 3.9). Hence, no antifungal activity was observed. On the contrary, it was observed that CATPO production was significantly ($P<0.001$) inhibited in response to increase in resorcinol concentration (95 % inhibition in catalase activity and 75 % inhibition in phenol oxidase activity). The inhibitory effect of resorcinol may be due to a direct inhibitory effect on CATPO-phenol oxidase activity. However, catalase activity was also decreased, suggesting an effect on enzyme production, rather than activity.

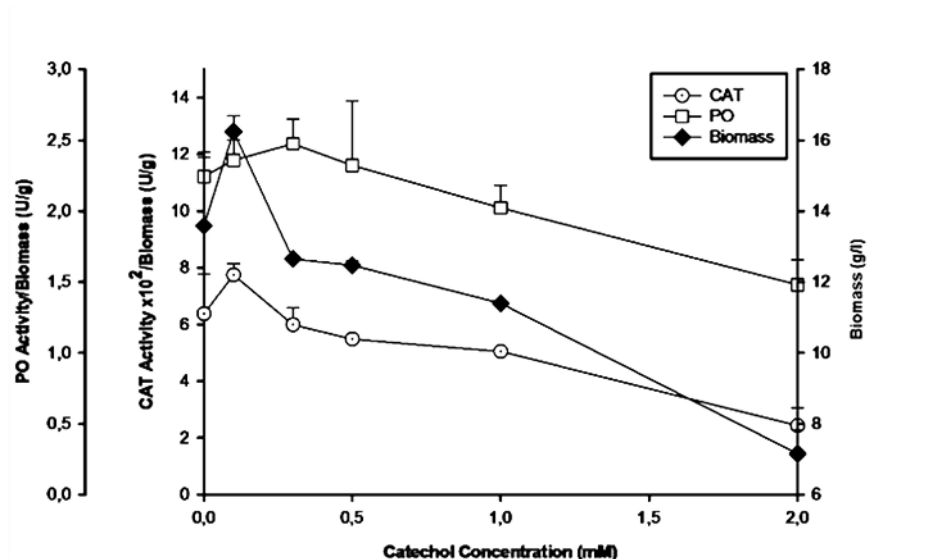


Figure 3.7 Catechol effect on *S. thermophilum* CATPO production and biomass generation.

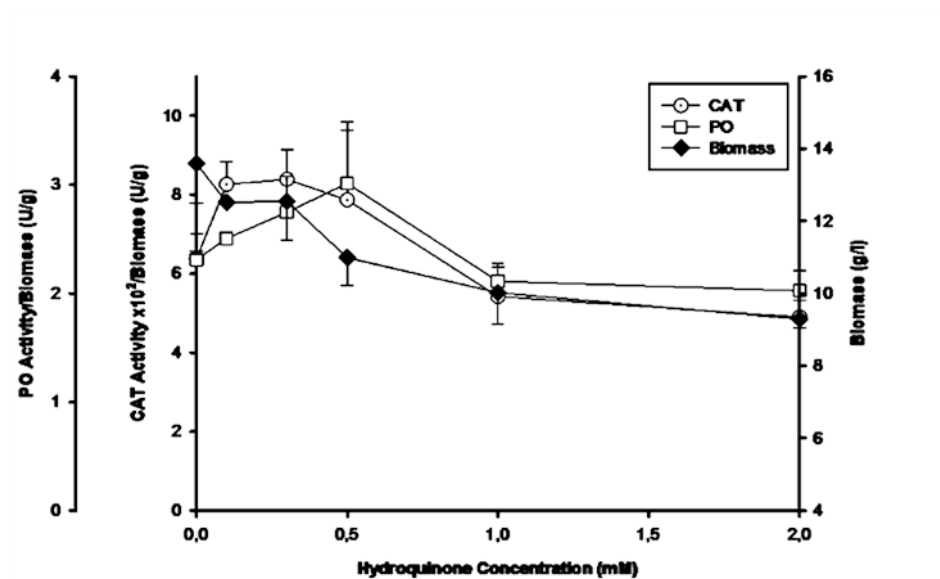


Figure 3.8 Hydroquinone effect on *S. thermophilum* CATPO production and biomass generation.

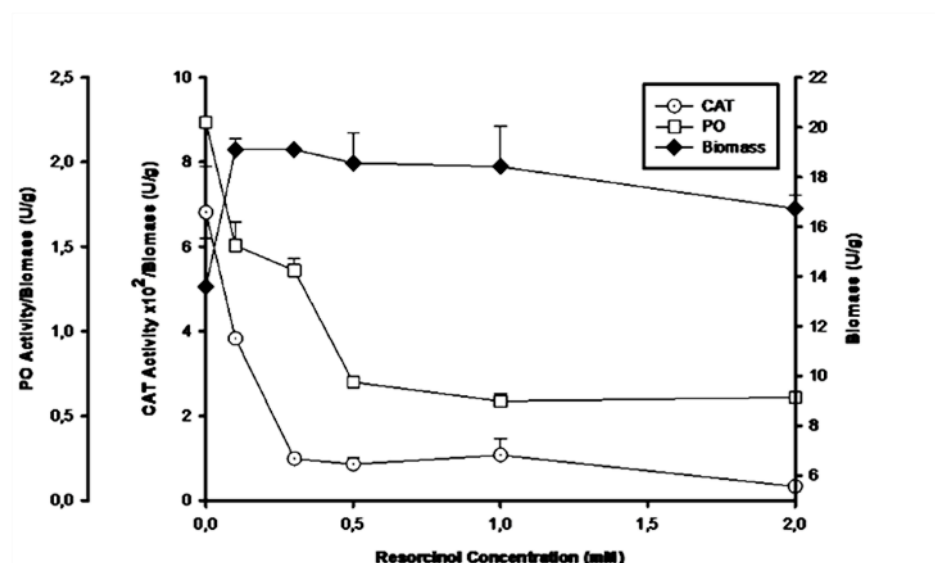


Figure 3.9 Resorcinol effect on *S. thermophilum* CATPO production and biomass generation.

In general, diphenolic compounds acted on *S. thermophilum* growth and enzyme production in a different manner. Catechol (*o*-diphenol) and hydroquinone (*p*-diphenol) were found to have negative effect on fungal growth (47 % growth inhibition for catechol and 32 % for hydroquinone). Catechol and hydroquinone exhibited inhibitory effect in a dose dependent manner. On the other hand, resorcinol (*m*-diphenol) was shown to enhance fungal biomass production (41 % increase). In fact, Passi and his colleagues (1987) reported that *o*- and *p*-diphenols were more toxic than *m*-diphenol resorcinol, supporting our findings.

Enzyme production was observed to be affected negatively by all three diphenolic compounds. With catechol and hydroquinone, the reduction was in parallel to a decrease in cellular growth, whereas with resorcinol, there was an inverse relationship. The observed differences may suggest different functionalities for these phenolics, whereby catechol and hydroquinone are likely to act in a different manner than resorcinol. The data for resorcinol suggest an

antioxidant function, while those obtained for catechol and hydroquinone suggest a possible toxic effect.

3.2.5.2 Phenolic Acids

Phenolic acids are known as antioxidants, whereas their antimicrobial activity has also been well documented (Shahidi and Naczki, 1995). Two representative groups, hydroxybenzoic acids and hydroxycinnamic acids, of phenolic acids were used to analyse their dose effect on fungal growth and CATPO production at a range, similar to that tested for the diphenolics (0.1-2 mM). Among hydroxybenzoic acids gallic and vanillic acids, for hydroxycinnamic acids caffeic, coumaric and chlorogenic acids were selected.

Except *p*-coumaric acid, all phenolic acids positively affected fungal growth. Gallic, vanillic and caffeic acid were found to have a noticeable stimulatory effect on biomass production ($P < 0.05$). Figure 3.10 illustrated 26 % increase in growth at low gallic acid concentrations. Even high amounts of gallic acid did not inhibit cellular growth with respect to control, showing no antifungal activity. Similar to gallic acid and resorcinol, vanillic and caffeic acid caused significant increase (28 % for vanillic acid and 24 % for caffeic acid) in biomass production relative to the control (Figure 3.11 & 3.12).

Chlorogenic acid exerted stimulatory effect on the growth of *S. thermophilum* (Figure 3.13), up to 0.3 mM, but acted negatively above this concentration.

p-Coumaric acid was the only phenolic acid significantly ($P < 0.001$) reducing fungal growth above 0.1 mM (Figure 3.14). This compound resulted in 42 % inhibition in biomass production at 2 mM, showing that *p*-coumaric acid was more toxic than *p*-hydroquinone but less than catechol.

Gallic and vanillic acids were shown to decrease CATPO production significantly ($P < 0.001$ for gallic acid, $P < 0.01$ for vanillic acid). Initial increase (28 %) in catalase activity was observed at low gallic acid concentration

($P > 0.05$). But its higher doses resulted in 46 % decrease in catalase activity and 25 % in phenol oxidase activity, while vanillic acid caused 43 % and 65 % inhibition, respectively. For gallic acid, the reduction in enzyme activity appeared to be in parallel to a decrease in growth (Figure 3.10). On the other hand, for vanillic acid, cellular biomass did not run parallel with enzyme activity showing the possibility of antioxidant effect (Figure 3.11).

Chlorogenic acid effect on enzyme activity was unnoticeable. The initial increase in enzyme activity followed by reduction at higher doses was in parallel with the change in biomass (Figure 3.13). Like chlorogenic acid, *p*-coumaric acid caused insignificant change in enzyme production. However, it appeared to be more toxic upon fungal cells than chlorogenic acid.

The effect of caffeic acid on biomass production was similar to gallic and chlorogenic acid (Figure 3.12). However, caffeic acid caused 47 % increase in catalase and about 10 % increase in phenol oxidase activity

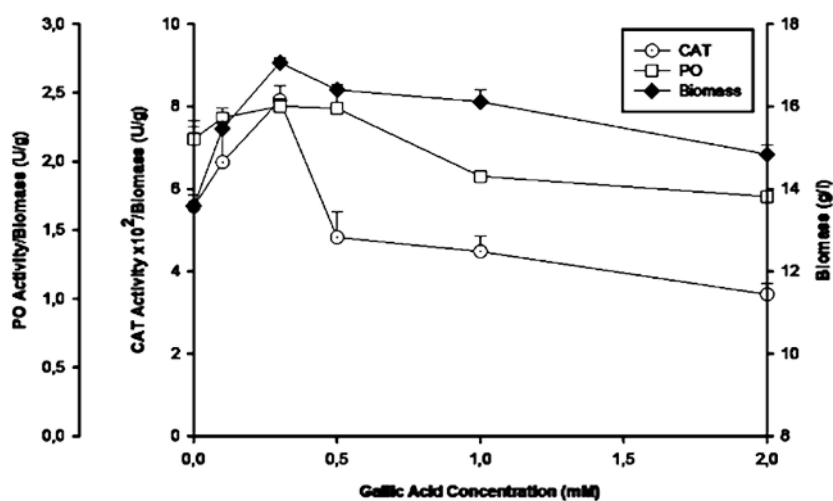


Figure 3.10 Gallic acid effect on *S. thermophilum* CATPO production and biomass generation.

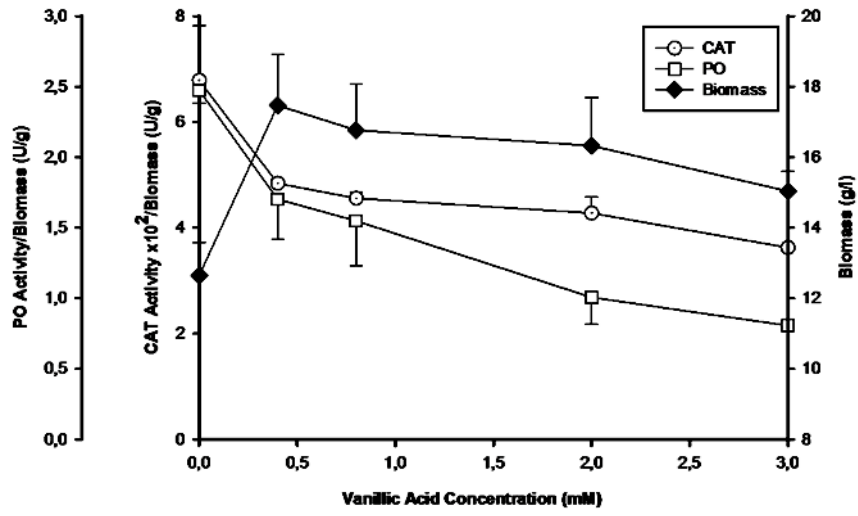


Figure 3.11 Vanillic acid effect on *S. thermophilum* CATPO production and biomass generation.

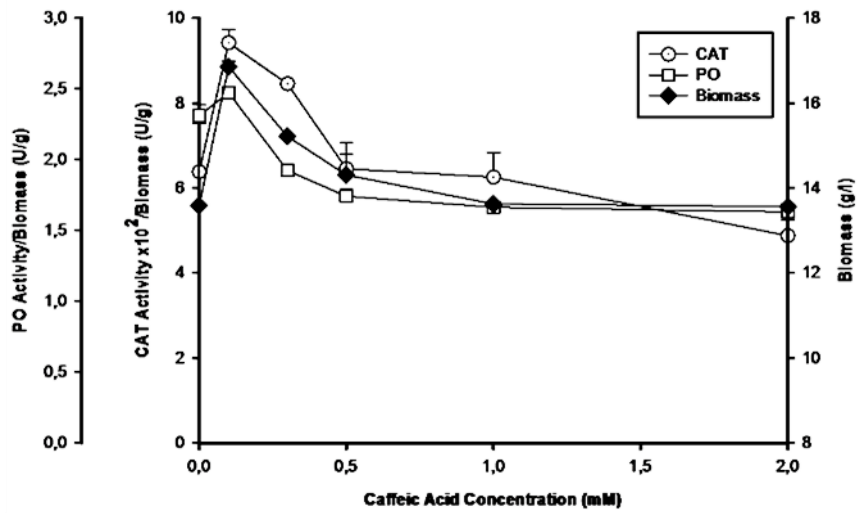


Figure 3.12 Caffeic acid effect on *S. thermophilum* CATPO production and biomass generation.

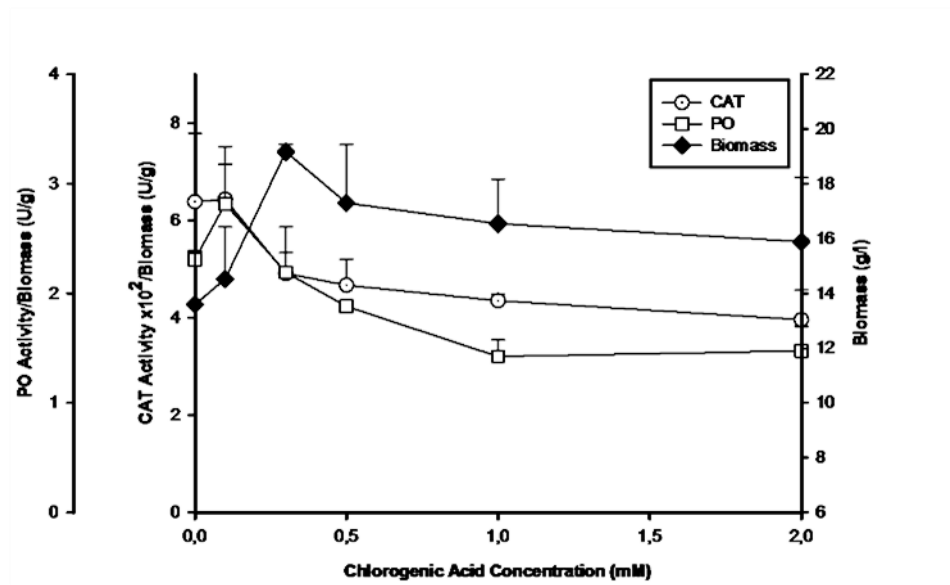


Figure 3.13 Chlorogenic acid effect on *S. thermophilum* CAT/PO production and biomass generation.

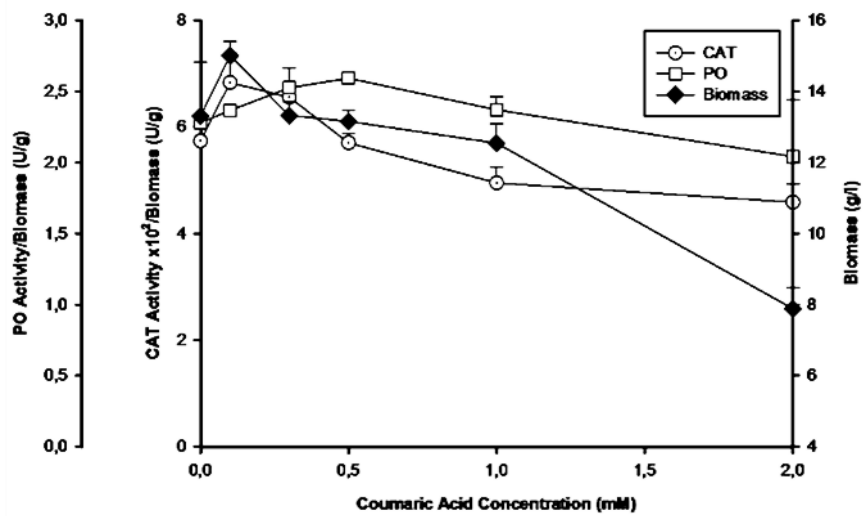


Figure 3.14 Coumaric acid effect on *S. thermophilum* CAT/PO production and biomass generation.

Most of the compounds caused an initial increase in biomass and corresponding enzyme activity possibly due to an antioxidant activity, followed by a gradual decrease in biomass and related enzyme activity in a dose-dependent manner suggesting a pro-oxidant activity.

3.2.5.3 Flavonoids

Flavonoids are strong antioxidants. Their antioxidant and chelating abilities can be improved by the presence of a catechol-like structure in the B-ring, an unsaturated 2,3 double bond and 3-hydroxyl group in the C-ring (Figure 1.14; Rice-Evans, 2001). The most powerful flavonoid antioxidant is known to be quercetin (Trolox equivalent antioxidant capacity=TEAC, 4.7 mM), followed by catechin (TEAC, 2.4 mM) and kaempferol (TEAC, 1.3 mM) (Rice-Evans *et al.*, 1997).

Effect of flavonoid concentration on *S. thermophilum* growth and CATPO production was performed using two sources, flavanols and flavonols, in a concentration range of 0.0025-0.1 mM and 0.04-0.16 mM, respectively.

Quercetin (Figure 3.16), catechin (Figure 3.18) and epicatechin (Figure 3.19) caused an initial increase in biomass production (5 %, 36 %, and 15 %, respectively). The stimulatory effect on cellular growth was significant with catechin ($P < 0.05$), while epicatechin and quercetin action was unnoticeable though. This early induction was then followed by a slow decrease in response to increase in dose. However, the biomass produced at the highest concentration was even higher than control.

Flavonols kaempferol and myricetin exerted strong inhibitory effect on fungal growth as presented in Figure 3.15 & 3.17 ($P < 0.01$ for kaempferol, $P < 0.05$ for myricetin). Myricetin was shown to have higher antifungal effect than kaempferol since the growth inhibition was 36 % with myricetin but 26 % with kaempferol.

Except myricetin, all flavonoids tested here were found to affect enzyme production in an insignificant manner. Myricetin caused 49 % increase in catalase and 43 % in phenol oxidase activities (Figure 3.17). Even at 0.2 mM myricetin concentration, catalase activity was shown to be induced by 24 % and phenol oxidase activity by 18 %.

Higher amounts of kaempferol and quercetin resulted in slight inhibition in which kaempferol effect was more observable. For kaempferol (0.1 mM), 32 % inhibition was observed for catalase activity, while quercetin (0.1 mM) gave rise to 19 % inhibition.

Catechin and epicatechin action on enzyme production was a bit different from that of the flavonols presented. These flavanols were detected to reduce enzyme production without an initial increase at lower doses. They caused approximately 20 % inhibition in catalase activity, which was found to be insignificant.

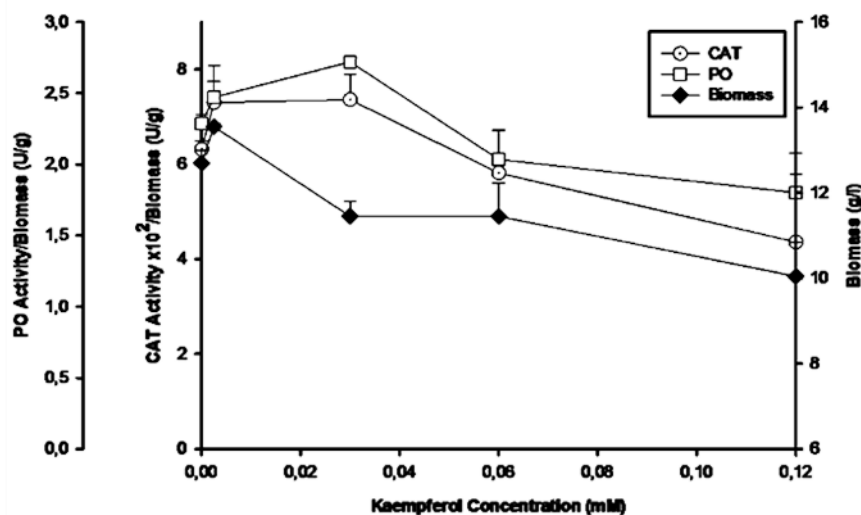


Figure 3.15 Kaempferol effect on *S. thermophilum* CATPO production and biomass generation.

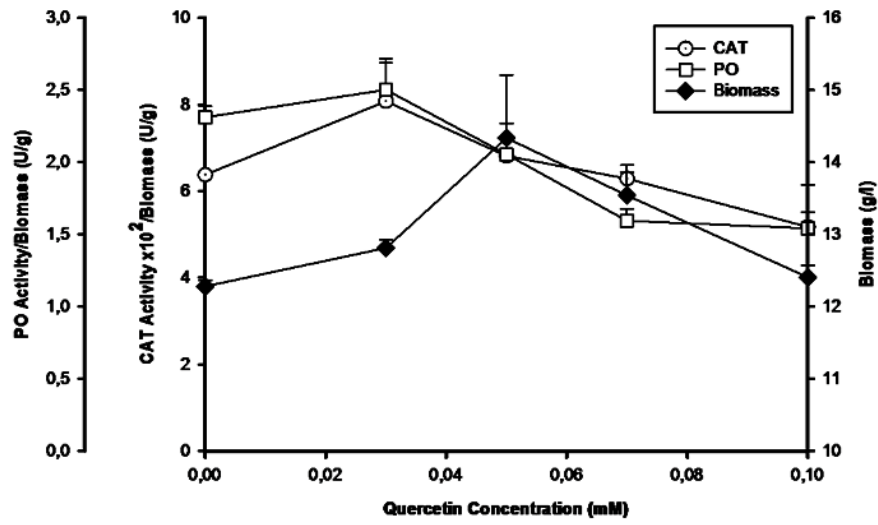


Figure 3.16 Quercetin effect on *S. thermophilum* CATPO production and biomass generation.

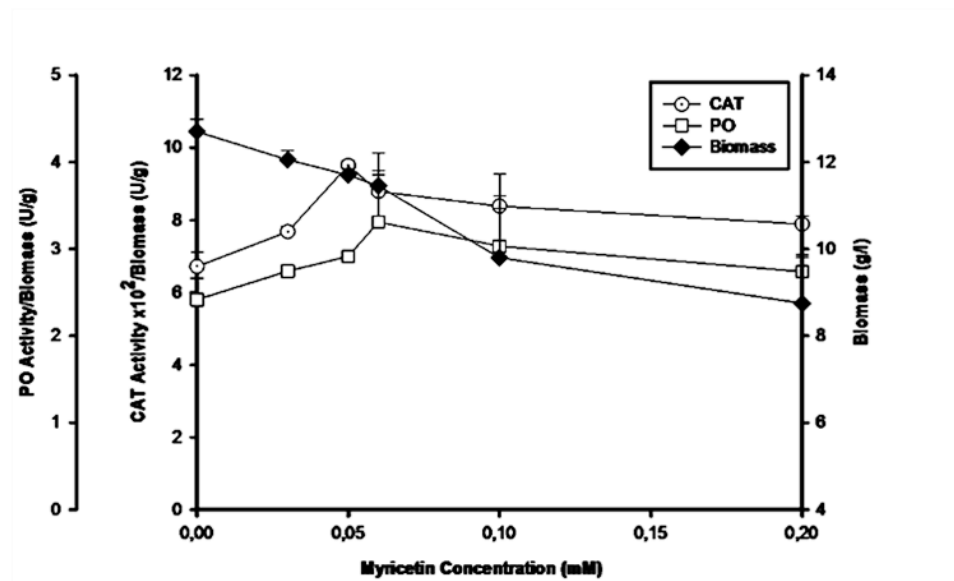


Figure 3.17 Myricetin effect on *S. thermophilum* CATPO production and biomass generation.

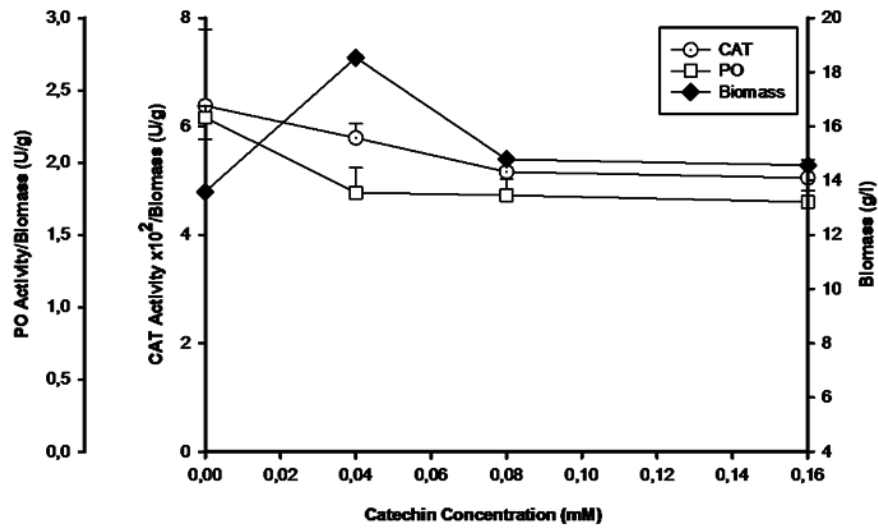


Figure 3.18 Catechin effect on *S. thermophilum* CATPO production and biomass generation.

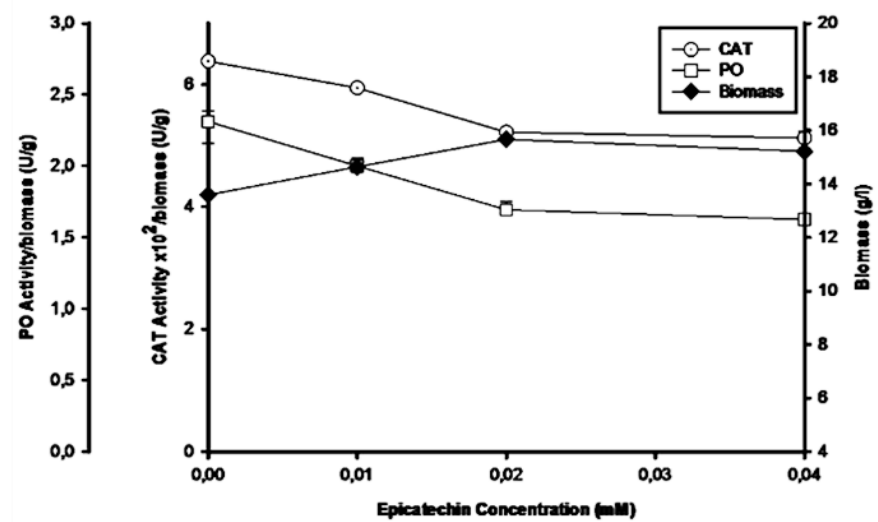


Figure 3.19 Epicatechin effect on *S. thermophilum* CATPO production and biomass generation.

3.2.5.4 Resveratrol

Effect of *t*-resveratrol was investigated at 0.1-1 mM. As shown in Figure 3.20, *t*-resveratrol did neither display any antifungal effect nor a significant growth promoting effect (only 12 % increase).

In terms of CATPO activity, up to 0.3 mM, an 11 % increase in catalase activity was determined, but 2.5 fold in phenol oxidase activity (significant, $P < 0.001$) which is the most pronounced effect observed so far. The significant change in phenol oxidase activity appeared to be dose sensitive since 0.5 mM caused a half reduction in activity but still higher than the control (Figure 3.20). This result may be due to a possible induction of other phenol oxidases in culture supernatant or a specific stimulating effect of resveratrol on the phenol oxidase activity of CATPO.

Resveratrol is also known as anti-aging compound. Initial experiments with yeast cells and higher eukaryotic cells showed that the anti-aging properties of *t*-resveratrol are related to its positive effect on sirtuins through increasing DNA stability (Baxter, 2008). Sirtuin proteins function as histone acetylating agents, leading to a decrease in DNA degradation by enhancing histone-DNA interaction, hence DNA stability.

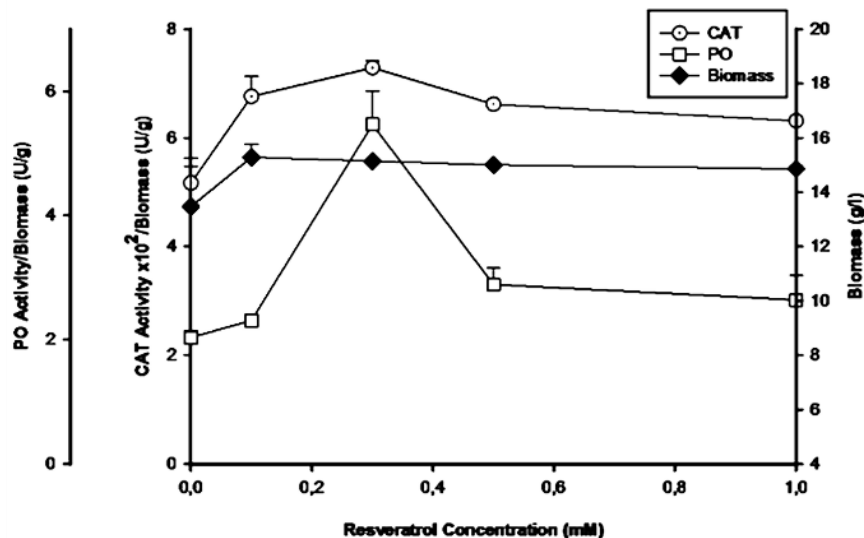


Figure 3.20 Resveratrol effect on *S. thermophilum* CATPO production and biomass generation.

3.2.5.5 Phenylactic Acid

Effect of phenylactic acid (PLA) concentration on fungal growth and enzyme production was performed at 0.1-0.5 mM. PLA, known as an antifungal compound in the literature, did not affect *S. thermophilum* growth negatively to a significant level. The initial increase (14 %) observed in CATPO production at 0.1 mM, followed by a reduction above 0.1 mM, was similar to the effects of some other phenolic compounds described above (Figure 3.21). However, in this case, the reduction in CATPO production was insignificant and enzyme production even at 0.5 mM concentration of PLA was higher than the control.

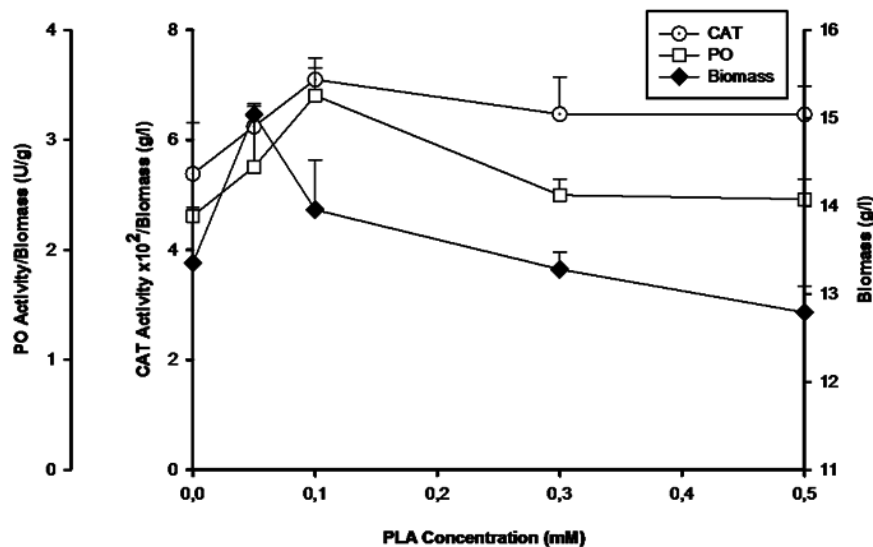


Figure 3.21 PLA effect on *S. thermophilum* CATPO production and biomass generation.

In the literature, PLA is shown to present antifungal activity at low pH (Lavermicocca *et al.*, 2003). In general, thermophilic fungi provide alkaline environment; therefore thermostable enzymes become more active at neutral or alkaline pH. Previous studies have shown that *S. thermophilum* growth environment is not acidic. For this reason, it was thought that PLA could not exhibit antifungal activity.

3.2.5.6 Evaluation of the Effect of Phenolic Compounds on CATPO Production

Thermophilic fungi are known as the most heat-resistant organisms. It is proposed that they have evolved from their mesophilic counterparts by adaptation to higher temperatures (Feofilova and Tereshina, 1999). Therefore, they continuously produce antioxidant chemicals and enzymes to compensate for excessive reactive oxygen species generated due to heat-stress. CATPO of *S.*

thermophilum is a growth associated enzyme and is produced constitutively, even in the absence of phenolic compounds.

Most phenolic compounds can act as antioxidant/pro-oxidant in a dose dependent manner (Won Lee and Joo Lee, 2006). Therefore, the growth of thermophilic fungi and corresponding antioxidant enzyme (CATPO) production could be changed in response to phenolic compounds having different structure and functionality.

Depending on the results obtained, *S. thermophilum* exhibited different sensitivity towards different phenolic compounds. In fact, except quercetin, epicatechin and phenyllactic acid, all phenolic compounds tested were seen to have a significant effect on either growth and/or CATPO production (Table 3.4). These functions may be suggested to be antifungal (a continuous decrease in growth as concentration increases) or antioxidant/pro-oxidant (an initial increase in growth followed by decrease) for fungal growth. For enzyme production, activity per biomass produced was considered. Those that showed a significance increase were said to enhance production, while those that showed a significance decrease were said to suppress production.

Accordingly, catechol, *p*-coumaric acid and kaempferol caused a significant decrease in fungal growth above a particular concentration, while *p*-hydroquinone and myricetin resulted in a continuous decrease with respect to increase in concentration. For phenolic compounds presenting antioxidant/prooxidant behaviour, the change in enzyme production was in parallel to that in cellular growth. In such a case, those phenolics might exhibit toxicity upon cells at higher doses. Thus, this toxic effect on enzyme production was suppressive rather than inductive. On the other hand, *p*-hydroquinone and myricetin, showing antifungal effect, were observed to enhance production. Therefore, it is believed that CATPO production increases in response to antifungal effect.

Resorcinol, gallic, vanillic, caffeic and chlorogenic acid, and catechin were shown to enhance fungal growth in a dose-dependent manner. Those compounds were

found to suppress enzyme production either above a particular concentration or in a constant behaviour. The most prominent suppression was observed with resorcinol and vanillic acid. Hence, it can be said that those phenolics might have an antioxidant effect and when this effect encountered, *S. thermophilum* CATPO production was decreased continuously or above certain doses.

The antioxidant/pro-oxidant effect might be related to the thermophilic nature of the fungus. When an antioxidant is already present in the environment, the fungus might produce less antioxidant and reduce the energy needed for the antioxidant mechanism. Therefore, the excess energy could be used for growth.

Since CATPO production is growth-associated, the action of phenolics on enzyme production has resulted in the protein inhibition or antioxidant/pro-oxidant behaviour in a dose-dependent manner. Inhibition of enzyme could stem from direct interaction of compound with the enzyme active site (Shahidi and Naczki, 1995) or from phenol oxidation products through reaction with sulfhydryl groups or through more nonspecific interactions with the proteins (Cowan, 1999).

Table 3.4 Dose-dependent effect of phenolic compounds on *S. thermophilum* CATPO production and biomass generation (statistically significant values are illustrated in bold)

Phenolic compound	%	%	% Relative CATPO production		% Relative min CATPO production	
	Relative max biomass	Relative min biomass	CAT	PO	CAT	PO
Control (no phenol)	100	100	100	100	100	100
Catechol	119	53	121	107	38	36
Hydroquinone	-	68	131	130	77	88
Resorcinol	141	-	-	-	5	25
Gallic acid	126	-	128	100	54	75
Vanillic acid	128	-	-	-	57	35
Caffeic acid	124	-	147	107	76	72
Chlorogenic acid	141	-	101	122	62	64
Coumaric acid	110	58	107	112	72	88
Kaempferol	102	74	115	118	68	78
Quercetin	105	-	126	108	81	66
Myricetin	-	64	149	143	-	-
Catechin	136	-	-	-	79	75
Epicatechin	115	-	-	-	80	70
Resveratrol	112	-	111	236	-	-
Phenyllactic acid	111	94	114	124	-	-

3.3 Biocatalysis using CATPO

Biotransformation studies include the use of biological agents, in the form of whole cells or isolated enzymes, to catalyze chemical reactions (Burton, 2001). Fungal CATPO seems to be an efficient biocatalyst for the biotransformation of some chiral organic compounds in racemic mixtures due to being highly stable in organic solvents like DMSO (Kaptan, 2004) and having high activity in the desired reaction (Ögel *et al.*, 2006).

Here it was aimed to analyse activity of CATPO on a number of organic compounds, to investigate product formation by thin layer chromatography, and to characterize the reaction products by high performance liquid chromatography (HPLC) or gas chromatography (GC).

3.3.1 CATPO Biocatalysis with Organic Compounds

Bioorganic conversion of pharmaceutically important compounds in the presence of fungal CATPO was investigated. These organic compounds included catechol, hydroquinone, resorcinol, gallic acid, caffeic acid, coumaric acid, chlorogenic acid, 4-tert-butylcatechol, L-dopa, phenyllactic acid, resveratrol and *meso*-hydrobenzoin. The molecular formula of organic substrates is given in Figure 3.22.

Catechol is an important intermediate in manufacturing pesticides and medicines and can also be used to produce perfumes (piperonal), dyes, photosensitive materials, electroplating materials, special inks, antioxidants, fungicides, light stabilizers, anticorrosive agents and promoters. Hydroquinone is mainly used in manufacturing film developers, anthraquinone dyes, azo dyes, desulfurization co-solvents in making ammonia, rubber antioxidants, polymerization inhibitors and coatings stabilizer. Resorcinol is mainly utilised in cosmetic preparations.

Gallic acid is found in gallnuts, sumac, witch hazel, tea leaves, oak bark, and other plants (Reynolds and Wilson, 1991). Gallic acid and its catechin derivatives are also present as one of the main phenolic components of both black and green tea. Esters of gallic acid have a diverse range of industrial uses, as antioxidants in food, in cosmetics and in the pharmaceutical industry (Ow and Stupans, 2003).

Caffeic acid and *p*-coumaric acid are rarely found in the free form, except in processed food that has undergone freezing, sterilization, or fermentation. Caffeic and quinic acid combine to form chlorogenic acid, which is found in many types of fruits at high concentrations in coffee (Manach *et al.*, 2004).

L-Dopa (3,4-dihydroxy phenyl L-alanine) is used to increase dopamine concentrations in the treatment of Parkinson's disease and Dopamine-Responsive Distonia. L-Dopa is produced from the amino acid L-tyrosine by the enzyme tyrosinase. The most common plant source of L-Dopa marketed in this manner is *Mucuna pruriens* (Velvet Bean).

4-tert-Butylcatechol is a derivative of catechol. It is added as a stabilizer and an inhibitor of polymerization to butadiene, styrene, vinyl acetate and other reactive monomer streams. It is 25 times better than hydroquinone at 60°C for polymerization inhibitory effect. Also used as a stabilizer in the manufacture of polyurethane foam. It also can be used as an antioxidant for synthetic rubber, polymers and oil derivatives. It can be used as purification agent for aminoformate catalysts (<http://en.wikipedia.org>).

Phenyllactic acid is present in honey and reported to have strong antifungal activity over a wide spectrum of fungi including *Aspergillus*, *Penicillium* and *Fusarium* (Lavermicocca *et al.*, 2003).

trans-Resveratrol (3,5,4'-trihydroxystilbene) is found in grape vines and reported to have antimicrobial, anti-HIV, anti-inflammatory effect. This compound is also known as important cancer chemoprotective agent (Nicotra *et al.*, 2004). In recent years, resveratrol has been reported to increase life span in eukaryotes (yeast, mice, *etc.*) related to its positive effect on sirtuins (Baxter, 2008).

meso-Hydrobenzoin (*meso*-1,2-Diphenyl-1,2-ethanediol) is a chiral compound. Chiral synthesis has become more and more important in research and industry, which is partly due to the always increased need for enantiopure chiral drugs.

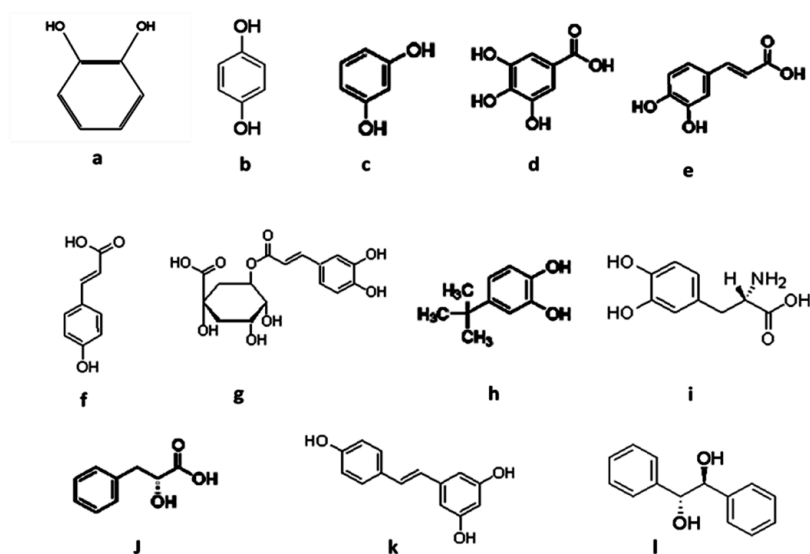


Figure 3.22 Structures of organic compounds used in CATPO biotransformation studies, a: *o*-catechol, b: *p*-hydroquinone, c: *m*-resorcinol, d: gallic acid, e: caffeic acid, f: *p*-coumaric acid, g: chlorogenic acid, h: 4-tert-butylcatechol, i: L-dopa, j: PLA (phenyllactic acid), k: *trans*-resveratrol, l: *meso*-hydrobenzoin.

All reactions with the above mentioned organic substrates were carried out at 60°C and at pH 7.0. The substrates were dissolved in either ethanol or DMSO (dimethyl sulfoxide) and used at a concentration of 10 mg/mL. The culture supernatant was used as a source of CATPO.

The chromatographic conditions for the analysis of phenolic compounds by thin layer chromatography (TLC) are presented in Appendix H.

The regioselective oxidation of hydrobenzoin in *meso* form and possible oxidation products of other chemicals were investigated. Based on the results presented in Table 3.5, except coumaric acid and resorcinol, all substrates gave oxidation products from their reaction with CATPO-containing culture supernatant of *S. thermophilum*. Both resorcinol (Shahidi and Naczka, 1995; Table 3.4) and *p*-coumaric acid (Table 3.2) were found to be potential inhibitors for

phenol oxidases. Hence, it was not surprising that oxidation products of those two were not observed by TLC.

The reaction products of resveratrol and benzyl formation via benzoin generation from *meso*-hydrobenzoin were further analysed.

Table 3.5 TLC results of biotransformation experiments with extracellular CATPO

Substrate	Product Formation on TLC Plate
Catechol	+
Hydroquinone	+
Resorcinol	-
Gallic acid	+
Caffeic acid	+
Coumaric acid	-
Chlorogenic acid	+
L-DOPA	+
4-tertbutylcatechol	+
PLA	+
Resveratrol	+
Hydrobenzoin	+

3.3.2 High Performance Liquid Chromatography (HPLC) Results

The reaction was set up between culture supernatant including CATPO and twelve different organic compounds for the biocatalytic process. Product

formation was monitored by TLC using authentic compounds as references, which is followed by HPLC or GC, as described in section 2.2.12.

HPLC was performed to detect the oxidation products, benzoin and benzil, of *meso*-hydrobenzoin.

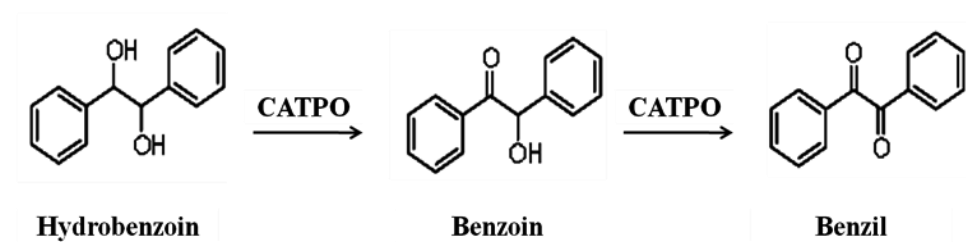


Figure 3.23 Oxidation of hydrobenzoin to benzil via benzoin formation by *S. thermophilum* CATPO.

Figure 3.24 demonstrates the retention times of compounds eluted from the chiral column. 6.9 retention time belongs to benzil and 37.2 retention time with 26.5 area percent belongs to hydrobenzoin. Benzoin was shown to have two different peaks at 19.1 and 28.6 retention time. Two different peaks of benzoin represent the stereoselective oxidation of hydrobenzoin by CATPO. R-benzoin was excess in the ratio of 65:35 percent enantiomeric excess.

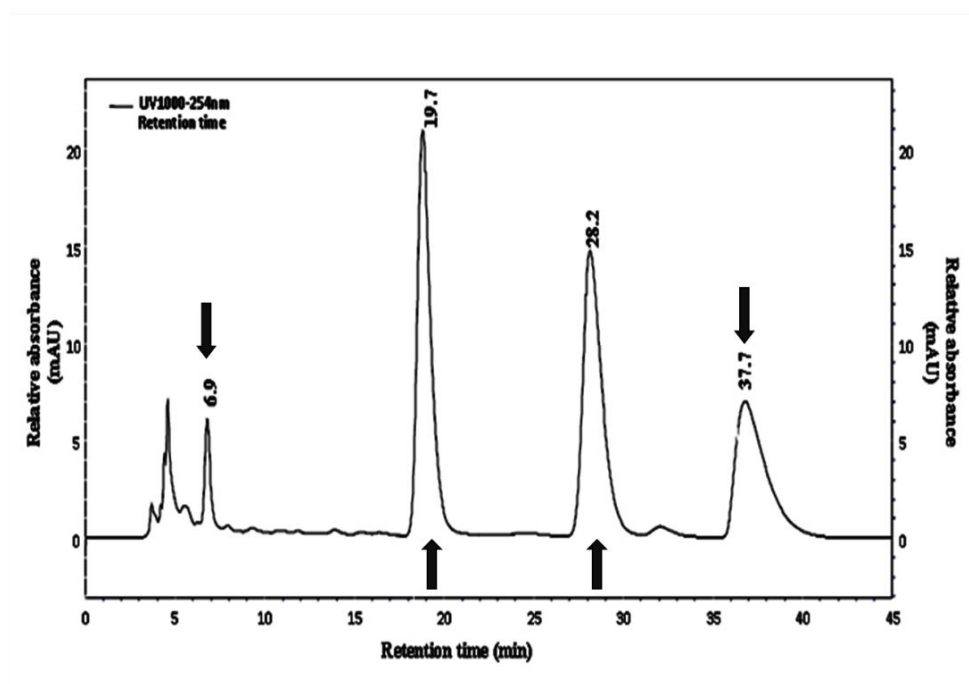


Figure 3.24 Chromatogram of reaction products from the oxidation of hydrobenzoin by *S. thermophilum* CATPO. The number indicates the retention time of each peak and the arrows correspond to the peaks of benzil (at ca. 6.9), benzoin (at ca. 19.1 and 28.6 for the R- and S-enantiomers) and hydrobenzoin (at ca. 37.2).

The conversion of hydrobenzoin to benzil via benzoin production was also performed by commercially available laccase isolated from *Trametes versicolor*. After monitoring products by TLC, they were detected by HPLC.

As presented in Figure 3.25, benzil formation was detected at the same retention time with respect to that observed with CATPO. The non-oxidised hydrobenzoin peak was seen at 37.7 retention time. R- and S-enantiomers of benzoin were monitored at retention times of 19.7 and 28.2, respectively. R-benzoin was excess in the ratio of 80:20 percent enantiomeric excess, which was considerably higher than that obtained in the presence of CATPO in reaction medium.

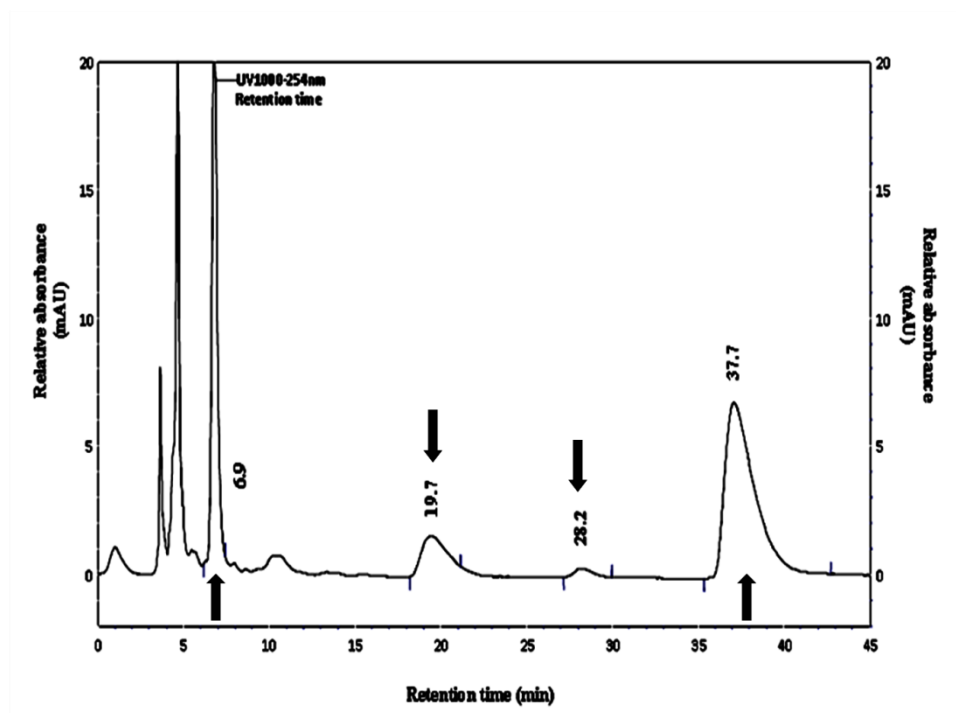


Figure 3.25 Chromatogram of reaction products from the oxidation of hydrobenzoin by *T. versicolor* laccase. The number indicates the retention time of each peak and the arrows correspond to the peaks of benzil (at *ca.* 6.9), benzoin (at *ca.* 19.7 and 28.2 for the R- and S-enantiomers) and hydrobenzoin (at *ca.* 37.7).

A summary of HPLC results including the retention time and the area percent of hydrobenzoin used in the biocatalysis experiments with both CATPO and *T. versicolor* laccase with regard to its oxidation products are documented in Table 3.6.

Table 3.6 HPLC results of hydrobenzoin oxidation with *S. thermophilum* CATPO and *T. versicolor* laccase

Biocatalyst	Organic compound	Retention time (min)	Area percent (%)
CATPO	Hydrobenzoin	37.2	26.5
	Benzoin	19.1	35.2
		28.6	34.6
Benzil	6.9	3.69	
Laccase	Hydrobenzoin	37.7	56.9
	Benzoin	19.7	9.3
		28.2	1.8
Benzil	6.9	31.9	

3.3.3 Gas Chromatography (GC) Results

Biotransformation of resveratrol was analysed by gas chromatography. The oxidation and possible sequential oligomerization of resvetarol to viniferin, known as chemoprotective agent (Cichewicz and Kouzi, 2002; Ohyama *et al.*, 1999), was investigated (Figure 3.26).

Similar to resveratrol, oligomeric stilbenes, called viniferins, have been found in plants as a result of infection or stress (Cichewicz and Kouzi, 2002; Nicotra *et al.*, 2004). Viniferins are reported to present antimicrobial, anti-HIV, and anti-inflammatory activities. They are also documented to play a role in the prevention of carcinogenesis, being able to inhibit cellular events in cancer cells (Ohyama *et al.*, 1999).

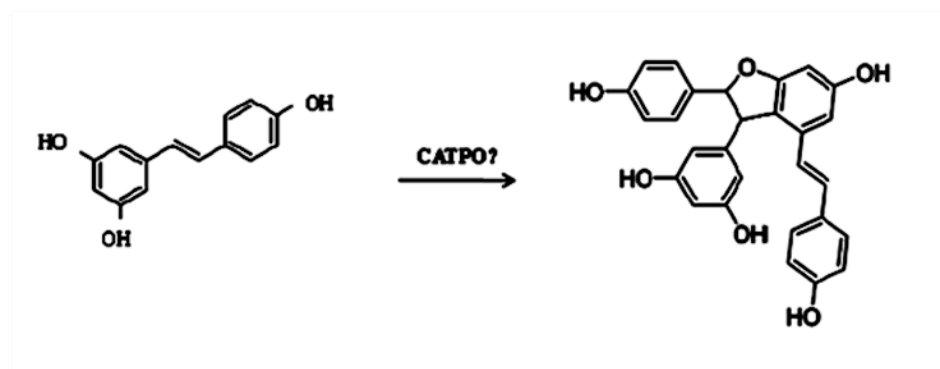
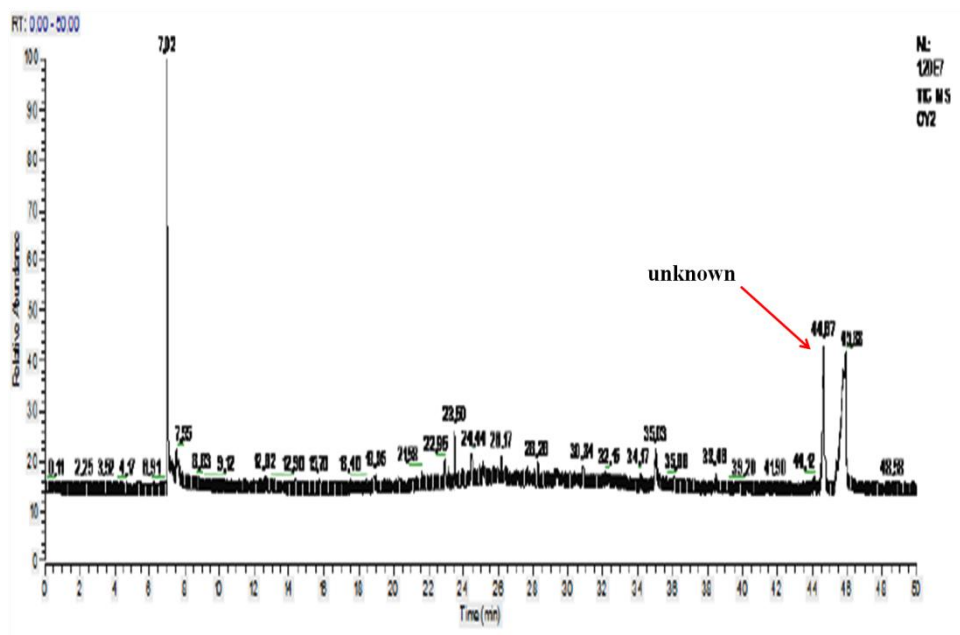
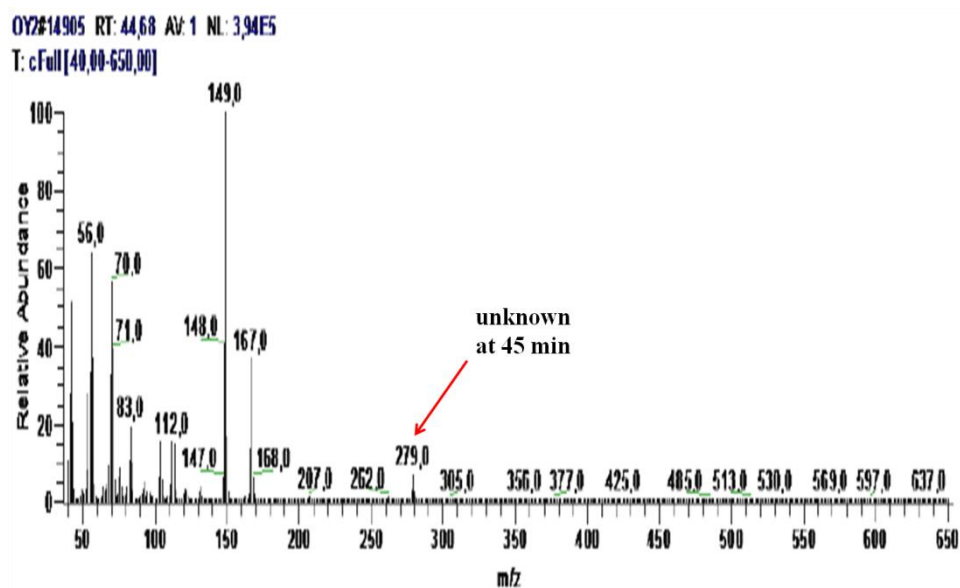


Figure 3.26 Viniferin production from *t*-resveratrol.

Figure 3.27 illustrates the retention times and the mass to charge ratios of resveratrol and its oxidation products. Reaction product was observed to come out of the column at 44.8 retention time and to give a molecular ion peak at m/z 279. This did not correspond to the structure of viniferin, m/z calculated for $C_{28}H_{22}O_6$ is 454. The unknown compound could not be a dimer; but might have furan rings additional to two phenol rings of resveratrol. Since it was not an oligomeric stilbene, the compound was not further analysed.



(a)



(b)

Figure 3.27 GC/MS result of resveratrol; (a), the chromatogram generated by GC; (b), the molecular weight of the fragments.

3.4 Molecular Studies on CATPO

S. thermophilum catalase-phenol oxidase (CATPO) is a bifunctional enzyme. Its major function is the removal of hydrogen peroxide. Besides that, enzyme is also capable of oxidizing various phenolic compounds as described in section 3.1.2.

In order to study the oxidase mechanism of catalase, the *catpo* gene from *S. thermophilum* was PCR amplified from pUC57 clone, which was synthesized by Genscript (section 2.2.3), transformed into *E. coli* BL21(DE3)star cells and was subjected to site directed mutation to obtain different mutant types. The overall experimental strategy followed is presented in Figure 3.28.

The nucleic acid sequence encoding *S. thermophilum* catalase gene was first introduced by Novo Nordisk (United States Patent, No. 5646025). Therefore, based on the sequence (Appendix J), codon optimised *catpo* exon gene was synthesized by GenScript through cloning onto pUC57 via EcoRV digestion (GenScript Corporation, USA). Specific primers were designed to amplify *catpo* gene excluding the signal peptide region (≈ 19 amino acids) from pUC57 clone. Then, amplified gene fragment was digested, ligated into vector pET28a (N-terminal 6xHis-tag followed by a TEV cleavage site replacing the native thrombin site; a generous gift from Prof. R. E. Sockett and made by Dr. John Taylor, University of Nottingham) and cloned into *E. coli* XL-1 Blue cells. Following restriction digestion, sequencing was performed in order to control the specificity of the amplified fragment. Two confirmed positive clones were transformed into *E. coli* BL21(DE3)star and expression studies were carried out. The presence of *catpo* gene (Appendix K) was confirmed by PCR using the genomic DNA of transformants and enzyme activity analysis.

To differentiate between phenol oxidation and catalase activity two mutants were designed targeting two conserved residues (histidine and valine) at the active site of catalases. QuickChange primers were designed to generate H101N and V142F mutational variants. The desired amino acid changes were confirmed by DNA sequencing and quantitative enzyme assays.

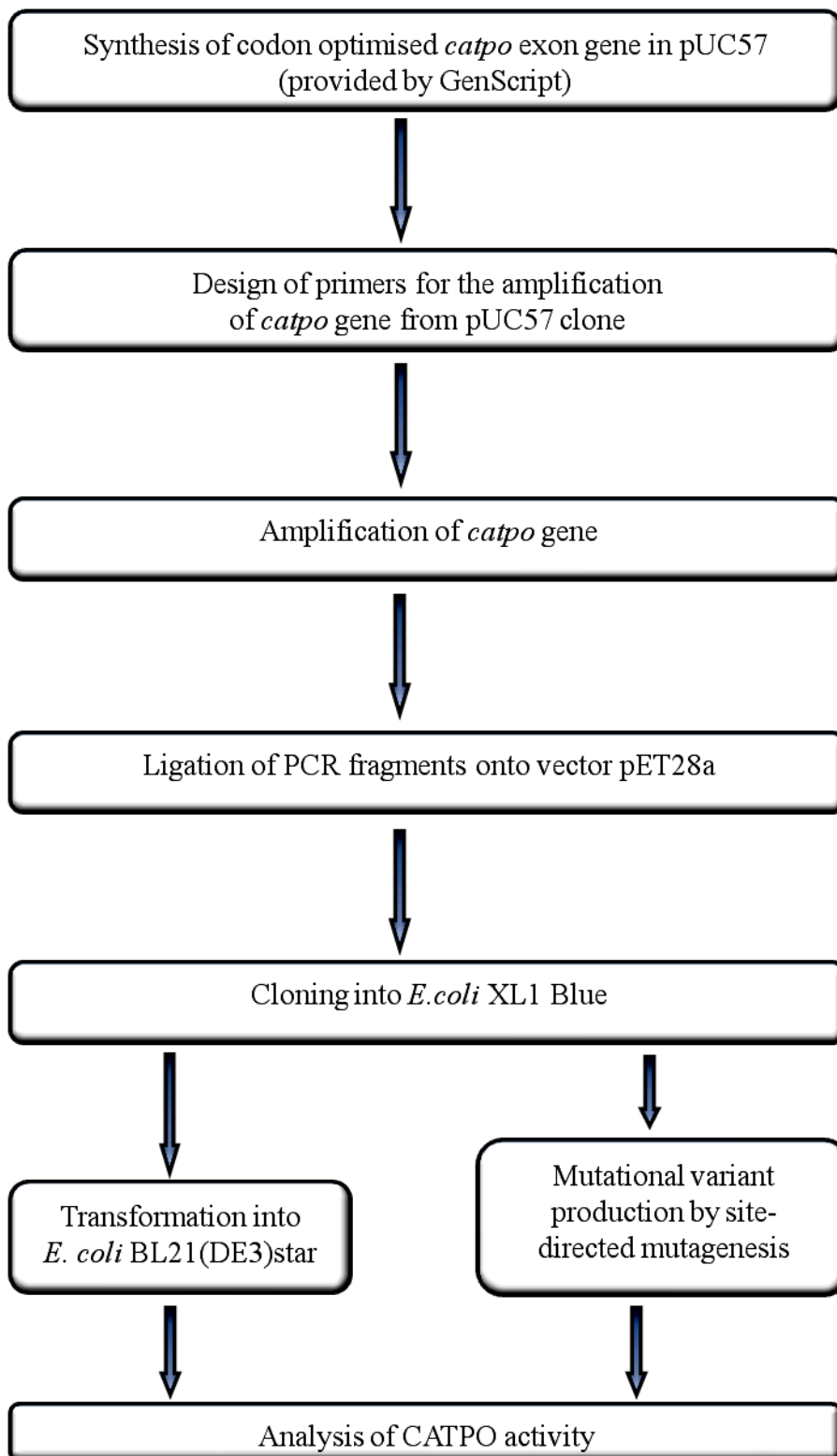


Figure 3.28 Experimental strategies for molecular studies on CATPO.

3.4.1 Cloning and Expression of *S. thermophilum catpo* Gene

3.4.1.1 PCR Cloning of *catpo* Gene onto the *E. coli* Expression Vector

The *catpo* gene from *S. thermophilum* was PCR amplified from a pUC57 clone (provided by GenScript) using two specific primers, namely NdeI20 and HindIIIend (Figure 3.29). The primers were designed (section 2.2.3) to start at the Threonine (Thr) residue predicted by Signal P, program for signal peptide cleavage prediction, as the first amino acid of the mature protein. Structure of *Penicillium vitale*, showing 63 % sequence homology, starts from at 39th residue of CATPO (Appendix L), suggesting that the first 20 residues after the signal sequence are not structured.

The amplification gave a product of an expected size of *ca.* 2.1 kbp (Figure 3.30).

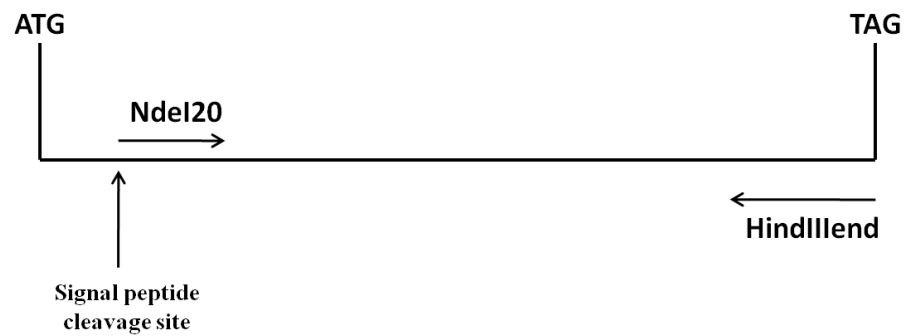


Figure 3.29 The schematic illustration of the location of primers NdeI20 and HindIIIend.

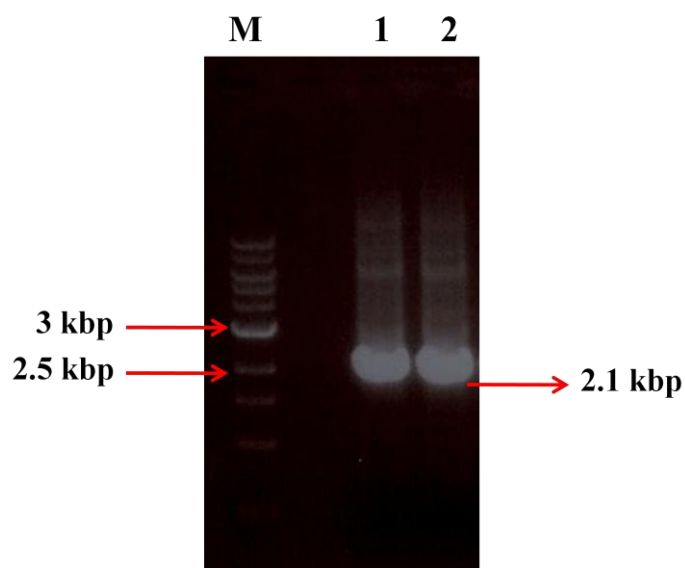


Figure 3.30 Amplification of *catpo* gene from *S. thermophilum* using primers NdeI20 and HindIIIend. PCR amplification yielded a major band of approximately 2.1 kbp sized. *M*, molecular size marker (1 kbp DNA Ladder, NEB); *Lane 1&2*, amplified gene fragments

3.4.1.2 Isolation of Recombinant Plasmids containing the *catpo* Gene

Following ligation of the amplified product onto pET28a TEV vector (Appendix B) and selection of *E. coli* transformants, the isolated recombinant plasmid was named as pETCATPO (approximate size *ca* 8 kbp, Appendix B). Plasmid isolates were analysed for the presence of insert by PCR reactions. Two positive clones (clone 1 and 4) were confirmed by restriction digestion and subsequent sequencing (Figure 3.31).

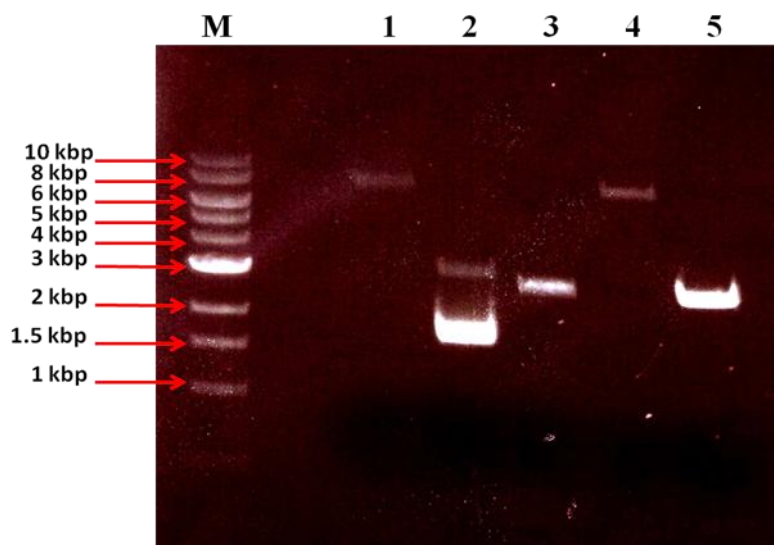


Figure 3.31 Isolated plasmids from *E. coli* pETCATPO transformants. *M*, molecular size marker (1 kbp DNA Ladder, NEB); *Lane 1-5*, analysis of isolated plasmid DNAs

3.4.2 Transformation of pETCATPO into *E. coli* BL21(DE3)star

E. coli BL21(DE3)star strains are designed for improving protein yield in a T7 promoter-based expression system. Because T7 RNA polymerase synthesizes mRNA more rapidly than *E. coli* RNA polymerases, transcription from the T7 promoter is uncoupled to translation in *E. coli*. This result in mRNA transcripts unprotected by ribosomes, which are then subject to enzymatic degradation by endogenous RNases. The reduced level of transcripts in the cell often leads to greatly reduced levels of protein yield. The BL21(DE3)star strains contain a mutation in the gene encoding RNaseE (*rne131*), which is one of the major sources of this mRNA degradation. BL21(DE3)star cells significantly improve the stability of mRNA transcripts and increase protein expression yield from the T7 promoter-based vectors.

Based on the pETCATPO construct, CATPO was expressed in the cytoplasm of *E. coli* and its expression was induced through adding IPTG. This is beneficial as

(i) *E. coli* produces endogenous catalase (HPI and HPII) in the cytoplasm, which are induced independently (Loewen *et al.*, 1985) and differently from CATPO and (ii) purified native CATPO from *S. thermophilum* is green in colour suggesting the presence of heme *d* and (iii) the closest structure homologue of *S. thermophilum* CATPO from BLAST analysis is the *P. vitale* catalase (PDB, 2IUJ) (Appendix L) which is again related to *E. coli* HPII catalase (PDB, 1GGE). Both of which are heme *d* containing catalases.

The four different factors are prone to have an effect on the activity and the yield of the ensuing catalase: growth temperature, induction time, exogenous heme addition and culture oxygenation.

Heme *d* containing HPII is expressed in *E. coli* during stationary phase (section 1.1.4). Heme *d* is also required for the part of the respiratory (membrane-bound) cytochrome *bd* quinol oxidase during oxygen limitation (Rice and Hempfling, 1978). Therefore, cells were grown until stationary phase at low aeration (120 rpm). However, under poor or no aeration growth conditions, *E. coli* produces HPII containing a mixture of hemes *b* and *d*. The heme *b* of HPII is converted into heme *d* by treatment with hydrogen peroxide (Loewen *et al.*, 1993), which is also likely to be case for *S. thermophilum* CATPO when activated in the cytoplasm of *E. coli*, and because T7 promoter on pET28a gives strong induction the temperature was dropped to 30°C and the IPTG concentration was minimised to 0.1 mM. No hemin or δ -aminolevulinic acid was added as it is possible that this reduces heme *d* content and favors heme *b* production (Kimoto *et al.*, 2008).

Considering the information related to the expression of catalases given above, initial expression was carried out at three different temperatures (20, 30 and 37°C) all at 120 rpm with *ca.* 2.5x head space versus the volume of the flask for 24 hours. No protein of *ca.* 79 kDa (theoretical mass, estimated from *expasy*) was observed when IPTG was added and cells were expressed at 20°C (Figure 3.32). However, inducible bands were observed in the soluble fraction and pellets were significantly greener when induced with IPTG and grown at 30°C or 37°C (Figure 3.32). Pellets were also more intensely green when tested at 5x head space-however this was linked to increasingly insoluble expression.

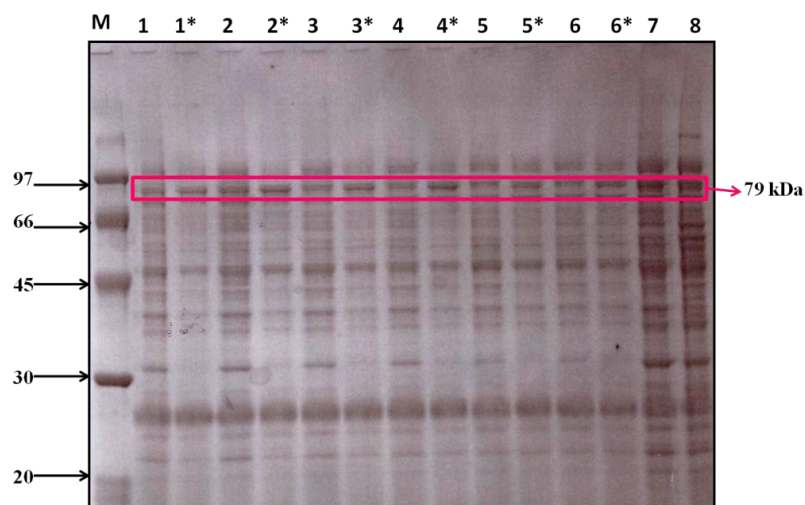


Figure 3.32 Expression profile of CATPO at different temperatures and in the presence of IPTG. *M*, molecular size marker (Low molecular weight-SDS marker, GE Healthcare); *, 0.1 mM IPTG addition; *Lane 1-7*, BL21(DE3)star growth at different temperatures and shaking rates; *Lane 8*, XL-1 Blue (Control) growth at 37°C and 200 rpm; *Lane 1-2**, growth at 37°C and 120 rpm; *Lane 3-4**, growth at 30°C and 120 rpm; *Lane 5-6**, growth at 20°C and 120 rpm; *Lane 7*, growth at 37°C and 200 rpm

Catalase activity results showed that activity was higher for those expressed at 30°C under IPTG induction (Table 3.7). An increase in catalase activity was correlated with induction of the *catpo* gene which was above that of basal levels of endogenous HPII tested using pETCATPO transformed in *E. coli* XL-1 Blue cells (which lack the λ DE3 lysogen and can therefore not express genes from a pET vector using the T7 system). *E. coli* BL21 and XL-1 are unlikely to differ significantly with respect to their endogenous HPII activities.

Table 3.7 Catalase activity measurements under different growth conditions

Conditions	Relative catalase activity (%)
Control (XL-1 Blue)	7.96
No IPTG, 30°C growth T, 200rpm *	34
0.1 mM IPTG, 30°C growth T, 200 rpm *	42,5
No IPTG, 37°C growth T, 200rpm *	47.7
0.1 mM IPTG, 37°C growth T, 200rpm *	15.9
No IPTG, 30°C growth T, 120rpm *	11.8
0.1 mM IPTG, 30°C growth T, 120rpm *	63
No IPTG, 37°C growth T, 120rpm *	21
0.1 mM IPTG, 37°C growth T, 120rpm *	21
No IPTG, 30°C growth T, 120rpm **	36
0.1 mM IPTG, 30°C growth T, 120rpm **	100
No IPTG, 37°C growth T, 120rpm **	34
0.1 mM IPTG, 37°C growth T, 120rpm **	47

**, Cells were grown for 16 hours; **, Cells were grown for 24 hours*

As presented in Figure 3.33, band at *ca.* 79 kDa appears in induced *E. coli* BL21(DE3)star, but not uninduced expression host or XL-1 Blue control. Induced band corresponds to increased catalase activity (Figure 3.33 & Table 3.7).

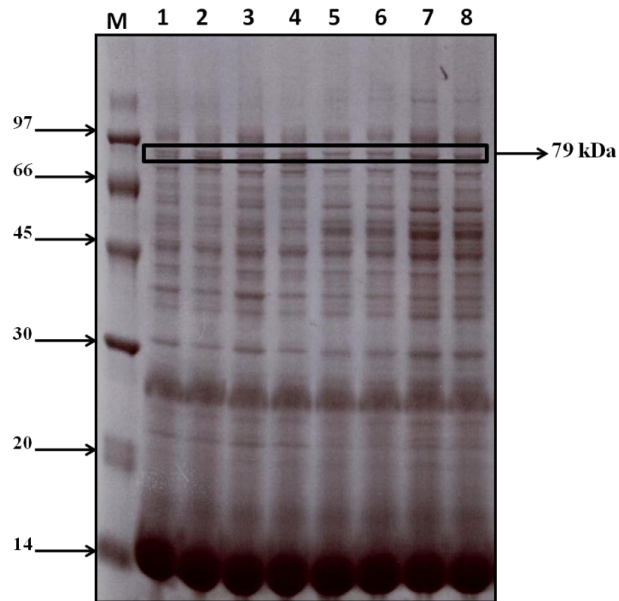


Figure 3.33 Optimisation of CATPO expression. *M*, molecular size marker (Low molecular weight-SDS marker, GE Healthcare); *Lane 1*, 2.5x head space, BL21(DE3)star, no IPTG; *Lane 2*, 2.5x head space, BL21(DE3)star, 0.1 mM IPTG; *Lane 3*, 5x head space, BL21(DE3)star, no IPTG; *Lane 4*, 5x head space, BL21(DE3)star, 0.1 mM IPTG; *Lane 5*, 2.5x head space, XL-1 Blue, no IPTG; *Lane 6*, 2.5x head space, XL-1 Blue, 0.1 mM IPTG; *Lane 7*, 5x head space, XL-1 Blue, no IPTG; *Lane 8*, 5x head space, XL-1 Blue, 0.1 mM IPTG

To conclude from optimisation results, both specific catalase and phenol oxidase activities were higher, when pETCATPO was transformed into *E. coli* BL21(DE3)star cells and expressed at 30°C in the presence of IPTG in 2.5x head space volume at 120 rpm shaking rate (Table 3.8).

Table 3.8 Expression optimisation results of CATPO

	Catalase activity (U/mL)	Phenol oxidase activity (U/mL)	Protein concentration (mg/mL)	Specific activity of catalase (U/mg)	Specific activity of phenol oxidase (U/mg)
XL-1 Blue cells, no IPTG, 2.5x head space	0	0.05	3.06	0	0.016
XL-1 Blue cells, 0.1mM IPTG, 2.5x head space	0.7	0.3	3.58	0.18	0.08
BL-21(DE3)star cells, no IPTG, 2.5x head space	2.9	0.46	4.33	0.68	0.1
BL-21(DE3)star cells, 0.1mM IPTG, 2.5x head space	8.7	0.49	4.37	2	0.11
XL-1 Blue cells, no IPTG, 5x head space	0	0.09	3.75	0	0.02
XL-1 Blue cells, 0.1mM IPTG, 5x head space	0.4	0.14	4	0.09	0.03
BL-21(DE3)star cells, no IPTG, 5x head space	3.8	0.1	3.67	1.	0.026
BL-21(DE3)star cells, 0.1mM IPTG, 5x head space	2.34	0.3	4.6	0.50	0.06

3.4.3 Site-Directed Mutagenesis on *catpo* Gene of *S. thermophilum*

Mutations were performed to explore the oxidase activity of catalase from *S. thermophilum*. Two conserved residues, histidine and valine, in the active site of almost all monofunctional catalases were targeted to analyse the effect of these mutations on the phenol oxidase and catalase activities.

These mutations are expected to inhibit the catalase activity. If the phenol oxidase activity shares the same active site, phenol oxidase activity should also be inhibited or negatively affected.

3.4.3.1 Primer Design for QuickChange Site-Directed Mutagenesis

A number of highly conserved residues are situated in the main channel (section 1.1.8.3). These include His101 and Val142 (according to *S. thermophilum* catalase numbering). His101 lies directly above the heme *d* and is essential for activity (Melik-Adamyan *et al.*, 2001), while the importance of Val142 is to constrict the narrowest, hydrophobic portion of the channel (Chelikani *et al.*, 2003).

Two specific primers were designed to mutate His101 and Val142, as described in section 2.2.9.1. The distal His101 residue is absolutely required for the protoheme (heme *b*) to heme *d* conversion and a change of histidine to asparagine results in heme *b* (Loewen *et al.*, 1993). In turn, Val142 is situated 8 Å from heme *d* and responsible for the entry of larger organics (e.g. phenolic-like compounds) (Chelikani *et al.*, 2003). The mutation of Val142 equivalent in *E. coli* HP11 (V169) has been demonstrated to reduce catalase activity by 12-fold but still retaining the heme *d* (Chelikani *et al.*, 2003).

Therefore, the H101N and V142F variants would test the hypothesis that there are two separate active sites in CATPO by abolishing either catalysis at the heme site and V142F which should exclude the entry of larger organics and although still reducing catalase activity should be observable. The V142F variant should also give an idea whether phenol oxidation occurs at another site by analogy to the *P. vitale* and *E. coli* HP11 catalases, together with the presence of heme *d* in *S. thermophilum* CATPO, catalase activity is likely to at this heme *d* active centre.

3.4.3.2 QuickChange Application to Generate Mutational Variants

Following mutation by thermal cycling and *DpnI* digestion according to the procedure given in section 2.2.9.2, *E. coli* XL-1 Blue competent cells were transformed with the plasmids carrying desired mutations (H101N and V142F). The bands with expected size of approximately 7500 bp were visualized for H101N and V142F by agarose gel electrophoresis (Figure 3.34 & 3.35).

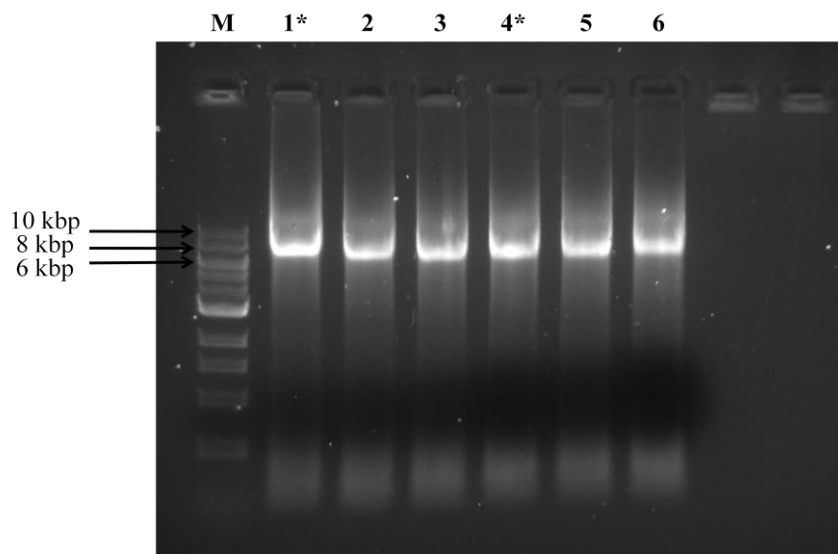


Figure 3.34 Isolation of plasmid carrying H101N mutation. *M*, molecular size marker (1 kbp DNA Ladder, NEB); *Lane 1-6*, analysis of isolated plasmid DNAs; *, positive clone confirmed by sequencing

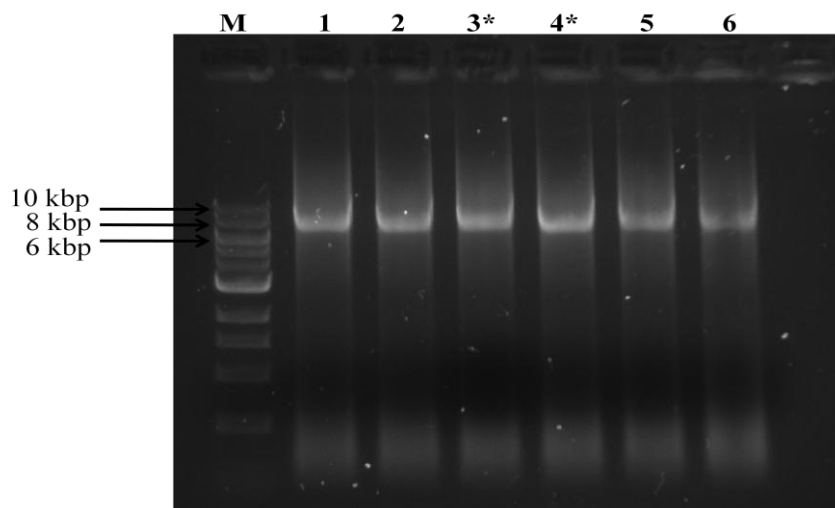


Figure 3.35 Isolation of plasmid carrying V142F mutation. *M*, molecular size marker (1 kbp DNA Ladder, NEB); *Lane 1-6*, analysis of isolated plasmid DNAs; *, positive clone confirmed by sequencing

3.5 Purification Results

Native and recombinant CATPO and mutational variants, H101N and V142F, of CATPO were purified corresponding to the protocols provided in section 2.2.13.

3.5.1 Purification of Native CATPO

Native CATPO was purified by anion exchange followed by gel filtration chromatography as described in section 2.2.13.1.

Purity of CATPO after anion (Figure 3.36) and gel filtration (Figure 3.37) chromatography was checked by running SDS-PAGE. Following collecting fractions of highly pure protein and subsequent concentration, 6-9 mg/mL of pure CATPO (>80 % purity, 44.8 % purification yield) was obtained at the end of the purification process. Specific activities of catalase and phenol oxidases were determined as 46 and 0.4 U/mg, respectively.

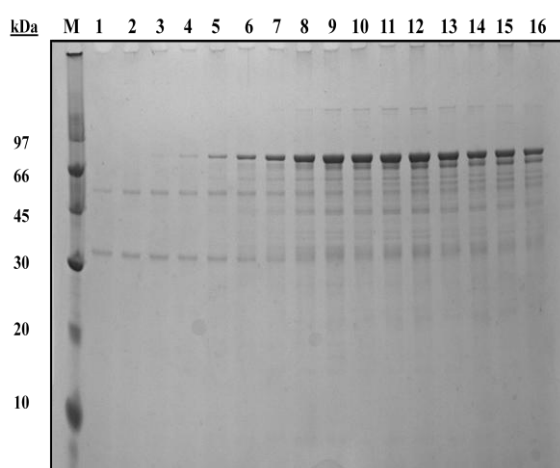


Figure 3.36 SDS-PAGE analysis of fractions from anion exchange chromatography. *M*, molecular size marker (Low molecular weight-SDS marker, GE Healthcare); *Lane 1-16*, fractions in 0.20-0.28 M NaCl region

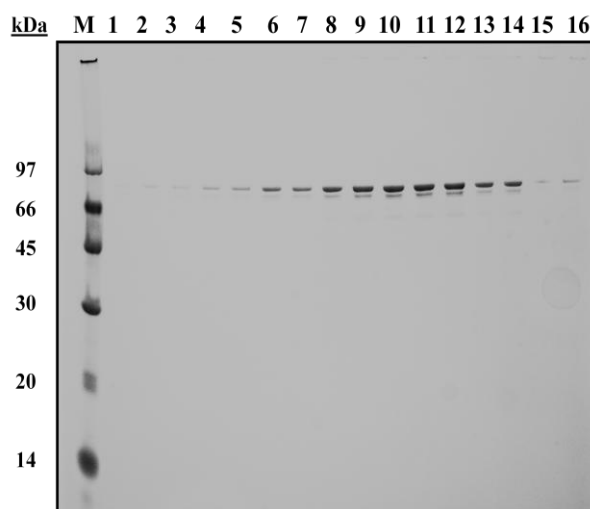


Figure 3.37 SDS-PAGE analysis of fractions from gel filtration chromatography. *M*, molecular size marker (Low molecular weight-SDS marker, GE Healthcare); *Lane 1-16*, fractions eluted between 140-170 min elution time

3.5.2 Purification of Recombinant CATPO

Recombinant wild-type and two variants (H101N and V142F) were purified by one-step affinity chromatography technique. HiTrap Chelating HP (GE Healthcare), when charged with Ni^{2+} ions, selectively retains histidine molecules on the surface of protein. Since all the recombinant variants of CATPO used in this study were histidine-tagged, these proteins were eluted from HiTrap Chelating HP with 20 mM NaPhosphatate buffer containing 0.5 M NaCl and 0.5 M imidazole (to compete with the His-tags for nickel binding), pH 7.4 (as explained in section 2.2.13.2).

Recombinant wild-type CATPO was eluted by collecting 1 mL fractions with imidazole gradient in the range of 0.1-0.5 M. Fractions of 0.19-0.34 M imidazole region were analysed by SDS-PAGE (Figure 3.38). Highly purified recombinant CATPO was detected in the concentration interval of 0.22-0.25 M imidazole.

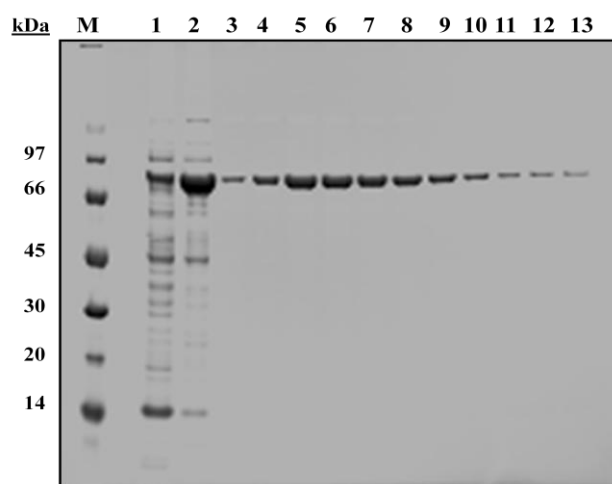


Figure 3.38 SDS-PAGE analysis of fractions of recombinant CATPO eluted from HiTrap Chelating column. *M*, molecular size marker (Low molecular weight-SDS marker, GE Healthcare); *Lane 1*, flow through; *Lane 2*, wash (20 mM NaPhosphate, 0.5 M NaCl, 0.1 M imidazole); *Lane 3-13*, fractions in 0.19-0.34 M imidazole region

H101N and V142F variants were also eluted from the chelating column with imidazole gradient in the range of 0.1-0.5 M. Their degree of purity was investigated by performing SDS-PAGE (Figure 3.39 & Figure 3.40). The fractions including H101N and V142F were collected between 0.32-0.4 M and 0.25-0.31 M imidazole region, respectively.

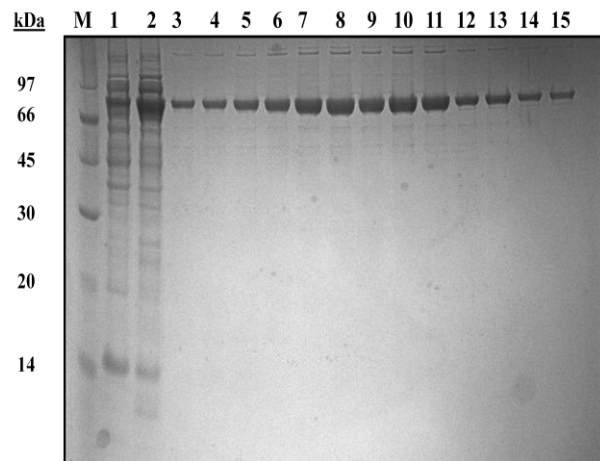


Figure 3.39 SDS-PAGE analysis of fractions of H101N eluted from HiTrap Chelating column. *M*, molecular size marker (Low molecular weight-SDS marker, GE Healthcare); *Lane 1*, flow through; *Lane 2*, wash (20 mM NaPhosphate, 0.5 M NaCl, 0.1 M imidazole); *Lane 3-15*, fractions in 0.28-0.45 M imidazole region

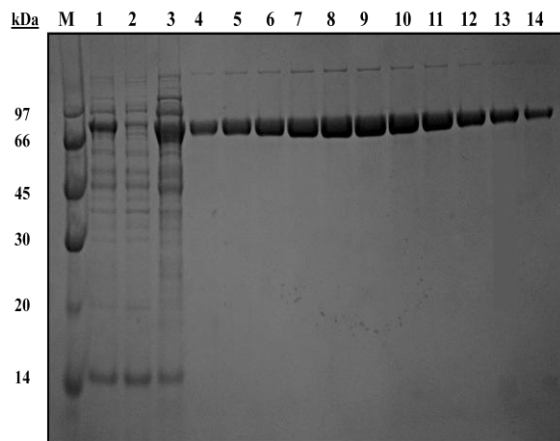


Figure 3.40 SDS-PAGE analysis of fractions of V142F eluted from HiTrap Chelating column. *M*, molecular size marker (Low molecular weight-SDS marker, GE Healthcare); *Lane 1*, flow through; *Lane 2*, wash (20 mM NaPhosphate, 0.5 M NaCl, 0.1 M imidazole); *Lane 3*, crude extract; *Lane 4-14*, fractions in 0.21-0.36 M imidazole region

3.6 Molecular Weight Determination of CATPO

To determine the molecular mass of CATPO, both SDS-PAGE and Native-PAGE were performed as described in section 2.2.10.1 & 2.2.10.2, respectively. Accordingly, CATPO was detected as distinct band of molecular mass *ca.* 320 kDa on native gel and *ca.* 80 kDa on denaturing gel (Figure 3.41).

This outcome showed that CATPO was a tetramer having four identical subunits, supporting the same results observed by Sutay, 2007. The tetrameric structure in catalases (especially monofunctional) is very common (Nicholls *et al.*, 2001). Large subunit catalase like HP11 from *E. coli* (Loewen, 1996) and small subunit catalase BLC (Kirkman and Gaetani, 1984) have been reported to be homotetramers.

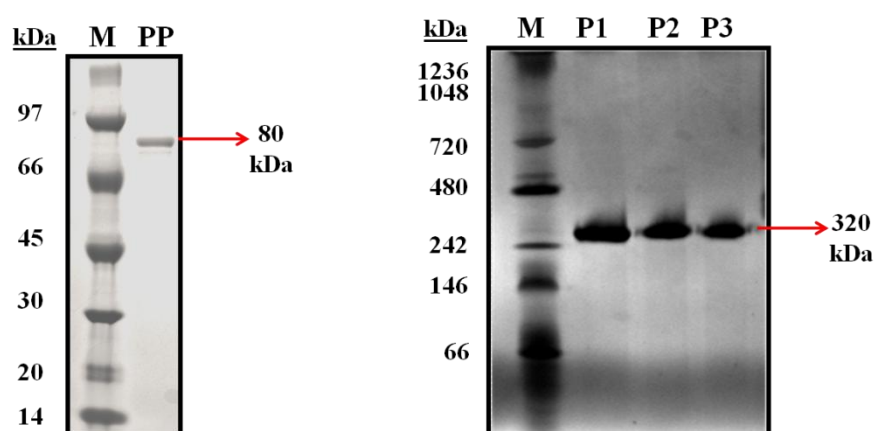


Figure 3.41 Molecular weight determination of CATPO. *Left* shows the SDS-PAGE analysis result: *M*, molecular size marker (Low molecular weight-SDS marker, GE Healthcare); *PP*, purified protein. *Right* shows the Native PAGE analysis result: *M*, molecular size marker (NativeMark™ Unstained Protein Standard, Invitrogen); *P1*, purified protein; *P2&P3*, 2- and 5-fold diluted protein

3.7 UV-Vis Spectra of Native and Recombinant CATPO

To compare the heme contents of native and recombinant CATPO, the UV-Vis spectra of purified native, recombinant wild-type and mutational variants of CATPO were determined in a range of 200-900 nm (Figure 3.42 and 3.43).

The UV-Vis spectrum of native CATPO (6 mg/mL) had absorption maxima at 280, 406, 592 and 691 nm (Figure 3.42). While, the first peak indicates the protein content, the second peak corresponds to Soret band showing the heme content of the sample. The other peaks are responsible for the identification of heme type. This result is similar to that of HPII catalase from *E. coli*, with absorption maxima 407, 590 and 715 nm (Loewen *et al.*, 1993). Since HPII is known to be heme *d* containing green coloured-catalase, this suggests the presence of heme *d* in CATPO.

From the spectrum data, the R_z value (A_{406}/A_{280}) was established as *ca.* 0.5, which is considerably lower than that found in other catalases in nature like *Saccharomyces cerevisiae* (Zámocký and Koller, 1999) having R_z value of *ca.* 1. This suggests that *S. thermophilum* produces CATPO with lower heme content under normal conditions.

The UV-Vis spectra of recombinant wild-type and its variants (H101N and V142F) were presented in Figure 3.43. Accordingly, wild-type and V142F were observed to have absorption maxima at 590 and 714 nm. On the other hand, H101N was shown to have these absorption maxima shifted to 536 and 629 nm, respectively. In other words, the characteristic heme *d* peak at 590 nm disappeared in H101N showing the change of heme *d* into heme *b*.

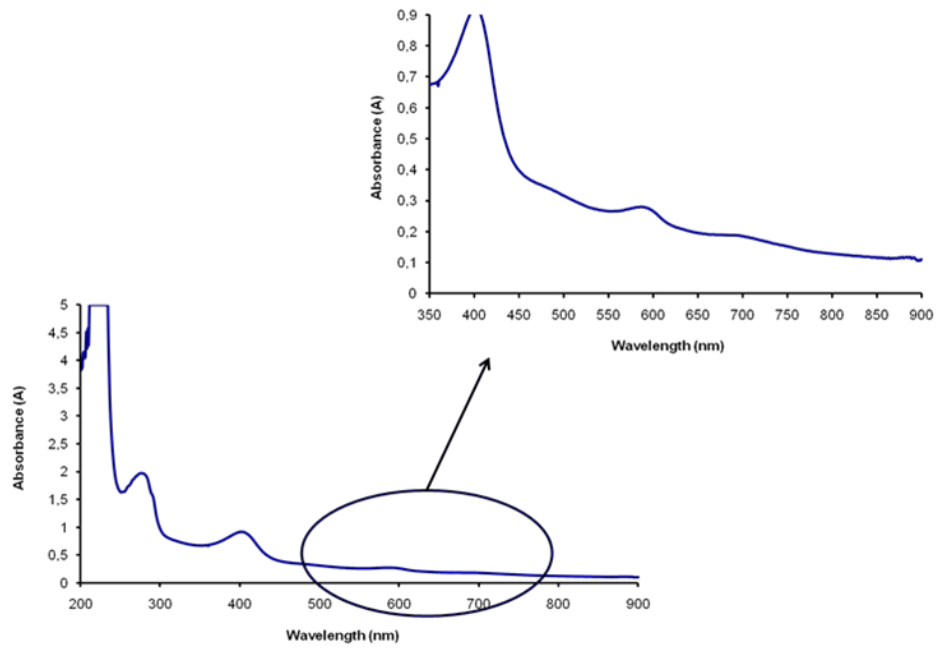


Figure 3.42 UV-Vis spectra of native CATPO.

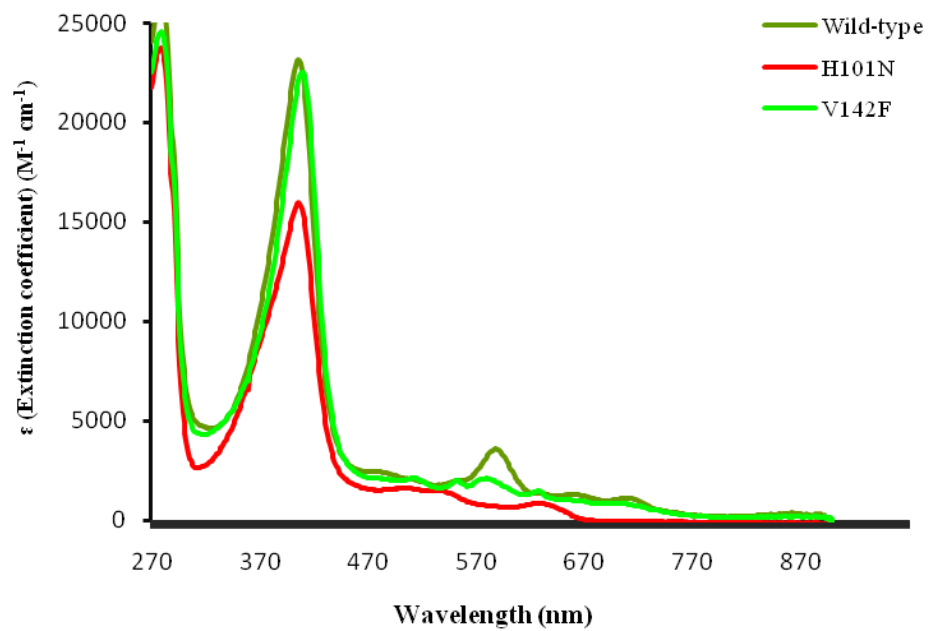


Figure 3.43 The comparison of UV-Vis spectra of recombinant wild-type CATPO, H101N and V142F.

The spectral data for these peaks, normalized to the main Soret absorption at 406 nm, are summarized in Table 3.9. In view of that, the recombinant enzymes show a Soret band ratio ($A_{406}/A_{280} = 0.8$ to 0.9) which indicates a higher heme content than in the native enzyme ($A_{406}/A_{280} = 0.5$). The native CATPO seems to be deficient in heme *d*. This could be due to the process of catalase tetramerization requiring a minimum of one or two heme monomers to fold the enzyme correctly like *Proteus mirabilis* iron deprived catalase produced in *E. coli* (Andreoletti *et al.*, 2003).

Heme *d* containing *E. coli* HP11 catalase has a 407 nm Soret band and a 2-banded high spin ferriheme visible spectrum (590 and 715 nm). A protoheme (heme *b*)-containing enzyme such as HPI has these absorption maxima shifted to 535 and 630 nm, respectively. Considering the characteristic absorption ratios for heme *d* (for recombinant wild type and V142F variants) and heme *b* (for H101N) from Table 3.9, they were consistent with those obtained for *E.coli* HP11 wild type and H128N mutant (for HP11 (wild type) - heme *d*: $A_{590}/A_{407}=0.17$ and $A_{715}/A_{407}=0.06$; for HP11 (H128N) - heme *b*: $A_{535}/A_{407}=0.14$ and $A_{630}/A_{407}=0.09$).

Table 3.9 Absorption spectra data for wild-type and mutant catalase-phenol oxidases produced by *E. coli* BL21(DE3)star cells

Variant	Absorption maxima	Rz (A406/A280)	A536/A406	A590/A406	A629/A406	A714/A406
Wild type	280, 406, 590, 714	0.9		0.15		0.05
H101N	280, 406, 536, 629	0.8	0.099		0.06	
V142F	280, 406, 590, 714	0.8		0.05		0.008

3.8 Specific Activities of Native, Recombinant Wild Type and Mutant CATPOs

Purification and characterisation of native, recombinant wild type and mutant catalase-phenol oxidases was performed. Catalase and phenol oxidase assays were performed at 60°C by the method described in section 2.2.10.5 and their specific activities were compared in Table 3.10.

Recombinant wild type enzyme exhibited the highest catalase and phenol oxidase activities as shown in Table 3.10. This means that heterologous expression of *catpo* gene of *S. thermophilum* caused an increase in the catalase enzyme production by almost 2-fold, but phenol oxidase activity did not change much. It might be related to the heme content of enzyme. As native CATPO contains lower heme *d* than recombinant one, it was not surprising to find lower catalase activity in native enzyme.

H101N and V142F mutants were designed to differentiate catalase and phenol oxidase activities. Namely, the mutations were carried out to test the hypothesis that there are two separate active sites in CATPO for the catalase and phenol oxidase activities. First approach was to abolish catalysis at the heme site and second, to perform V142F mutation which should exclude entry of larger organics like phenolic-like compounds while reducing catalase activity.

As shown in Table 3.11, H101N revealed activities that are 0.21 and 22 % of wild type catalase and phenol oxidase, respectively. Accordingly, H101N seems to have less effect on phenol oxidase activity. This was consistent with the conversion of heme *d* to heme *b*. The absence of the imidazole group of His101, the distal side essential histidine of CATPO, precludes the formation of compound I and results in the H101N variant lacking catalytic activity.

V142F variant showed 0.80 % of wild type catalase activity and 8 % of wild type phenol oxidase activity (Table 3.11). This was reliable since the presence of larger side chain interferes with substrate access to the active site. The catalytic activity was also diminished, but still higher than H101N. V142F had more inhibitory effect on phenol oxidase activity, although both activities were reduced.

As a conclusion, two variants affected catalase and phenol oxidase activities in a negative manner. Both mutations had a dramatic effect on catalase activity and greatly inhibited the phenol oxidase activity. The V142F mutation had a more dramatic effect on phenol oxidase activity. Based on these results, both activities are probably associated with the heme centre.

Table 3.10 Specific activities of purified catalase-phenol oxidase variants

Variant	Specific catalase activity (U/mg)	Specific phenol oxidase activity (U/mg)
Native CATPO	46+/-3	0.4+/-0.03
Recombinant wild type	76+/-0.3	0.5+/-0.01
H101N	0.16+/-0.02	0.11+/-0.03
V142F	0.6+/-0.03	0.04+/-0.02

Table 3.11 Relative activities of purified catalase-phenol oxidase variants

Variant	% Relative catalase activity	% Relative phenol oxidase activity
Recombinant wild type	100	100
H101N	0.21	22
V142F	0.8	8

3.9 Three Dimensional Structure Determination of CATPO

The determination of the protein structure by X-ray crystallography requires growing high-quality crystals of the purified protein, measuring the directions and intensities of X-ray beams diffracted from the crystals, and using a computer to simulate the effects of an objective lens and therefore producing an image of the crystal's contents (Rhodes, 2000).

Scytalidium thermophilum catalase-phenol oxidase (CATPO) structure was determined by obtaining brownish-green crystals by sitting-drop method and sequential X-ray diffraction.

3.9.1 CATPO Crystallisation

During crystallisation experiments, two steps were followed including the determination of initial crystallisation conditions and the optimisation of crystallisation to get high-quality crystals.

Two problems can be faced during crystal growth; to reach a point of saturation at which crystals are formed and then to grow the crystals big enough for diffraction studies. The point of saturation depends on the variation of solubility with the protein concentration, ionic strength, and temperature, the presence of organic solvent, pH and binding of counter ions to the protein (Blundell and Johnson, 1976).

3.9.1.1 Initial Crystallisation Screening

Hundreds of crystallisation experiments were performed for initial screening of crystallisation conditions. Once initial crystals were obtained and confirmed as the crystals of the target macromolecule using X-ray diffraction, the crystallisation conditions were further optimized.

For initial screening, ten different screening kits including Crystal Screen I and II, Index I and II, Membfac and Natrix, SaltRx I and II produced by Hampton Research (USA) covering 296 conditions and Wizard I and II produced by Emerald Biosystems (USA) covering 96 conditions were used. The first observed crystals were needle shaped under the condition of PEG2000 (precipitant) and 0.1 M Bis-Tris buffer (Figure 3.44). Using the initial conditions, large scale crystal trays were prepared.



Figure 3.44 Initial small scale CATPO crystal grown at 18°C.

3.9.1.2 Optimisation of Crystallisation Conditions

After screening the chemical and physical conditions under which the protein has a propensity to crystallize, the chemical and physical parameters were refined to produce crystals suitable for analysis by X-ray diffraction through optimisation stage.

By changing the precipitate type and concentration, buffer type and pH, the brownish-green were observed in a condition of 18-24 % PEG2000, at 0.1 M Bis-Tris buffer at pH between 6.4 and 7.0 (Figure 3.45). These crystals were rod-shaped and rising one from the other. They were better ordered than initial crystals, but not suitable for X-ray data collection. Therefore, additive screening test was performed to find out the best additive promoting single good quality crystal.



Figure 3.45 Rod-shaped CATPO crystals in 22 % PEG2000, at pH 6.8 and 18°C.

It was found that addition of some additives including taurine, iso-propanol, spermidine, and barium chloride improved the quality of crystal. Diamond shaped crystals were obtained at a condition of 18-24 % PEG2000 at pH between 6.4-6.8 and 0.1 M Bis-Tris buffer with either 0.1 M Barium chloride or 0.1 M Taurine. Under these conditions, several crystal trays were set and many single crystals were obtained in 5-7 days (Figure 3.46). Unfortunately, most crystals contained cracks inside, which prevented the good data collection with X-ray.

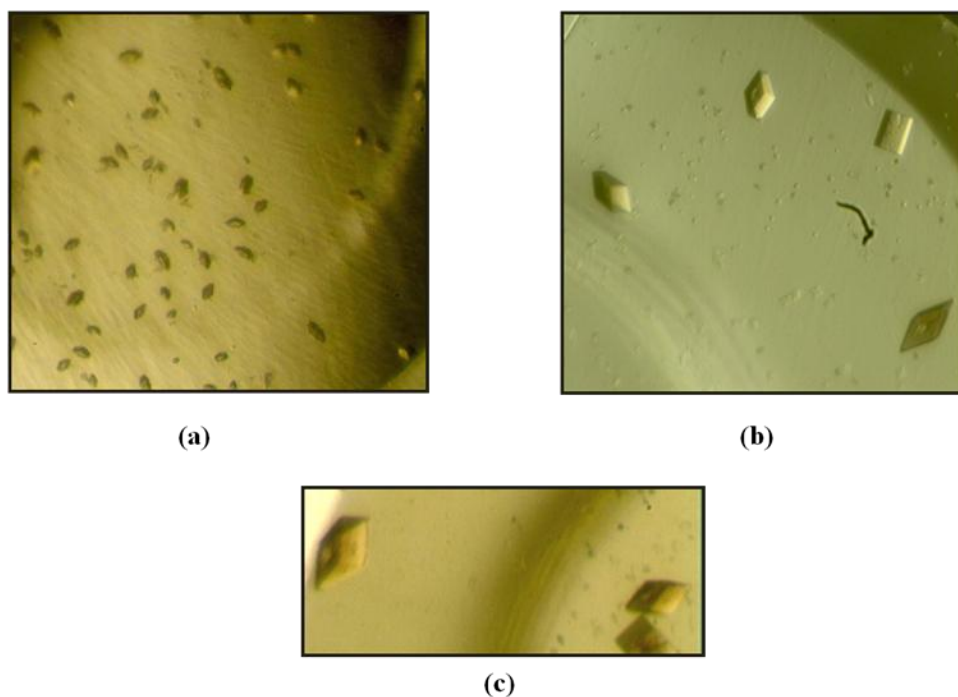


Figure 3.46 CATPO crystals in 24 % PEG2000 at 18°C and (a) pH 6.8 with 0.1 M Taurine, (b) pH 6.4 with 0.1 M Barium chloride (c) pH 6.6 with 0.1 M Barium chloride.

Finally, protein concentration was optimised to enhance the crystal quality. Purified CATPO was utilized at 3-9 mg/mL for setting up crystallisation trays. As shown in Figure 3.47, the best crystal was observed under the condition of 18 % PEG2000 at pH 6.4 with 0.1 M Barium chloride when 9 mg/mL of CATPO was used. This crystal was then cryocooled in liquid nitrogen using PEG2000 as cryoprotectant. Cryoprotectant PEG2000 was added to drop indirectly in diffusion controlled system. Final concentration of PEG2000 was 45 % in reservoir solution.



(a)



(b)

Figure 3.47 The best CATPO crystal in 18 % PEG2000 at pH 6.4 0.1 M Bis-Tris buffer with 0.1 M Barium chloride (a) crystals in drop, (b) single crystal used for X-ray data collection.

3.9.2 Crystallisation of CATPO Variants

Following initial screening test using ten different kits that cover 392 conditions, green coloured crystals of V142F variant were observed as shown in Figure 3.48. Small scale V142F crystals were observed under the condition of 0.2 M potassium chloride, 0.01 M calcium chloride dehydrate, 0.05 M sodium cacodylate trihydrate at 6.0 with 10 % w/v PEG 4000. Large scale crystallisation trays were set at this condition to obtain well ordered crystals at suitable size for X-ray data collection.

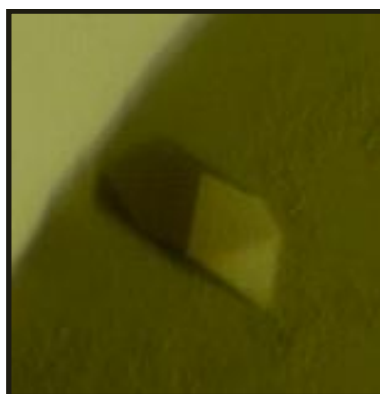


Figure 3.48 Single V142F crystal in 10 % PEG4000 at pH 6.0 0.5 M Sodium cacodylate trihydrate buffer with 0.2 M potassium chloride and 0.01 M calcium chloride dehydrate.

V142F crystal with good quality was then flash cooled with liquid nitrogen using glycerol as cryoprotectant and used for X-ray diffraction. However, high resolution data were not collected due to the lack of cryoprotectant optimisation studies.

3.9.3 Structure of CATPO

Diffraction data were collected using synchrotron radiation at the beam line I04 (Diamond Light Source, UK) at a wavelength of 2.7 Å. CATPO crystals were orthorhombic, space group $P2_12_12$ with four subunits in the crystal asymmetric unit. Diffraction data were obtained from crystals cooled with a nitrogen cryostream giving unit cell parameters of $a=185.4$, $b=216.3$, and $c=68.6$ Å and α , β , and $\gamma=90.0^\circ$.

To solve the structure, the diffraction data set was processed using the program MOSFLM (Collaborative Computational Project, Number 4, 1994), scaled with the program SCALA (Evans, 1997) and reduced using SCALA and TRUNCATE from the CCP4 program suite (Collaborative Computational Project, Number 4,

1994). Structure determination was carried out with the program MOLREP (Vagin and Teplyakov, 1997) using the native PVC structure as the searching model. Refinements were completed using the program REFMAC (Murshudov *et al.*, 1997). Six regions (residues 638-642, 668-670, 673-674, 677, 690-692 and 717) were predicted from gene sequence as they were not detected in electron density map. Model building and refinement were performed using *Coot* and *REFMAC5*.

Preliminary refinement studies showed that the electron density map defines the main chain and side chain atoms of 2,680 amino acids, 20 water molecules and 20 di-NAG compounds with four subunits. The map shows clear continuity in all subunits over the complete length from Glu46 to Ala637. The thirteen residues at the carboxy-domain predicted from gene sequence are disordered in four subunits. Refinement and model building are still in progress.

The preliminary structure of CATPO, shown in Figure 3.49, is composed of four monomers which are interacting with each other.

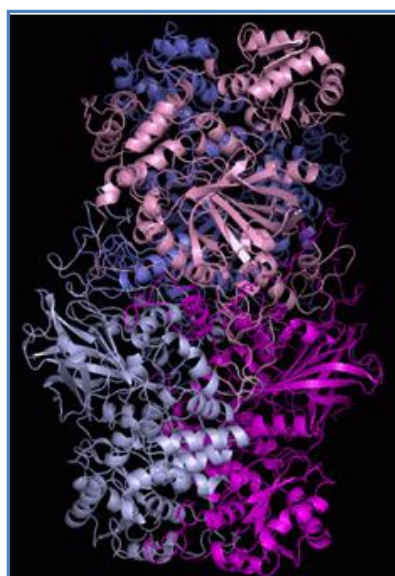


Figure 3.49 Three dimensional structure of CATPO.

The CATPO subunit conformation can be described; similar to those defined by other catalases (Bravo *et al.*, 1999; Díaz *et al.*, 2009; Vainshtein *et al.*, 1986) as being composed of five different regions, including a long amino-terminal arm, an antiparallel eight-stranded β -barrel, an extended wrapping loop, a four helical domain and, in large catalases, a carboxy-terminal domain with flavodoxin like topology joined by a long loop (Figure 3.50a).

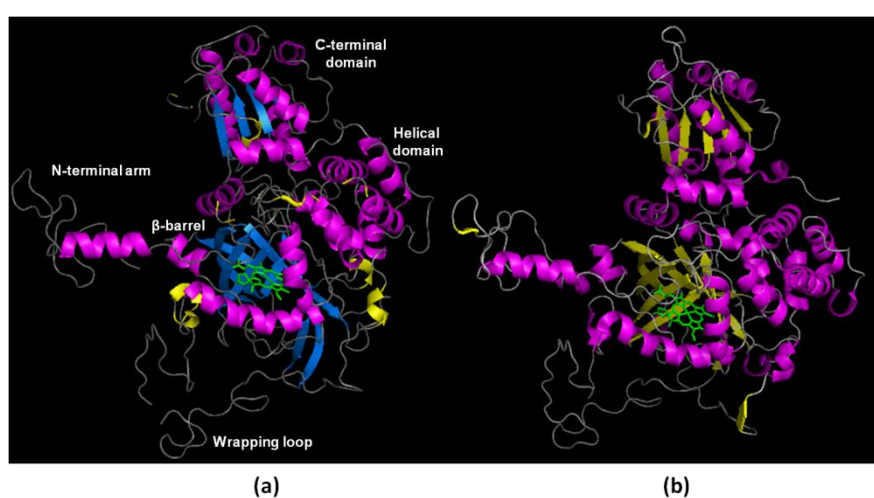


Figure 3.50 Structure of CATPO (a) and PVC (b) monomers.

The structure was very similar to *P. vitale* catalase (PVC) structure (Figure 3.50). The overall amino acid sequence homology with PVC is found to have 63 % identity (NCBI Blast). Similar to PVC, heme molecule is deeply buried inside CATPO structure at about 20 Å from the nearest molecular surface. Both catalases contain the heme *d* group characterised in the active centre of refined CATPO crystal having the cis-hydroxy γ -spirolactone structure, which can be clearly deduced from the electron density map (Figure 3.51). The presence of γ -spirolactone ring and hydroxyl group make the heme *d* more asymmetric with respect to heme *b* in small clade 3 catalases (Murshudov *et al.*, 1996).

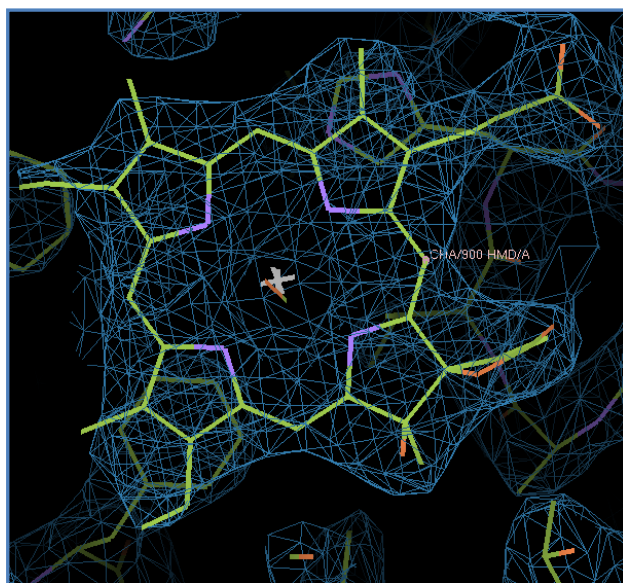


Figure 3.51 Stereo view of (Fo - Fc) omit map of CATPO heme group.

Three residues, tyrosine in the heme proximal side pocket and histidine and asparagines in the distal side, appear to be directly involved in catalysis. In CATPO these residues are Tyr387, His101 and Asn173 (Figure 3.52). As mentioned before, Val142 possibly responsible for the entry of larger organic substrates appeared to be essential for catalytic activity (Figure 3.52).

Tyr387 forms the fifth coordination bond to the iron of the heme (Figure 3.52 & 3.53). Residues governing heme orientation appear to be Pro328, Val246 and Leu379. These residues are also preserved in PVC (Pro291, Val209 and Leu342) (Appendix L).

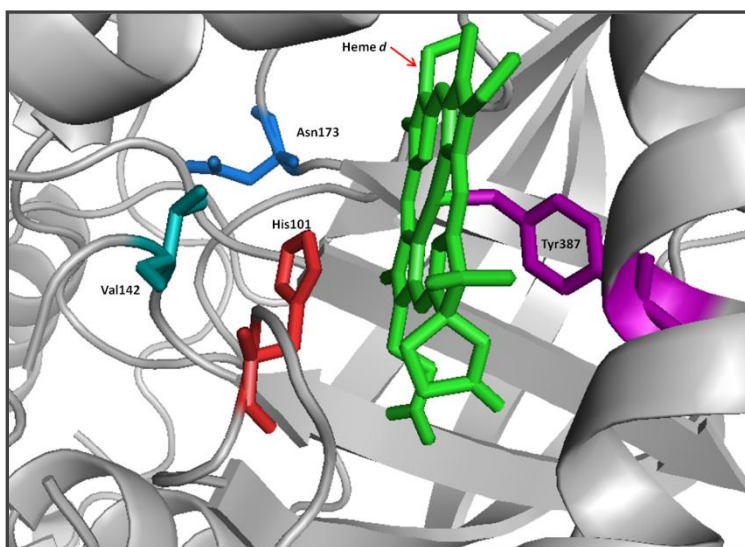


Figure 3.52 View of distal and proximal sites in CATPO.

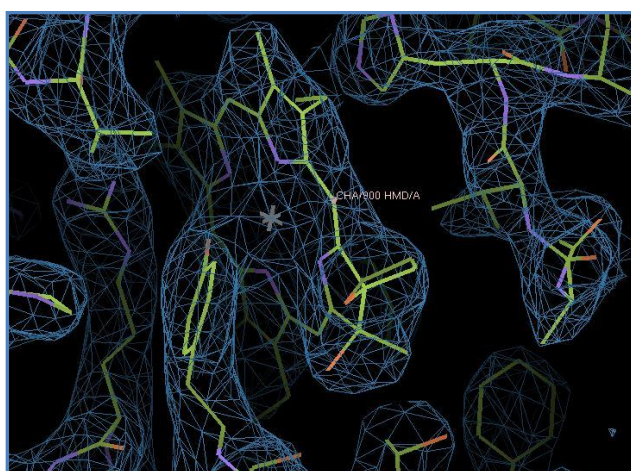


Figure 3.53 Heme centre in CATPO structure with electron density map.

CHAPTER 4

CONCLUSIONS

Catalase-phenol oxidase (CATPO) was the first reported example of a fungal enzyme displaying bifunctional catalase-phenol oxidase activity.

The enzyme was incapable of oxidising tyrosinase and laccase-specific substrates. Its phenol oxidation nature was found to resemble mainly catechol oxidases.

Enzyme production was shown to be enhanced in the presence of caffeic acid, myricetin and resveratrol, while catechol, resorcinol and vanillic acid caused suppression of CATPO production.

CATPO was observed as an efficient biocatalyst for biotransformation of pharmaceutically important organic compounds including L-dopa, hydrobenzoin and resveratrol. The oxidation product of hydrobenzoin, benzoin, was obtained as 65:35 enantiomeric excess of R-benzoin. This result was promising since R enantiomer of benzoin is a valuable drug intermediate in pharmaceutical industry.

Spectroscopic and mutagenesis studies showed that catalase-phenol oxidase (CATPO) contain a heme *d* centre. Both catalase and phenol oxidase activities appeared to occur at the heme.

X-ray crystallography analysis stated that CATPO structure is a tetramer consisting of four monomers which are interacting with each other. The heme component is cis-hydroxychlorin γ -spirolactone which is rotated 180° with

respect to small subunit catalases. Three important residues of heme pocket are shown to be proximal Tyr387 and distal His101 and Asp173.

Bifunctionality may provide some advantages for industrial applications. This novel function of catalase might be important for detoxification and/or in the action of chemoprotective agents.

CHAPTER 5

RECOMMENDATIONS

For future studies, analysis of three dimensional structure of native CATPO should be performed. The structure determination of recombinant CATPO could be completed to compare both native and recombinant forms of the enzyme. The metal content of enzyme can be examined to see any possible metals present other than heme. Optimisation of conditions for kinetic constants determination is indispensable. EPR (Electron paramagnetic resonance) could be performed to identify reaction intermediates in catalytic cycle(s) of CATPO. Further mutagenesis studies could be also done to dissent reaction mechanisms.

REFERENCES

- Abril, N., Pueyo, C., 1990, "Mutagenesis in *Escherichia coli* lacking catalase", *Environmental and Molecular Mutagenesis*, 15: 184-189.
- Aguirre, J., Rios-Momberg, M., Hewitt, D., Hansberg, W., 2005, "Reactive oxygen species and development in microbial eukaryotes", *Trends in Microbiology*, 13(3): 111-118.
- Akagawa, M., Shigemitsu, T., Suyama, K., 2003, "Production of hydrogen peroxide by polyphenols and polyphenol-rich beverages under quasiphysiological conditions", *Bioscience, Biotechnology and Biochemistry*, 67(12): 2632-2640.
- Alfonso-Prieto, M., Borovik, A., Carpena, X., Murshudov, G., Melik-Adamyan, W., Fita, I., Rovira, C., Loewen, P.C., 2007, "The structures and electronic configuration of compound I intermediates of *Helicobacter pylori* and *Penicillium vitale* catalases determined by X-ray crystallography and QM/MM density functional theory calculations", *Journal of American Chemical Society*, 129: 4193-4205.
- Allgood, G.S., Perry, J.J., 1986, "Characterization of a manganese-containing catalase from the obligate thermophile *Thermoleophilum album*", *Journal of Bacteriology*, 168: 563-567.
- Amorim, A.M., Gasques, M.D.G., Andreaus, J., Scharf, M., 2002, "The application of catalase for the elimination of hydrogen peroxide residues after bleaching of cotton fabrics", *Annals of the Brazilian Academy of Sciences*, 74(3): 433-436.
- Andreoletti, P., Sainz, G., Jaquinod, M., Gagnon, J., Jouve, H.M., 2003, "High-resolution structure and biochemical properties of a recombinant *Proteus mirabilis* catalase depleted in iron", *Proteins*, 50: 261-71.
- Angelova, M.B., Pashova, S.B., Spasova, B.K., Vassilev, S.V., Slokoska, L.S., 2005, "Oxidative stress response of filamentous fungi induced by hydrogen peroxide and paraquat", *Mycological Research*, 109(2): 150-158.
- Aoshima, H. Ayabe, S., 2007, "Prevention of the deterioration of polyphenol-rich beverages", *Food Chemistry*, 100: 350-355.
- Arnao, M.B., Acosta, M., del Río, J.A., Varón, R., García-Cánovas, F., 1990, "A kinetic study on the suicide inactivation of peroxidase by hydrogen peroxide", *Biochimica et Biophysica Acta*, 1041(1): 43-47.

- Ashby, J., Tinwell, H., Pennie, W., Brooks, A., Lefevre, P., Beresford, N., Sumpter, J., 1999, "Partial and weak oestrogenicity of the red wine constituent resveratrol: consideration of its superagonist activity in MCF-7 cells and its suggested cardiovascular protective effects", *Journal of Applied Toxicology*, 19: 39-45.
- Ates, S., Cortenlioglu, E., Bayraktar, E., Mehmetoglu, U., 2007, "Production of L-dopa using Cu-alginate gel immobilized tyrosinase in a batch and packed bed reactor", *Enzyme and Microbial Technology*, 40: 683-687.
- Bajpai, P., 1999, "Application of enzymes in the pulp and paper industry", *Biotechnology Progress*, 15: 147-157.
- Baxter, R.A., 2008, "Anti-aging properties of resveratrol: review and report of a potent new antioxidant skin care formulation", *Journal of Cosmetic Dermatology*, 7: 2-7.
- Beers, Jr., R.F., Sizer, I.W., 1952, "A spectrophotometric method for measuring the breakdown of hydrogen peroxide by catalase", *Journal of Biological Chemistry*, 195(1): 133-140.
- Belozerskaya, T.A., Gessler, N.N., 2006, "Oxidative stress and differentiation in *Neurospora crassa*", *Microbiology*, 75(4): 427-431.
- Blundell, T.L., Johnson, L.N., 1976, "Protein Crystallography", 1st Ed., *Academic Press Inc.*, London, Great Britain.
- Bonnichsen, R.K., Chance, B., Theorell, H., 1947, "Catalase activity", *Acta Chemica Scandinavica*, Vol: 1.
- Bowers, J.L., Tyulmenkov, V.V., Jernigan, S.C., Klinge, C.M., 2000, "Resveratrol acts as a mixed agonist/antagonist for estrogen receptors {alpha} and {beta}", *Endocrinology*, 141: 3657-3667.
- Bradford, M.M., 1976, "A rapid and sensitive method for the quantitation of microgram quantities of protein utilizing the principle of protein-dye binding", *Analytical Biochemistry*, 72: 248-254.
- Bravo, J., Verdager, N., Tormo, J., Betzel, C., Switala, J., Loewen, P.C. and Fita, I., 1995, "Crystal structure of catalase HPII from *Escherichia coli*", *Structure*, 3: 491-502.
- Bravo, J., Fita, I., Ferrer, J.C., Ens, W., Hillar, A., Switala, J., Loewen, P.C., 1997, "Identification of a novel bond between a histidine and the essential tyrosine in catalase HPII of *Escherichia coli*", *Protein Science*, 6: 1016-1023.
- Bravo, J., Mate, M.J., Schneider, T., Switala, J., Wilson, K., Loewen, P.C., Fita, I., 1999, "Structure of catalase HPII from *Escherichia coli* at 1.9 Å resolution", *Proteins*, 34: 155-66.

- Burdon, R.H., 1995, "Superoxide and hydrogen peroxide in relation to mammalian cell proliferation", *Free Radical Biology and Medicine*, 18: 775-794.
- Burton, S.G., 2001, "Development of bioreactors for application of biocatalysts in biotransformations and bioremediation", *Pure and Applied Chemistry*, 73(1): 77-83.
- Burton, S.G., 2003, "Laccases and phenol oxidases in organic synthesis-a review", *Current Organic Chemistry*, 7: 1317-1331.
- Bussink, H.J., Oliver, R., 2001, "Identification of two highly divergent catalase genes in the fungal tomato pathogen *Cladosporium fulvum*", *European Journal of Biochemistry*, 268: 15-24.
- Calera, J.A., Sánchez-Weatherby, J., López-Medrano, R., Leal, F., 2000, "Distinctive properties of the catalase B of *Aspergillus nidulans*", *FEBS Letters*, 475: 117-120.
- Caridis, K.A., Christakopoulos, P., Macris, B.J., 1991, "Simultaneous production of glucose oxidase and catalase by *Alternaria alternate*", *Applied Microbiology and Biotechnology*, 34: 794-797.
- Carpena, X., Soriano, M., Klotz, M.G., Duckworth, H. W., Donald, L.J., Melik-Adamyanyan, W., Fita, I., Loewen, P.C., 2003, "Structure of the clade 1 catalase, *CatF* from *Pseudomonas syringae* at 1.7 Å resolution", *Proteins*, 50: 423-436.
- Carvalho, G.M.J., Alves, T.L.M., Freire, D.M.G., 2000, "L-dopa production by immobilized tyrosinase", *Applied Biochemistry and Biotechnology*, 84-86: 791-800.
- Cattani, L., Ferri, A., 1994, "The function of NADPH bound to catalase", *J Biol Res-Boll Soc It Biol Sper*, 70: 75-82.
- Ceni, G.C., Baldissera, E.M., Antunes, O.A., Vladimir Oliveira, J., Dariva C, de Oliveira D., 2008, "Oxidases from mate tea leaves (*Ilex paraguariensis*): extraction optimization and stability at low and high temperatures", *Bioprocess and Biosystems Engineering*, 31: 541-50.
- Chayen, N.E., Saridakis, E., 2008, "Protein crystallization: from purified protein to diffraction-quality crystal", *Nature Methods*, 5(2): 147-153.
- Chelikani, P., Carpena, X., Fita, I., Loewen, P.C., 2003, "An electrical potential in the access channel of catalases enhances catalysis", *The Journal of Biological Chemistry*, 278: 31290-31296.
- Chelikani, P., Donald, L.J., Duckworth, H.W., Loewen, P.C., 2003, "Hydroperoxidase II of *Escherichia coli* exhibits enhanced resistance to proteolytic cleavage compared to other catalases", *Biochemistry*, 42: 5729-5735.

- Chelikani, P., Fita, I., Loewen, P.C., 2004, "Diversity of structures and properties among catalases", *CMLS Cellular and Molecular Life Sciences*, 61: 192-208.
- Cichewicz, R.H.; Kouzi, S.A., 2002, "Resveratrol oligomers: structure, chemistry, and biological activity". In studies in natural products chemistry; *Atta-Ur-Rahman, Ed.; Elsevier Press, Oxford*, 26: 507-579.
- Chu, H., Leeder, J., Gilbert, S., 1975, "Immobilized catalase reactor for use in peroxide sterilization of dairy products", *Journal of Food Science*, 40, 641-643.
- Claus, H., Faber, G., König, H., 2002, "Redox-mediated decolorization of synthetic dyes by fungal laccase", *Applied Microbiology and Biotechnology*, 59: 672-678.
- Claus, L., 2003, "Laccases and their occurrence in prokaryotes", *Archives of Microbiology*, 179: 145-150.
- Collaborative Computational Project, Number 4, 1994, "The CCP4 Suite: Programs for Protein Crystallography", *Acta Crystallographica Section D*, 50: 760-763.
- Cooney, D.G., Emerson, R., 1964, "Thermophilic Fungi: An Account of Their Biology, Activities and Classification", W.H. Freeman Publishers, San Francisco, USA.
- Cowan, M.M., 1999, "Plant products as antimicrobial agents", *Clinical Microbiology Reviews*, 12: 564-582.
- Crystianson, D.W., 1997, "Structural chemistry and biology of manganese metalloenzymes", *Progress in Biophysics and Molecular Biology*, 67: 217-252.
- Deisseroth, A., Dounce, A.L., 1970, "Catalase: Physical and chemical properties, mechanism of catalysis, and physiological role", *Physiological Reviews*, 50: 319-375.
- Díaz, A., Horjales, E., Rudiño-Piñera, E., Arreola, R., Hansberg, W., 2004, "Unusual Cys-Tyr Covalent Bond in a Large Catalase", *Journal of Molecular Biology*, 342: 971-985.
- Díaz, A., Muñoz-Clares, R.A., Rangel, P., Valdés, V.J., Hansberg, W., 2005, "Functional and structural analysis of catalase oxidized by singlet oxygen", *Biochimie*, 87: 205-214.
- Díaz, A., Valdés, V.J., Rudiño-Piñera, E., Horjales, E., Hansberg, W., 2009, "Structure-function relationships in fungal large-subunit catalases", *Journal of Molecular Biology*, 386: 218-32.
- Durán, N., Esposito, E., 2000, "Potential applications of oxidative enzymes and phenoloxidase-like compounds in wastewater and soil treatment: a review", *Applied Catalysis B: Environmental*, 28: 83-99.

- Durante, D., Casadio, R., Martelli, L., Tasco, G., Portaccio, M., De Luca, P., Bencivenga, U., Rossi, S., Di Martino, S., Grano, V., Diano, N., Mita, D.G., 2004, "Isothermal and non-isothermal bioreactors in the detoxification of waste waters polluted by aromatic compounds by means of immobilised laccase from *Rhus vernicifera*", *Journal of Molecular Catalysis B: Enzymatic*, 27(4-6): 191-206.
- Eicken, C., Zippel, F., Büldt-Karentzopoulos, K., Krebs, B., 1998, "Biochemical and spectroscopic characterization of catechol oxidase from sweet potatoes (*Ipomoea batatas*) containing a type-3 dicopper center", *FEBS Letters*, 436: 293-299.
- Emsley, P., Cowtan, K., 2004, "Coot: model-building tools for molecular graphics", *Acta Crystallographica Section D*, 60: 2126-2132.
- Eugenio, M.E., Carbajo, J.M., Martín, J.A., González, A.E., Villar, J.C., 2009, "Laccase production by *Pycnoporus sanguineus* under different culture conditions", *Journal of Basic Microbiology*, 49: 1-8.
- Evans, P.R., 1997, "Scala", *Joint CCP4 and ESF-EACBM Newsletter*, 33: 22-24.
- Evans, P., 2005, "Scaling and assessment of data quality", *Acta Crystallographica D*, 62: 72-82.
- Feofilova, E.P., Tereshina, V.M., 1999, "Thermophilicity of mycelial fungi in the context of biochemical adaptation to thermal stress", *Applied Biochemistry and Microbiology* 35: 486-494.
- Ferguson, L.R., 2001, "Role of plant polyphenols in genomic stability", *Mutation Research*, 475: 89-111.
- Fita, I., Rossmann, M.G., 1985, "The active center of catalase", *Journal of Molecular Biology*, 185: 21-37.
- Fita, I., Silva, A.M., Murthy, M.R.N., Rossmann, M.G., 1986, "The refined structure of beef liver catalase at 2.5 Å resolution", *Acta Crystallographica-Section B: Structural Crystallography and Crystal Chemistry*, 42: 497-515.
- Fraaije, M.W., Roubroeks, H.P., Hagen, W.R., Van Berkel, W.J.H., 1996, "Purification and characterization of an intracellular catalase-peroxidase from *Penicillium simplicissimum*", *European Journal of Biochemistry*, 235: 192-198.
- Frugoli, J.A., McPeck, M.A., Thomas, T.L., McClung, C.R., 1998, "Catalase is encoded by a multigene family in *Arabidopsis thaliana* Heynh. *Landsberg erecta*", *Plant Physiology*, 112: 327-336.
- Garcia-Molina, F., Hiner, A.N.P., Fenoll, L.G., Rodriguez-Lopez, J.N., Garcia-Ruiz, P.A., Garcia-Canovas, F., Tudela, J., 2005, "Mushroom tyrosinase: Catalase activity, inhibition and suicide inactivation", *Journal of Agricultural and Food Chemistry*, 53: 3702-3709.

- Garman, E.F., Owen, R.L., 2006, "Cryocooling and radiation damage in macromolecular crystallography", *Acta Crystallographica Section D*, 62: 32-47.
- Gehm, B., McAndrews, J., Chien, P., Jameson, J., 1997, "Resveratrol, a polyphenolic compound found in grapes and wine, is an agonist for the estrogen receptor", *Proceedings of the National Academy of Sciences*, 94: 14138-14143.
- Gerdemann, C., Eicken, C., Krebs, B., 2002, "The crystal structure of catechol oxidase: new insight into the function of type-3 copper proteins", *Accounts of Chemical Research*, 35: 183-191.
- Gerdemann, C., Eicken, C., Magrini, A., Meyer, H.E., Rompel, A., Spener, F., Krebs, B., 2001, "Isoenzymes of *Ipomoea batatas* catechol oxidase differ in catalase-like activity", *Biochemica et Biophysica Acta*, 1548: 94-105.
- Gessler, N.N., Sokolov, A.V., Bykhovsky, V.Y., Belozerskaya, T.A., 2002, "Superoxide Dismutase and Catalase Activities in Carotenoid-Synthesizing Fungi *Blakeslea trispora* and *Neurospora crassa* Fungi in Oxidative Stress", *Applied Biochemistry and Microbiology*, 38: 205-209.
- Gouet, P., Jouve, H.M., Dideberg, O., 1995, "Crystal structure of *Proteus mirabilis* PR catalase with and without bound NADPH", *Journal of Molecular Biology*, 249: 933-954.
- Griffith, G.W., 1994. "Phenoloxidases", *Progress in Industrial Microbiology*, 29: 763-788.
- Hakansson, K.O., Brugna, M., Tasse, L., 2004, "The three dimensional structure of catalase from *Enterococcus faecalis*", *Acta Crystallographica D*, 60: 1374-1380.
- Halaouili, S., Asther, M., Sigoillot, J-C, Hamdi, M., Lomascolo, A., 2006a, "Fungal tryrosinases: new prospects in molecular characteristics, bioengineering and biotechnological applications", *Journal of Applied Microbiology*, 100: 219-232.
- Hara, I., Ichise, N., Kojima, K., Kondo, H., Ohgiya, S., Matsuyama, H., Yumoto, I., 2007, "Relationship between the size of the bottleneck 15 Å from iron in the main channel and the reactivity of catalase corresponding to the molecular size of substrates", *Biochemistry*, 46: 11-22.
- Hearn, V.M., Wilson, E.V., Mackenzie, D.W.R., 1992, "Analysis of *Aspergillus fumigatus* catalases possessing antigenic activity", *Journal of Medical Microbiology*, 36: 61-67.
- Heim, K.E., Tagliaferro, A.R., Bobilya, D.J., 2002, "Flavonoid antioxidants: chemistry, metabolism and structure-activity relationships", *The Journal of Nutritional Biochemistry*, 13: 572-584.

- Hillar, A., Nicholls, P., 1992, "A mechanism for NADPH inhibition of catalase compound II formation", *FEBS Letters*, 314:179-182.
- Hisada, H., Hata, Y., Kawato, A., Abe, Y., Akita, O., 2005, "Cloning and expression analysis of two catalase genes from *Aspergillus oryzae*", *Journal of Bioscience and Bioengineering*, 99: 562-568.
- Hortner, H., Ammerer, G., Hartter, E., Hamilton, B., Rytka, J., Bilinski, T., Ruis, H., 1976, "Regulation of synthesis of catalases and iso-1-cytochrome C in *Saccharomyces cerevisiae* by glucose, oxygen and heme", *European Journal of Biochemistry*, 128: 179-184.
- Isobe, K., Inoue, N., Takamatu, Y., Kamada, K., Wakao, N., 2006, "Production of catalase by fungi growing at low pH and high temperature", *Journal of Bioscience and Bioengineering*, 101: 73-76.
- Jeandet, P., Douillet-Breuil, A.C., Bessis, R., Debord, S., Sbaghi, M., Adrian, M., 2002, "Phytoalexins from the vitaceae: biosynthesis, phytoalexin gene expression in transgenic plants, antifungal activity, and metabolism", *Journal of Agricultural Food Chemistry*, 50, 2731-2741.
- Jolley, R.L. Jr., Evans, L.H., Makino, N., Mason, H.S., 1974, "Oxytyrosinase", *The Journal of Biological Chemistry*, 249(2): 335-345.
- Jones, P., 2001, "Roles of water in heme peroxidase and catalase mechanisms" *The Journal of Biological Chemistry*, 276: 13791-13796.
- Jones, P., Dunford, H.B., 2005, "The mechanism of compound I formation revisited", *Journal of Inorganic Biochemistry*, 99: 2292-2298.
- Kalko, S.G., Gelpí, J.L., Fita, I., Orozco, M., 2001, "Theoretical study of the mechanisms of substrate recognition by catalase", *Journal of American Chemical Society*, 123: 9665-9672.
- Kamel M.Y., Tahany M.N., 1973, "*Penicillium notatum* catalase purification and properties", *Acta biologica et medica Germanica*, 30: 13-23.
- Kaptan, Y., 2004, "Utilization of *Scytalidium thermophilum* phenol oxidase in bioorganic synthesis", M.Sc. Thesis, METU, Ankara, Turkey.
- Kawasaki L., Aguirre, J., 2001, "Multiple catalase genes are differentially regulated in *Aspergillus nidulans*", *Journal of Bacteriology*, 1434-1440.
- Khan, A.U., Wilson, T., 1995, "Reactive oxygen species as cellular messengers", *Chemistry and Biology*, 2: 437-445.
- Khangulov, S.V., Barynin, V.V., Antonyuk-Barynina, S.V., 1990(a), "Manganese-containing catalase from *Thermus thermophilus* peroxide e-induced redox transformation of manganese ions in presence of specific inhibitors of catalase activity", *Biochimica et Biophysica Acta*, 1020: 25-33.

Khangulov, S.V., Barynin, V.V., Voevodskaya, N.V., Grebenko, A. I., 1990(b), "ESR spectroscopy of the binuclear cluster of manganese ions in the active center of Mn-catalase from *Thermus thermophilus*", *Biochimica et Biophysica Acta*, 1020: 305-310.

Khangulov, S.V., Goldfeld, M.G., Gerasimenko, V.V., Andreeva, N.E., Barynin, V.V., Grebenko, A. I., 1990(c), "Effect of anions and redox state on the activity of manganese containing catalase from *Thermus thermophilus*", *Journal of Inorganic Biochemistry*, 40: 279-292.

Kim, J.A., Sha, Z., Mayfield, J.E., 2000, "Regulation of *Brucella abortus* catalase", *Infection and Immunity*, 68: 3861-3866.

Kimoto, H., Matsuyama, H., Yumoto, I., Yoshimune, K., 2008, "Heme content of recombinant catalase from *Psychrobacter sp.* T-3 altered by host *Escherichia coli* cell growth conditions", *Protein Expression and Purification*, 59: 357-359.

Kirkman, H.N., Gaetani, G.F., 1984, "Catalase: a tetrameric enzyme with four tightly bound molecules of NADPH", *Proceedings of the National Academy of Sciences*, 81: 4343-4347.

Kirkman, H.N., Gaetani, G.F., 2006, "Mammalian catalase: a venerable enzyme with new mysteries", *Trends in Biochemical Sciences*, 32(1): 44-50.

Klotz, M., Klassen, G., Loewen, P.C., 1997, "Phylogenetic relationships among prokaryotic and eukaryotic catalases", *Molecular Biology and Evolution*, 14: 951-958.

Klotz, M.G., Loewen, P.C., 2003, "The molecular evolution of catalatic hydroperoxidases: Evidence for multiple lateral transfer of genes between Prokaryota and from Bacteria into Eukaryota", *Molecular Biology and Evolution* 20: 1098-1112.

Ko, T-P, Safo, M.K., Musayev, F.N., Di Salvo, M.L., Wang, C., Wu, S-H, Abraham, D.J., 1999, "Structure of human erythrocyte catalase", *Acta Crystallographica Section D Biological Crystallography*, 56: 241-245.

Kocabas, D.S., Bakir, U., Phillips, S.E.V., McPherson, M.J., Ogel, Z.B., 2008, "Purification, characterization, and identification of a novel bifunctional catalase-phenol oxidase from *Scytalidium thermophilum*", *Applied Microbiology and Biotechnology*, 79: 407-415.

Kocabas, D.S., Pearson, A.R., Phillips, S.E.V., Bakir, U., Ogel, Z.B., McPherson, M.J., Trinh, C., 2009, "Crystallization and preliminary X-ray analysis of a bifunctional catalase-phenol oxidase from *Scytalidium thermophilum*", *Acta Crystallographica Section F: Structural Biology and Crystallization Communications*, 65: 486-488.

- Kono, Y., Fridovich, I., 1983, "Isolation and characterization of the pseudocatalase of *Lactobacillus plantarum*", *Journal of Biological Chemistry*, 258: 6015-6019.
- Krebs, B., 1995, "Purple acid phosphatases and catechol oxidase and their model compounds. Crystal structure of purple acid phosphatase from kidney beans", *In Bioinorganic Chemistry: An Inorganic Perspective of Life*, Edited by Kessissoglou DP. Dordrecht, Kluwer Academic Publishers: 371-384.
- Kwon, S., Anderson, A.J., 2001, "Catalase activities of *Phanerochaete chrysosporium* are not coordinately produced with ligninolytic metabolism: catalases from a white-rot fungus", *Current Microbiology*, 42: 8-11.
- Lafay, S., Gueux, E., Rayssiguier, Y., Mazur, A., Rémésy, C., Scalbert, A., 2005, "Caffeic acid inhibits oxidative stress and reduces hypercholesterolemia induced by iron overload in rats", *International Journal for Vitamin and Nutrition Research*, 75: 119-125.
- Lafay, S., Morand, C., Manach, C., Besson, C., Scalbert, A., 2006, "Absorption and metabolism of caffeic acid and chlorogenic acid in the small intestine of rats", *British Journal of Nutrition*, 96: 39-46.
- Lavermicocca, P., Valerio, F., Evidente, A., Lazzaroni, S., Corsetti, A. & Gobbetti, M., 2000. "Purification and characterization of novel antifungal compounds from the sourdough *Lactobacillus plantarum* strain 21B", *Applied and Environmental Microbiology*, 66: 4084-4090.
- Lee, K.W., Lee, H.J., 2006, "Biphasic effects of dietary antioxidants on oxidative stress-mediated carcinogenesis", *Mechanisms of Ageing and Development*, 127: 424-431.
- Leonowicz, A., Cho, N.S., Luterek, J., Wilkolazka, A., Wojtas-Wasilewska, M., Matuszewska, A., Hofrichter, M., Wesenberg, D., Rogalski, J., 2001, "Fungal laccase: properties and activity on lignin", *Journal of Basic Microbiology*, 41: 185-227.
- Lerch, K., 1976, "*Neurospora* tyrosinase: molecular weight, copper content and spectral properties", *FEBS Letters*, 69(1): 157-60.
- Lerch, K., Ettlinger, L., 1972, "Purification and properties of a tyrosinase from *Streptomyces glaucescens*", *Pathologia et Microbiologia*, 38(1): 23-25.
- Leslie, A.G.W., 2006, "The integration of macromolecular diffraction data", *Acta Crystallographica Section D*, 62: 48-57.
- Levy, E., Eyal, Z., Hochmant, A., 1992, "Purification and characterization of a catalase-peroxidase from the fungus *Septoria tritici*", *Archives of Biochemistry and Biophysics*, 296: 321-327.

- Lim, J.-Y., Ishiguro, K., Kubo, I., 1999, "Tyrosinase inhibitory *p*-coumaric acid from ginseng leaves", *Phytotherapy Research*, 13: 371-375.
- Loewen, P.C., 1984, "Isolation of catalase-deficient *Escherichia coli* mutants and genetic mapping of *katE*, a locus that affects catalase activity", *Journal of Bacteriology*, 157: 622-626.
- Loewen, P.C., Switala, J., Triggs-Raine, B.L., 1985, "Catalases HPI and HPII in *Escherichia coli* are induced independently", *Archives of Biochemistry and Biophysics*, 243: 144-149.
- Loewen, P.C., Switala, J., 1986, "Purification and characterization of catalase HPII from *Escherichia coli* K12", *Biochemistry and Cell Biology*, 64: 638-646.
- Loewen, P.C., Switala, J., 1987, "Multiple catalases in *Bacillus subtilis*", *Journal of Bacteriology*, 169: 3601-3607.
- Loewen, P.C., Switala, J., von Ossowski, I., Hillar, A., Christie, A., Tattrie, B., Nicholls, P., 1993, "Catalase HPII of *Escherichia coli* catalyzes the conversion of protoheme to cis-heme *d*", *Biochemistry*, 32: 10159-10164.
- Loewen, P.C., 1996, "Probing the structure of catalase HPII of *Escherichia coli*-a review", *Gene*, 179(1): 39-44.
- Loewen, P.C., 1997, "Bacterial catalases", *Oxidative Stress and the Molecular Biology of Antioxidant Defences*, Cold Spring Harbor Laboratory Pres: 273-308.
- Loewen, P.C., Hu, B., Strutinsky, J., Sparling, R., 1998, "Regulation in the *rpoS* regulon of *Escherichia coli*", *Canadian Journal of Microbiology*, 44: 707-717.
- Loewen, P.C., 1999, *Encyclopedia of molecular biology*, A Wiley-Interscience Publication.
- Loewen, P.C., Klotz, M.G., Hassett, D.J., 2000, "Catalase- an "old" enzyme that continues to surprise us", *ASM (American Society for Microbiology) News*, 66: 76-82.
- Loewen, P.C., Carpena, X., Rovira, C., Ivancich, A., Perez-Luque, R., Haas, R., Odenbreit, S., Nicholls, P., Fita, I., 2004, "Structure of *Helicobacter pylori* catalase, with and without formic acid bound, at 1.6 Å resolution", *Biochemistry*, 43: 3089-3103.
- Lule, S.U., Xia, W.S., 2005, "Food phenolics, pros and cons: a review", *Food Reviews International*, 21: 367-388.
- Lyons, G.A., Sharma, H.S.S., 1998, "Differentiation of *Scytalidium thermophilum* isolates by thermogravimetric analyses of their biomass", *Mycological Research*, 102, 843-849.

- Maheswari, R., Bharadwaj, G., Bhat, M., 2000, "Thermophilic fungi: their physiology and enzymes", *Microbiology and Molecular Biology Reviews*, 64: 461-488.
- Maj, M., Loewen, P.C., Nicholls, P., 1998, "*E. coli* HP11 catalase interaction with high spin ligands: formate and fluoride as active site probes", *Biochimica et Biophysica Acta*, 1384: 209-222.
- Manach, C., Scalbert, A., Morand, C., Rémésy, C., Jiménez, L., 2004, "Polyphenols: food sources and bioavailability", *The American Journal of Clinical Nutrition*, 79: 727-47.
- Marusek, C.M., Trobaugh, N.M., Flurkey, W.H., Inlow, J.K., 2006, "Comparative analysis of polyphenol oxidase from plant and fungal species", *Journal of Inorganic Biochemistry*, 100: 108-123.
- Mate, M., Murshudov, G., Bravo, J., Melik-Adamyan, W., Loewen, P.C, Fita, I., 2001, "Heme-catalases", *Handbook of proteins*.
- Maté, M.J., Sevinc, M.S., Hu, B., Bujons, J., Bravo, J., Switala, J., Ens, W., Loewen, P.C., Fita, I., 1999, "Mutants that alter the covalent structure of catalase hydroperoxidase II from *Escherichia coli*", *The Journal of Biological Chemistry*, 274: 27717-27725.
- Maté, M.J., Zamocky, M., Nykyri, L. M., Herzog, C., Alzari, P.M., Betzel, C., Koller, F., Fita, I., 1999, "Structure of catalase A from *Saccharomyces cerevisiae*", *Journal of Molecular Biology*, 286: 135-139.
- Mayer, A.M., Harel, E., 1979, "Polyphenol oxidases in plants", *Phytochemistry*, 18: 193-215.
- Mayer, A.M., 1987, "Polyphenol oxidases in plants-recent progress", *Phytochemistry*, 26: 11-20.
- Mayer, A.M., 2006, "Polyphenol oxidases in plant and fungi: going places? A review", *Phytochemistry*, 67: 2318-2331.
- Mayfield, J.E, Duvall, M.R., 1996, "Anomalous phylogenies based on bacterial catalase gene sequences", *Journal of Molecular Evolution*, 42: 469-471.
- Mazzafera, P., Robinson, S.P., 2000, "Characterization of polyphenol oxidase in coffee", *Phytochemistry*, 55: 285-296.
- McCann, M.P., Kidwell, J.P., Matin, A., 1991, "The putative σ factor *KatF* has a central role in development of starvation-mediated general resistance in *Escherichia coli*", *Journal of Bacteriology*, 173: 4188-4194.
- Meir, E., Yagil, E., 1990, "Regulation of *Escherichia coli* catalases by anaerobiosis and catabolite repression", *Current Microbiology*, 20: 139-144.

Melik-Adamyan, W.R., Barynin, V.V., Vagin, A.A., Borisov, V.V., Vainshtein, B.K., Fita, I., Murthy, M.R.N., Rossmann, M.G., 1986, "Comparison of Beef Liver and *Penicillium vitale* Catalases", *Journal of Molecular Biology*, 188: 63-72.

Melik-Adamyan, W., Bravo, J., Carpena, X., Switala, J., Maté, M.J., Fita, I., Loewen, P.C., 2001, "Substrate flowing catalases deduced from the crystal structures of active site variants of HPII from *Escherichia coli*", *PROTEINS: Structure, Function, and Genetics*, 44: 270-281.

Merle, P.L., Sabourault, C., Richier, S., Allemand, D., Furla, P., 2007, "Catalase characterization and implication in bleaching of a symbiotic sea anemone", *Free Radical Biology and Medicine*, 42: 236-246.

Mete, S., 2003, "Scytalidium thermophilum polyphenol oxidase: production and partial characterization", M.Sc. Thesis, METU, Ankara, Turkey.

Meyer, A.S., Pedersen, L.H., Isaksen, A., 1997, "The effect of various food parameters on the activity and stability of catalase from *Aspergillus niger* and catalase from bovine liver", *Food Chemistry*, 60: 137-142.

Mikolasch, A., Schauer, F., 2009, "Fungal laccases as tools for the synthesis of new hybrid molecules and biomaterials", *Applied Microbiology and Biotechnology*, 82: 605-624.

Minussi, R.C., Pastore G.M., Duran N., 2002, "Potential applications of laccase in the food industry", *Trends Food Science and Technology*, 13: 205-216.

Miura, T., Muraoka, S., Fujimoto, Y., Zhao, K., 2000, "DNA damage induced by catechol derivatives", *Chemico-Biological Interactions*, 126: 125-136.

Morozova, O.V., Shumakovich, G.P., Gorbacheva, M.A., Shleev, S.V., Yaropolov, A.I., 2007, "Blue laccases", *Biochemistry (Moscow)*, 72: 1136-1150.

Moyer, D., 1997, "Scytalidium catalase gene", United States Patent, No. 5646025.

Mueller, S., Riedel, H., Stremmel, W., 1997, "Determination of catalase activity at physiological hydrogen peroxide concentrations", *Analytical Biochemistry*, 245: 55-60.

Mulvey, M.R., Switala, J., Borys, A., Loewen, P.C., 1990, "Regulation of transcription of *katE* and *katF* in *Escherichia coli*", *Journal of Bacteriology*, 172: 6713-6720.

Murshudov, G.N., Melik-Adamyan, W.R., Grebenko, A.I., Barynin, V.V., Vagin, A.A., Vainshtein, B.K., Dauter, Z., Wilson, K., 1992, "Three-dimensional structure of catalase from *Micrococcus lysodeikticus* at 1.5 Å resolution", *FEBS Letters*, 312: 127-131.

- Murshudov, G.N., Grebenko, A.I., Barynin, V., Dauter, Z., Wilson, K.S., Vainshtein, B.K., Melik-Adamyanyan, W., Bravo, J., Ferrer, J.C., Switala, J., Loewen, P.C., Fita, I., 1996, "Structure of the Heme *d* of *Penicillium vitale* and *Escherichia coli* Catalases", *The Journal of Biological Chemistry*, 271: 8863-8868.
- Murshudov, G.N., Vagin, A.A., Dodson, E.J., 1997, "Refinement of macromolecular structures by the maximum-likelihood method", *Acta Crystallographica. Section D: Biological Crystallography*, 53: 240-255.
- Murthy, M.R.N., Reid, T.J., Sicignano, A., Tanaka, N., Rossmann, M.G., 1981, "Structure of beef liver catalase", *Journal of Molecular Biology*, 152: 465-499.
- Nakamura, K., Go, N., 2005, "Function and molecular evolution of multicopper blue proteins", *Cellular and Molecular Life Sciences*: 1-17.
- Nardini, M., Natella, F., Gentili, V., DiFelice, M., Scaccini, C., 1997, "Effect of caffeic acid dietary supplementation on the antioxidant defense system in rat: an *in vivo* study", *Archives of Biochemistry and Biophysics*, 342: 157-160.
- Natella, F., Nardini, M., Giannetti, I., Dattilo, C., Scaccini, C., 2002, "Coffee drinking influences plasma antioxidant capacity in humans", *Journal of Agricultural and Food Chemistry*, 50: 6211-6216.
- Navarro, R.E., Stringer, M.A., Hansberg, W., Timberlake, W.E., Aguirre, J., 1996, "*CatA*, a new *Aspergillus nidulans* gene encoding a developmentally regulated catalase", *Current Genetics*, 29: 352-359.
- Nicholls, P., Fita, I., Loewen, P.C., 2001, "Enzymology and structure of catalases", *Advances in Inorganic chemistry*, 51: 51-106.
- Nicotra, S., Cramarossa, M.R., Mucci, A., Pagnoni, U.M., Riva, S., Forti, L., 2004, "Biotransformation of resveratrol: synthesis of trans-dehydrodimers catalyzed by laccases from *Myceliophthora thermophyla* and from *Trametes pubescens*", *Tetrahedron*, 60: 595-600.
- Ohyama, M., Tanaka, T., Ito, T., Iinuma, M., Bastow, K.F., Lee, K.-H., 1999, "Antitumor agents 200. ¹ cytotoxicity of naturally occurring resveratrol oligomers and their acetate derivatives", *Bioorganic and Medicinal Chemistry Letters*, 9: 3057-3060.
- Oikawa, S., Furukawaa, A., Asada, H., Hirakawa, K., Kawanishi, S., 2003, "Catechins induce oxidative damage to cellular and isolated DNA through the generation of reactive oxygen species", *Free Radical Research*, 37: 881-890.
- Oshino, N., Oshino, R., Chance, B., 1973, "The characteristics of the peroxidatic reaction of catalase in ethanol oxidation", *Biochemical Journal*, 131: 555-567.
- Ow, Y.Y., Stupans, I., 2003, "Gallic acid and gallic acid derivatives: effects on drug metabolising enzymes", *Current Drug Metabolism*, 4: 241-248.

Ögel, Z.B., Yarangümeli, K., Dü, H., Ifrij, İ., 2001, "Submerged cultivation of *Scytalidium thermophilum* on complex lignocellulosic biomass for endoglucanase production", *Enzyme and Microbial Technology*, 28: 689-695.

Ögel, Z.B., Yüzügüllü, Y., Mete, S., Bakir, U., Kaptan, Y., Sutay, D., Demir, A.S., 2006, "Production, properties and application to biocatalysis of a novel extracellular alkaline phenol oxidase from the thermophilic fungus *Scytalidium thermophilum*", *Applied Microbiology and Biotechnology*, 71: 853-862.

Paris, S., Wysong, D., Debeaupuis, J.P., Shibuya, K., Philippe, B., Diamond, R.D., Latge, J.P., 2003, "Catalases of *Aspergillus fumigatus*", *Infection and Immunity*, 71: 3551-3562.

Passi, S., Picardo, M., Nazzaro-Porro, M., 1987, "Comparative cytotoxicity of phenols *in vitro*", *Biochemical Journal*, 245: 537-542.

Pazarlıoğlu, N.K., Sarınsık, M., Telefoncu, A., 2005. "Laccase: production by *Trametes versicolor* and application to denim washing", *Process Biochemistry*, 40(5): 1673-1678.

Poulos, T.L, Kraut, J., 1980, "The stereochemistry of peroxidase catalysis", *Journal of Biological Chemistry*, 255: 8199-8205.

Penner-Hahn, J.E., 1992, "Manganese Redox Enzymes", ed. V.L. Pecoraro: 29-45. *VCH Publishers*, New York.

Pierson, M.D., Reddy, N.R., 1982, "Inhibition of *Clostridium botulinum* by antioxidants and related phenolic compounds in comminuted pork", *Journal of Food Science*, 47: 1-4.

Pourcel, L., Routaboul, J.-M., Cheynier, V., Lepiniec, L., Debeaujon, I., 2006, "Flavonoid oxidation in plants: from biochemical properties to physiological functions", *Trends in Plant Science*, 12: 29-36.

Putnam, C. D., Arvai, A. S., Bourne, Y., Tainer, J. A., 2000, "Active and inhibited human catalase structures: ligand and NADPH binding and catalytic mechanism", *Journal of Molecular Biology*, 296: 295-309.

Rahman, I., Biswas, S.K., Kirkham, P.A., 2006, "Regulation of inflammation and redox signaling by dietary polyphenols", *Biochemical Pharmacology*, 72: 1439-1452.

Rauha, J.-P., Remes, S., Heinonen, M., Hopia, A., Kähkönen, M., Kujala, T., Pihlaja, K., Vuorela, H., Vuorela, P., 2000, "Antimicrobial effects of Finnish plant extracts containing flavonoids and other phenolic compounds", *International Journal of Food Microbiology*, 56: 3-12.

Reynolds, L.D., Wilson, N.G., 1991, "Scribes and Scholars" 3rd Edition, Oxford: 193-194.

- Rescigno, A., Sollai, F., Pisu, B., Rinaldi, A., Sanjust, E., 2002, "Tyrosinase inhibition: general and applied aspects", *Journal of Enzyme Inhibition and Medicinal Chemistry*, 17(4): 207-218.
- Rhodes, G., 2000, "Crystallography made crystal clear: A guide for users of macromolecular models", 2nd Edition, Academic Press Inc., London, Great Britain.
- Rice-Evans, C., 2001, "Flavonoid antioxidants", *Current Medicinal Chemistry*, 8: 797-807.
- Richter, H.E., Loewen, P.C., 1982, "Catalase synthesis in *Escherichia coli* is not controlled by catabolite repression", *Archives of Biochemistry and Biophysics*, 215: 72-77.
- Rompel, A., Fischer, H., Meiwes, D., Büldt-Karentzopoulos, K., Magrini, A., Eicken, C., Gerdemann, C., Krebs, B., 1999, "Substrate specificity of catechol oxidase from *Lycopus europaeus* and characterization of the bioproducts of enzymic caffeic acid oxidation", *FEBS Letters*, 445: 103-110.
- Ruis, H., Koller, F., 1997, "Cell biology of yeast fungal catalases. In oxidative stress and the molecular biology of antioxidant defenses" (Scandalios, J.G., ed.), Cold Spring Harbor Laboratory Press, Cold Spring Harbor, NY.
- Sakaguchi, N., Inowe, M., Ogihara, Y., 1998, "Reactive oxygen species and intracellular Ca²⁺, common signals for apoptosis induced by gallic acid", *Biochemical Pharmacology*, 55: 1973-1981.
- Sammartano, L.J., Tuveson, R.W., Davenport, R., 1986, "Control of sensitivity to inactivation by H₂O₂ and broad-spectrum near-UV radiation by *Escherichia coli katF* locus", *Journal of Bacteriology*, 168: 13-21.
- Sanchez-Amat, A., Solano, F., 1997, "A pluripotent polyphenol oxidase from the melanogenic marine *Alteromonas sp* shares catalytic capabilities of tyrosinases and laccases", *Biochemical and Biophysical Research Communications*, 240: 787-792.
- Scandalios, J.G., Guan, L., Polidoros, A.N., 1997, "Catalase in plants: gene structure, properties, regulation, and expression". *Cold Spring Harbor Press*, Cold Spring Harbor, NY.
- Scandalios, J.G., 2005, "Oxidative stress: molecular perception and transduction of signals triggering antioxidant gene defenses", *Brazilian Journal of Medical and Biological Research*, 38: 995-1014.
- Schrader, M., Fahimi, H.D., 2006, "Peroxisomes and oxidative stress", *Biochimica et Biophysica Acta*, 1763: 1755-1766.
- Sevinc, M.S., Mate, M.J., Switala, J., Fita, I., Loewen, P.C., 1999, "Role of the lateral channel in catalase HP_{II} of *Escherichia coli*", *Protein Science*, 8: 490-498.

- Shahidi, F., Naczk, M., 1995, "Food phenolics", *Technomic Publishing Company*, U.S.A.
- Shannon, C.T., Pratt, D.E., 1967, "Apple polyphenol oxidase activity in relation to various phenolic compounds", *Journal of Food Science*, 32: 479.
- Shi, C., Dai, Y., Xia, B., Xu, X., Xie, Y., Liu, Q., 2001, "The purification and spectral properties of polyphenol oxidase I from *Nicotiana tabacum*", *Plant Molecular Biology Reporter*, 19: 381a-381h.
- Sies, H., 1997, "Oxidative stress: oxidants and antioxidants", *Experimental Physiology*, 82: 291-295.
- Silva, E.M., Machucab, A., Milagres, A.M.F., 2004, "Evaluating the growth and enzyme production from *Lentinula edodes* strains", *Process Biochemistry*, 40(1): 161-164.
- Stopper, H., Schmitt, E., Kobras, K., 2005, "Genotoxicity of phytoestrogens", *Mutation Research*, 574: 139-155.
- Storz, G., Tartaglia, L.A., 1992, "OxyR: A regulator of antioxidant genes", *The Journal of Nutrition*, 122: 627-630.
- Straatsma, G., Samson, R.A., Olijnsma, T.W., Op Den Camp, H.J.M., J Gerrits, J.P.G., Van Griensven, L.J.L.D., 1994, "Ecology of thermophilic fungi in mushroom compost, with emphasis on *Scytalidium thermophilum* and growth stimulation of *Agaricus bisporus* mycelium", *Applied and Environmental Microbiology*: 454-458.
- Sumner, J.B., Dounce, A.L., 1937, "Crystalline catalase", *Science*, 121: 417-424.
- Sutay, D., 2007, "Purification, characterization, crystallization and preliminary X-ray structure determination of *Scytalidium thermophilum* bifunctional catalase and identification of its catechol oxidase activity", Ph.D. Thesis, METU, Ankara, Turkey.
- Switala, J., O'Neil, J.O., Loewen, P.C., 1999, "Catalase HPII from *Escherichia coli* Exhibits Enhanced Resistance to Denaturation", *Biochemistry*, 38: 3895-3901.
- Switala, J., Loewen, P.C., 2002, "Diversity of properties among catalases" *ABB Archives of Biochemistry and Biophysisc*, 401: 145-154.
- Takasaka, T., Sayers, N.M., Anderson, M.J., Benbow, E.W., Denning, D.W., 1999, "*Aspergillus fumigatus* catalase: cloning of an *Aspergillus nidulans* catalase B homologue and evidence for at least three catalases", *FEMS Immunology and Medical Microbiology*, 23: 125-133.

Thavasi, V., Bettens, R.P.A., Leong, L.P., 2009, "Temperature and solvent effects on radical scavenging ability of phenols", *Journal of Physical Chemistry A*, 113: 3068-3077.

Timkovich, R., Bondoc, L.L., 1990, "Diversity in the structure of hemes" *Advances in Biophysical Chemistry*, 1: 203-247.

Tomás-Barberán, F.A., Espín, J.C., 2001, "Phenolic compounds and related enzymes as determinants of quality in fruits and vegetables", *Journal of Science of the Food and Agriculture*, 81: 853-876.

Tormo, J., Fita, I., Switala, J., Loewen, P.C., 1990, "Crystallization and preliminary X-ray diffraction analysis of catalase HPII from *Escherichia coli*", *Journal of Molecular Biology*, 213: 219-220.

Torres de Pinedo, A., P. Peñalver, P., Morales, J.C., 2006, "Synthesis and evaluation of new phenolic-based antioxidants: structure-activity relationship", *Food Chemistry*, 103: 55-61.

Trela, B.C., Waterhouse, A.L., 1996, "Resveratrol: isomeric molar absorptivities and stability", *Journal of Agricultural Food Chemistry*, 44: 1253-1257.

Tsuchiya, T., Suzuki, O., Igarashi, K., 1996, "Protective effects of chlorogenic acid on paraquat-induced oxidative stress in rats", *Bioscience, Biotechnology and Biochemistry*, 60: 765-768.

Tuomela, M., Vikman, M., Hatakka, A., Itävaara, M., 2000, "Biodegradation of lignin in a compost environment: a review", *Bioresource Technology*, 72: 169-183.

Urso, M.L., Clarkson, P.M., 2003, "Oxidative stress, exercise, and antioxidant supplementation", *Toxicology*, 189: 41-54.

Vagin, A., Teplyakov, A., 1997, "MOLREP: an automated program for molecular replacement", *Journal of Applied Crystallography*, 30: 1022-1025.

Vagin, A.A., Steiner, R.A., Lebedev, A.A., Potterton, L., McNicholas, S., Long, F., Murshudov, G.N., 2004, "REFMAC5 dictionary: organization of prior chemical knowledge and guidelines for its use", *Acta Crystallographica Section D*, 60: 2184-2195.

Vainshtein, B.K., Melik-Adamyanyan, W.R., Barynin, V.V., Vagin, A.A., Grebenko, A.I., 1981, "Three dimensional structure of the enzyme catalase", *Nature*, 197: 411-412.

Vainshtein, B.K., Melik-Adamyanyan, W.R., Bajyuiu, V.V., Vagiui, A.A., Grcbcuko, A.I., Borisov, V.V., Bartels, K.S., Fita, I., Rossmann, M.G., 1986, "Three-dimensional structure of catalase from *Penicillium vitale* at 2.0 Å resolution", *Journal of Molecular Biology*, 188: 49-61.

- Valko, M., Leibfritz, D., Moncol, J., Mark, T.D., Mazur, C.M., Telser, J., 2007, "Free radicals and antioxidants in normal physiological functions and human disease", *The International Journal of Biochemistry and Cell Biology*, 39: 44-84.
- van Gelder, C.W., Flurkey, W.H., Wichers, H.J., 1997, "Sequence and structural features of plant and fungal tyrosinases", *Phytochemistry*, 45: 1309-1323.
- Vetrano, A.M., Heck, D.E., Mariano, T.M., Mishin, V., Laskin, D.L., Laskin, J.D., 2005. "Characterization of the oxidase activity in mammalian catalase", *The Journal of Biological Chemistry*, 280(42): 35372-35381.
- Volkert, M.R., Loewen, P.C., Switala, J., Crowley, D., Conley, M., 1994, "The $\Delta(\text{argF-lacZ})_{205}(\text{U169})$ deletion greatly enhances resistance to hydrogen peroxide in stationary-phase *Escherichia coli*", *Journal of Bacteriology*, 176: 1297-1302.
- Waldo, G.S., Fronko, R.M., Penner-Hahn, J.E., 1991, "Inactivation and reactivation of manganese catalase: oxidation-state assignments using X-ray absorption spectroscopy", *Biochemistry*, 30: 10486-10490.
- Waldo, G.S., Yu, S., Penner-Hahn, J.E., 1992, "Structural characterization of the binuclear Mn site in *Lactobacillus plantarum* manganese catalase", *Journal of the American Chemical Society*, 114: 5869-5870.
- Waldo, G.S., Penner-Hahn, J.E., 1995, "Mechanism of manganese catalase peroxide disproportionation: determination of manganese oxidation states during turnover", *Biochemistry*, 34: 1507-1512.
- Walker, J.R.L., 1995, "Enzymatic browning in fruits", In C.Y. Lee and J.R. Whitaker (Eds.), *Enzymatic browning and its prevention*, 8-22. Washington, D.C: American Chemical Society.
- Walker, J.R.L., Ferrar, P.H., 1998, "Diphenol oxidase, enzyme-catalysed browning and plant disease resistance", *Biotechnology and Genetic Engineering Reviews*, 15, 457-498.
- Walker, J.R.L., McCallion, R.F., 1980, "The selective inhibition of *ortho* and *para*-diphenol oxidases", *Phytochemistry*, 19(3): 373-377.
- Walter, W.M., Jr. and Purcell, A.E., 1980, "Effect of substrate levels and polyphenol oxidase activity on darkening in sweet potato cultivars", *Journal of Agricultural and Food Chemistry*, 28: 941-944.
- Wang, H., Tokusige, Y., Shinoyama, H., Fujii, T., Urakami, T., 1998, "Purification and characterization of a thermostable catalase from culture broth of *Thermoascus aurantiacus*", *Journal of Fermentation and Bioengineering*, 85: 169-173.

- Whittaker, M.M., Barynin, V.V., Antonyuk, S.V., Whittaker, J.W., 1999, "The oxidized (3,3) state of manganese catalase: comparison of enzymes from *Thermus thermophilus* and *Lactobacillus pantarum*", *Biochemistry*, 38: 9126-9136.
- Wichers, H.J., Gerritse, Y.A., Chapelon, C.G.J., 1996, "Tyrosinase isoforms from the fruitbodies of *Agaricus bisporus*", *Phytochemistry*, 43: 333-337.
- Wiegant, W.M., 1992, "Growth characteristics of the thermophilic fungus *Scytalidium thermophilum* in relation to production of mushroom compost", *Applied and Environmental Microbiology*: 1301-1307.
- Wiegant, W.M., Wery, J., Buitenhuis, E.T., De Bont, J.A.M., 1992, "Growth-promoting effect of thermophilic fungi on the mycelium of the edible mushroom *Agaricus bisporus*", *Applied and Environmental Microbiology*: 2654-2659.
- Wikipedia, 4-tert-butylcatechol, <http://en.wikipedia.org>, last accessed date: 10/12/2009.
- Xu, F., 2001, "Dioxygen reactivity of laccase: dependence on laccase source, pH, and anion inhibition", *Applied Biochemistry and Biotechnology*, 95(2): 125-133.
- Yamazaki, S., Morioka, C., Itoh, S., 2004, "Kinetic evaluation of catalase and peroxxygenase activities of tyrosinase", *Biochemistry*, 43: 11546-11553.
- Yonei, S., Yokota, R., Sato, Y., 1987, "The distinct role of catalase and DNA repair systems in protection against hydrogen peroxide in *Escherichia coli*", *Biochemical and Biophysical Research Communications*, 143: 638-644.
- Zámocký, M., Herzog, C., Nykyri, L. M., Koller, F., 1995, "Site-directed mutagenesis of the lower parts of the major substrate channel of yeast catalase A leads to highly increased peroxidatic activity", *FEBS Letters*, 367: 241-245.
- Zámocký, M., Koller, F., 1999, "Understanding the structure and function of catalases: clues from molecular evolution and *in vitro* mutagenesis", *Progress in Biophysics & Molecular Biology*, 72: 19-66.
- Zámocký, M., Regelsberger, G., Jakopitsch, C., Obinger, C., 2001, "The molecular peculiarities of catalase-peroxidases", *FEBS Letters*, 492: 177-182.

APPENDIX A

GROWTH MEDIA, BUFFERS AND SOLUTIONS PREPARATIONS

Agarose Gel 0.8 % (w/v)

0.8 g agarose is dissolved in 100 mL 1X TAE buffer by heating in microwave.

Bis-Tris (1 M, pH 7)

20.9 g Bis-Tris is dissolved in 100 mL H₂O. It is stirred vigorously on a magnetic stirrer while the pH is adjusted to 7.0 with concentrated HCl.

Barium chloride (0.1 M)

1 g Barium chloride is dissolved in 40 mL H₂O. The volume is adjusted to 50 mL and sterilized by filtration.

CaCl₂ (1 M, 50 mL)

5.55 g of CaCl₂ is dissolved in 40 mL H₂O. The volume is adjusted to 50 mL and sterilized by filtration.

EDTA (0.5 M, pH 8.0)

186.1 g of ethylenedinitrilotetraacetic acid disodium salt dihydrate added to 800 mL of distilled water. It is stirred vigorously on a magnetic stirrer while the pH is adjusted to 8.0 with NaOH pellets. The solution is dispensed into aliquots and sterilized by autoclaving.

Ethanol (70%, 100 mL)

70 mL absolute ethanol is mixed with 30 mL distilled sterile water.

IPTG (1 M)

2.4 g IPTG is dissolved in 10 mL H₂O, filter sterilized, dispensed into aliquots and stored at -20°C.

MgSO₄ (20 mM, per Litre)

4.92 g MgSO₄·7H₂O is dissolved in 1 L distilled water. The solution is sterilized by autoclaving.

LB Broth (per Litre)

10 g Tryptone

5 g Yeast extract

10 g NaCl

Final volume is adjusted to 1 L with distilled water and pH is adjusted to 7.0 with NaOH and autoclaved. The medium is stored at 4°C.

LB Kanamycin Agar (per Litre)

10 g Tryptone

5 g Yeast extract

10 g NaCl

20 g Agar

Final volume is adjusted to 1 L with distilled water and pH is adjusted to 7.0 with NaOH and autoclaved. When it cools to 55°C, 50 µg/mL kanamycin is added and poured to petri dishes. The plates stored at 4°C.

Lysis Buffer (100 mL, pH 8.0)

50 mM HEPES (Na Salt)

25% Sucrose

1% Triton-X 100

5 mM MgCl₂.6H₂O

Final volume is adjusted to 100 mL with distilled water and pH is adjusted to 8.0 by adding a few drops of concentrated HCl. Then, it is sterilized by filtering through 0.22 µm filters and stored at room temperature. 1 mg/mL lysozyme, 5 µL omnicleave and 1 tablet protease inhibitor (ROSH) are added whenever it is used.

NaOH (10 N, 100 mL)

40 g of NaOH pellets is added slowly to 80 mL of H₂O. When the pellets have dissolved completely, the volume is adjusted to 100 mL with H₂O. The solution is stored at room temperature.

NE Buffer (10 X)

0.3 M NaAC (pH 7)

1 mM EDTA

Phosphate (Sodium) Buffer

Stock solution A

2 M monobasic sodium phosphate, monohydrate (276 g/L)

Stock solution B

2 M dibasic sodium phosphate (284 g/L)

Mixing an appropriate volume (mL) of A and B as shown in the table below and diluting to a total volume of 200 mL, a 1 M phosphate buffer of the required pH at room temperature.

Qiagen Buffer P1

50 mM Tris·Cl, pH 8.0

10 mM EDTA

100 µg/mL RNase A

Qiagen Buffer P2

0.2 M NaOH

10% (w/v) SDS

Qiagen Buffer EB

10 mM Tris-Cl, pH 8.5

SDS (10% w/v, per Litre)

100 g of SDS is dissolved in 900 mL of H₂O. The solution is heated to 68°C and stirred with a magnetic stirrer to assist dissolution. If necessary, pH is adjusted to 7.2 by adding a few drops of concentrated HCl. The volume of the solution is adjusted to 1 L with H₂O. It is stored at room temperature.

Saline Tween (ST)

0.8 % NaCl

0.005 % Tween-80 (1:100 dilutions from 0.5% (v/v) Tween-80 stock)

TAE Buffer (50X, per Litre)

242 g of Tris base is dissolved in 600 mL distilled water. The pH is adjusted to 8.0 with approximately 57 mL glacial acetic acid. Then, 100 mL 0.5 M EDTA (pH 8.0) is added and the volume is adjusted to 1 L.

TE Buffer

10 mM Tris- HCl (pH 8.0)

1 mM EDTA (pH 8.0)

TFB 1

30 mM Potassium acetate

10 mM CaCl₂

50 mM MnCl₂

100 mM RbCl

15% (v/v) Glycerol

Adjust pH to 5.8 using 1 M acetic acid. Sterilize through 0.22 μm filter and store at 4°C.

TFB 2

10 mM MOPS

75 mM CaCl₂

10 mM RbCl

15% (v/v) Glycerol

Adjust pH to 6.5 using 1 M KOH. Sterilize using 0.22 μm filter and store at 4°C.

Tris HCl Buffer (50 mM, pH 8.0)

6 g Tris base is dissolved in 800 mL of distilled water. The pH is adjusted to the desired value with concentrated hydrochloric acid. The solution is cooled to room temperature before making final adjustment to pH. The volume of the solution is then adjusted to 1 L with distilled water and sterilized by autoclaving.

YpSs Agar

4.0 g/L Yeast extract
1.0 g/L K_2HPO_4
0.5 g/L $MgSO_4 \cdot 7H_2O$
15.0 g/L Soluble starch
20.0 g/L Agar

YpSs Broth

4.0 g/L Yeast extract
1.0 g/L K_2HPO_4
0.5 g/L $MgSO_4 \cdot 7H_2O$
10 g/L Glucose

YpSs Broth (Modified)

4.0 g/L Yeast extract
1.0 g/L K_2HPO_4
0.5 g/L $MgSO_4 \cdot 7H_2O$
0.1 g/L $CuSO_4 \cdot 5H_2O$
40 g/L Glucose

APPENDIX B

VECTOR MAP

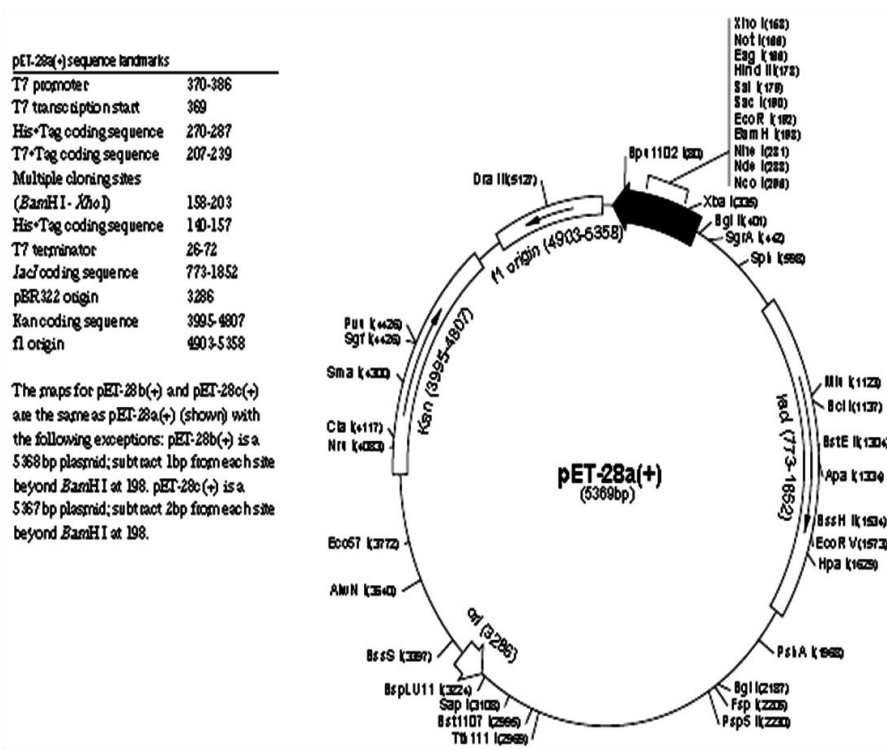


Figure B.1 Map of cloning vector, pET28a, Novagen.

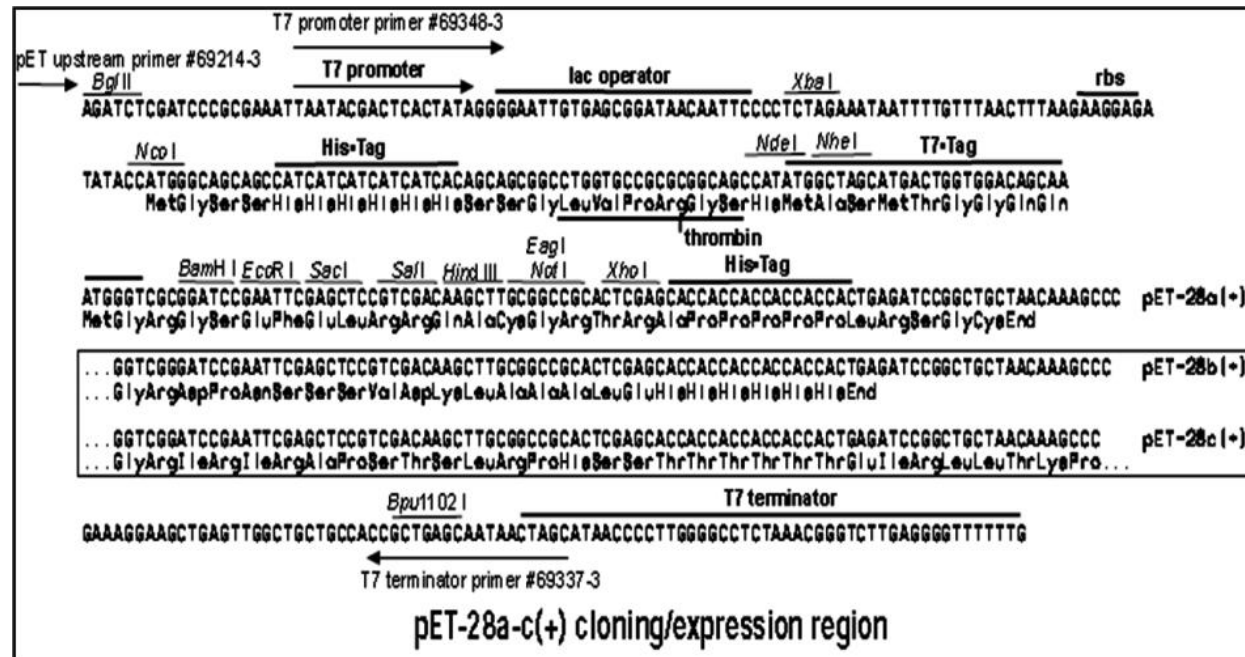


Figure B.1 (continued).

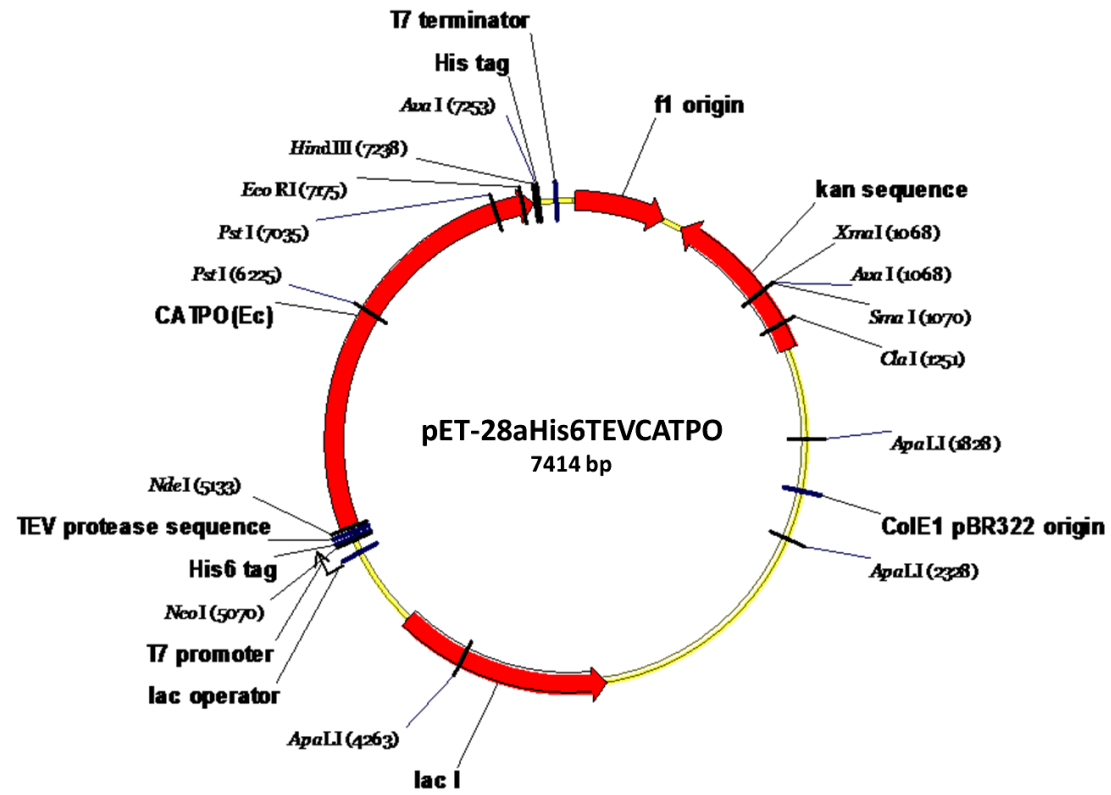


Figure B.2 Map of expression vector, pET-28aHis6TEVCATPO.

APPENDIX C

MOLECULAR SIZE MARKERS

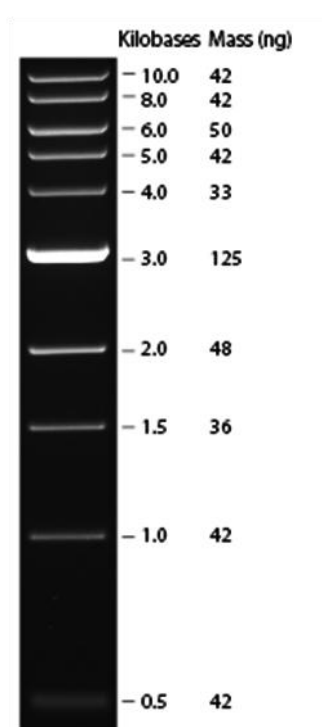


Figure C.1 1 kb DNA Ladder (NEB).

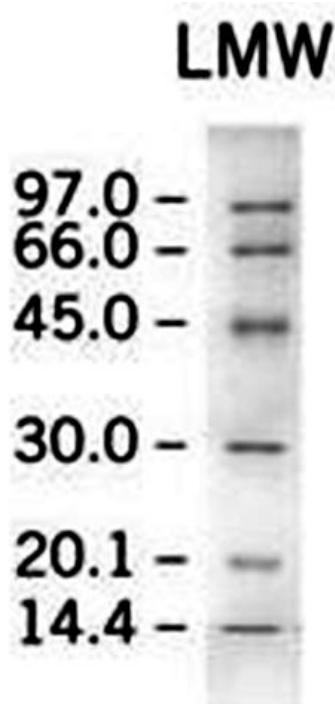
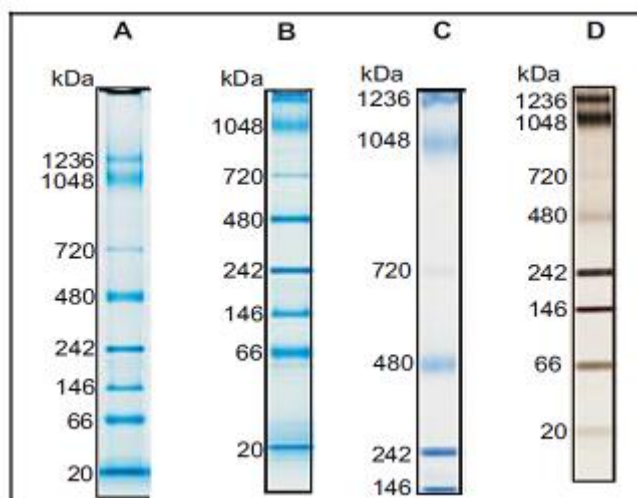


Figure C.2 Low Molecular weight-SDS Marker (GE Healthcare).



Protein Band	kDa
IgM Hexamer	1236
IgM Pentamer	1048
Apoferritin band 1	720
Apoferritin band 2	480
B-phycoerythrin	242
Lactate Dehydrogenase	146
Bovine Serum Albumin	66
Soybean Trypsin Inhibitor	20

Figure C.3 The NativeMark™ Unstained Protein Standard (5 μL) was stained with the Colloidal Blue Staining Kit after separation on a NativePAGE™ Novex® 3-12 % Bis-Tris Gel (A), NativePAGE™ Novex® 4-16 % Bis-Tris Gel (B), or a NuPAGE® Novex® 3-8 % Tris-Acetate Gel (C). The standard (5 μL of a 1:20 dilution) was also analyzed on a Novex® 4-12 % Tris-Glycine Gel (D) and stained with the SilverQuest™ Silver Staining Kit (Invitrogen).

APPENDIX D

SDS-PAGE PROTOCOL

SDS-Polyacrylamide Gel Electrophoresis was performed using NuPAGE[®] Novex[®] Bis-Tris gels according to the instructions provided from www.invitrogen.com web site.

Sample Preparation

Reagent	Reduced Sample	Non-reduced Sample
Sample	x μ L	x μ L
NuPAGE LDS Sample Buffer (4X)	2.5 μ L	2.5 μ L
NuPAGE Reducing Agent (10X)	1 μ L	--
Deionised Water	to 6.5 μ L	to 7.5 μ L
<hr/>		
Total Volume	10 μ L	10 μ L

Heat samples at 70°C for 10 min.

Running Buffer Preparation

Prepare 1X SDS Running Buffer by adding 50 mL 20X NuPAGE[®] MES or MOPS SDS Running Buffer to 950 mL of deionised water.

Sample Loading

Load the appropriate concentration of protein (of interest) on the gel.

Buffer Loading

Fill the Upper Buffer Chamber with 200 mL 1X NuPAGE[®] SDS Running Buffer. For reduced samples, use 200 mL 1X NuPAGE[®] SDS Running Buffer containing 500 μ L NuPAGE[®] Antioxidant. Fill the Lower Buffer Chamber with 600 mL 1X NuPAGE[®] SDS Running Buffer.

Running Conditions

Voltage: 200 V constant

Run time: 35 min (MES Buffer), 50 min (MOPS Buffer)

Expected current: 100-125 mA/gel (start), 60-80 mA/gel (end)

APPENDIX E

SIMPLYBLUE SAFESTAIN MICROWAVE PROTOCOL

Microwave Procedure

The microwave procedure is fast, takes just 12 min and yields results with sensitivity as low as 5 ng with an additional incubation with a salt solution. The procedure is for 1.0 mm mini-gels. For 1.5 mm mini-gels, use the values in parentheses.

Caution: Use caution while using the stain in a microwave oven. Do not overheat the staining solutions.

1. After electrophoresis, place the gel in 100 mL of ultrapure water in a loosely covered container and microwave on High (950 to 1,100 watts) for 1 min until the solution almost boils.
2. Shake the gel on an orbital shaker for 1 min. Discard the water.
3. Repeat Steps 1 and 2 two more times.
4. After the last wash, add 20 mL of SimplyBlue™ SafeStain and microwave on High for 45 s to 1 min until the solution almost boils.
5. Shake the gel on an orbital shaker for 5 min. Detection limit: 20 ng BSA.
6. Wash the gel in 100 mL of ultrapure water for 10 min on a shaker. Detection limit: 10 ng BSA.
7. Add 20 mL of 20 % NaCl for at least 5 min. Detection limit: 5 ng BSA. Gel can be stored for several weeks in the salt solution.

APPENDIX F

NATIVE-PAGE PROTOCOL

Native-Polyacrylamide Gel Electrophoresis was performed using NativePAGE™ Novex® 4-16 % Bis-Tris Gels according to the instructions provided from Invitrogen.

Sample Preparation

Reagent	Sample with detergent	Detergent free sample
Sample	x μ L	x μ L
NativePAGE™ Sample Buffer (4X)	2.5 μ L	2.5 μ L
NativePAGE™ 5 % G-250	0.25-1 μ L	optional
Sample Additive		
Deionised Water	to 10 μ L	to 10 μ L

Mix well. Do not heat samples for native gel electrophoresis.

Buffer Preparation

Running Buffer (Anode Buffer, 20X):

NativePAGE™ Running Buffer (20X)	50 mL
Deionised Water	950 mL
<hr/>	
Total Volume	1000 mL

Mix thoroughly and use ~600 mL of the 1X NativePAGE™ Anode Buffer in the Lower (Outer) Buffer Chamber.

NativePAGE™ Cathode Buffer Additive (20X):

Reagents	Dark Blue	Light Blue
NativePAGE™ Anode Buffer (20X)	10 mL	10 mL
NativePAGE™ Cathode Buffer Additive (20X)	10 mL	1 mL
Deionised Water	180 mL	189 mL
<hr/>		
Total Volume	200 mL	200 mL

Mix thoroughly and use ~200 mL of the appropriate 1X NativePAGE™ Cathode Buffer in the Upper (Inner) Buffer Chamber.

Sample Loading

Load the appropriate concentration of protein (of interest) on the gel.

Running Conditions

NativePAGE™ Bis-Tris Gel	Voltage	Run Time	Expected Current
Standard, Room Temperature Run	150 V Constant	90-115 min (3-12 % gel)	Start: 12-16 mA End: 2-4 mA
		105-120 min (4-16 % gel)	
Low Temperature (4°C) Run	150 V Constant for 60 min, then increase voltage to 250 V Constant for the remainder of the run (30-90 min)		Start: 8-10 mA End: 2-4 mA

APPENDIX G

BRADFORD ASSAY

The Bio-Rad Protein Assay (Bio-Rad) based on the method of Bradford (Bradford, 1976) was used.

Reagents:

1x Dye Reagent: 1 L of dye solution containing methanol and phosphoric acid. One bottle of dye reagent is sufficient for 200 assays using the standard 5 mL procedure or 4,000 assays using the microplate procedure.

Bovine Serum Albumin Standard Set: Set of 7 concentrations of BSA (2, 1.5, 1, 0.75, 0.5, 0.25, 0.125 mg/mL) in 1 mL tubes.

<u>Tube Number</u>	<u>Standard/μL</u>	<u>Source of Standard</u>	<u>Diluent/μL</u>	<u>Conc.(μg/mL)</u>
1	70	2 mg/mL stock	0	2000
2	75	2 mg/mL stock	25	1500
3	70	2 mg/mL stock	70	1000
4	35	Tube 2	35	750
5	70	Tube 3	70	500
6	70	Tube 5	70	250
7	70	Tube 6	70	125
8	0	0	70	0

1. Pipette each standard (20 μL) and unknown sample solution (20 μL) into separate clean test tubes.
2. Add 1mL of dye solution to each tube and vortex
3. Incubate at room temperature for at least 5 min. Samples should not be incubated longer than 1 h at room temperature.
4. Set the spectrophotometer to 595 nm. Zero the instrument with the blank sample. Measure the absorbance of the standards and unknown samples.
5. Plot standard curve versus sample to find unknown.

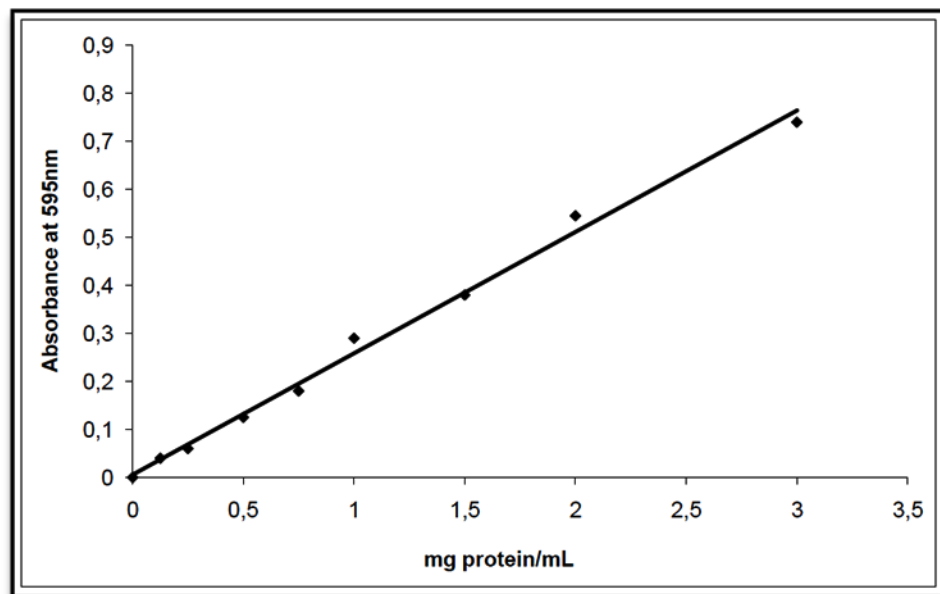


Figure G.1 Standard curve for Bradford method.

APPENDIX H

PREPARATION OF TLC PLATES AND SOLVENT SYSTEMS

TLC plates were cut horizontally at the size of 5 cm tall by various widths; depending on the number of samples running on a plate. Small amount of sample was spotted onto TLC plate sheet with the help of capillaries. The sheet was then placed in solvent beaker and a glass lid was replaced on top of the beaker. The solvent rose up the TLC plate by capillary action. The plate was removed when the solvent front is about half a cm below the top of the plate. Seven different mobile phases were used according to the substrate type as shown in Table H.1.

After removing the plate from beaker, the solvent was allowed to evaporate completely from the plate. To visualize the spots, plate was hold under UV light and any spots detected were marked with pencil.

Table H.1 Thin layer chromatographic systems used in the study

Chromatographic system No.	Organic substrate	Solvent (volume ratio)
1	Gallic acid	Ethylacetate:formic acid:acetic acid:water, 100:11:11:27
2	Catechol, hydroquinone, resorcinol	Benzene:acetic acid:water, 6:7:3
3	4-tert-Butylcatechol	Ethylacetate:n-hexane, 1:2
4	L-DOPA , PLA, (-)-epinephrine	Methanol:dichloromethane, 1:10
5	Caffeic acid	Petroleum ether:ethyl acetate:formic acid, 30:15:5
6	Resveratrol	Dichloromethane:methanol, 1:0.05
7	Hydrobenzoin	Ethylacetate:n-hexane, 1:6

APPENDIX I

AMMONIUM SULFATE PRECIPITATION PROTOCOL

The following protocol was used for *S. thermophilum* CATPO precipitation using ammonium sulfate as precipitant:

1. Take 100 mL of supernatant.
2. Slowly add solid ammonium sulfate to a final concentration of 50 % (232.8 g / 800 mL of solution) and stir at room temp for 15 min.
3. Centrifuge for 30 min at 10,000 rpm (at 4°C).
4. Separate the supernatant solution from the pellet and perform an 80 % ammonium sulfate precipitation by adding 155.2 g of solid ammonium sulfate per L of supernatant solution. Stir and centrifuge as above.
5. Save the pellet and resuspend in 50-100 mL of buffer.
6. Run SDS-PAGE, check the activity of CATPO.
7. Dialyze against 50 mM Tris-HCl, pH 8.0 overnight to remove any ammonium sulfate present in solution.

APPENDIX J

AMINO ACID SEQUENCE OF *SCYTALIDIUM THERMOPHILUM* CATALASE

The amino acid sequence of *S. thermophilum* catalase was first published by Mayer, 1997 (United States Patent, No. 5646025). The *catpo* gene of *S. thermophilum* is composed of 717 amino acids. The coding region encodes 19 amino acid signal peptide (coloured purple). Three residues indicated in different colours are essential for catalysis. Tyr387 (red) is located on the proximal side of heme, whereas His101 (pink) and Asn173 (blue) are found on the distal side.

MNRVTNLLAWAGAIGLAQATCPFADPAALYSRQDTTSGQSPLAAYEV
DDSTGYLTSDVGGPIQDQTSLKAGIRGPTLLEDFMFRQKIQHFDHERVPE
RAV**H**ARGAGAHGTFTSYADWSNITAASFLNATGKQTPVVFVRFSTVAGSR
GSADTARDVHGFATR FYTDEGNFIVG**N**NIPVFFIQDAIQFPDLIHSV KPRP
DNEIPQAATAHDSA WDFFSQQPSTMHTLFWAMSGHGIPRSYRHMDGFG
VHTFRFVKDDGSSKLIKWHFKSRQ GKASLVWEEAQVLSGKNADFHRQD
LWDAIESGNGPEWDVCVQIVDESQAQAFGFDLLDPTKIIPEEYAPLTKLG
LLKLDNRNPTNYFAETE QVMFQPGHIVRGIDFTEDPLLQGR LFS**Y**LDTQLN
RNGGPNFEQLPINMPRVPIHNNNRDGAGQMFIHRNKYPYTPNTLNSGYP
RQANQNAGR GFFTAPGRTASGALVREVSPTFNDHWSQPRLFFNSLTPVE
QQFLV NAMRFEISLVKSEEVKKNVLTQLNRVSHDVAVRVA AAI GLGAPD
ADDTYYHNNKTAGVSIVGSGPLPTIKTLRVGILATTSESSALDQAAQLRT
RLEKDGLVVTVVAETLREGVDQTYSTADATGFDGVVVVDGAAALFAST
ASSPLFPTGRPLQIFVDA YRWGKPVGVC GGSSEVLDAADV PEDGDGVY
SEESVDMFVEEF EKGLATFRFTDRFALDS

APPENDIX K

AMINO ACID SEQUENCE OF pETCATPO (Δ19aa CATPO pET28aTEV)

The amino acid sequence of codon optimised *catpo* gene for expression in *E. coli* is given below. It consists of 720 amino acids. Histidine tags (dark blue) and TEV cleavage site (red) are indicated in bold. Arrow shows the mature protein start site.



MGSS**HHHHH**HSSG**ENLYFQ**GHMTCPFADPAALYSRQDTTSGQSPLAAY
EVDDSTGYLTSDVGGPIQDQTSKAGIRGPTLLEDFMFRQKIQHFDHERV
PERAVHARGAGAHGTFTSYADWSNITAASFLNATGKQTPVFVRFSTVAG
SRGSADTARDVHGFATRFYTDEGNFDIVGNNIPVFFIQDAIQFPDLIHSVK
PRPDNEIPQAATAHDSA WDFFSQQPSTMHTLFWAMSGHGIPRSYRHMDG
FGVHTFRFVKDDGSSKLIKWHFKSRQGKASLVWEEAQVLSGKNADFHR
QDLWDAIESGNGPEWDVCVQIVDESQAQAFGFDLLDPTKIIPEEYAPLTK
LGLLKLDRNPTNYFAETE QVMFQPGHIVRGIDFTEDPLLQGRLFSYLDTQ
LNRNGGPNFEQLPINMPRVPIHNNNRDGAGQMFIHRNKYPYTPNTLNSG
YPRQANQNAGRGFFTAPGRTASGALVREVSPTFNDHWSQPRLFFNSLTP
VEQQFLVNAMEISLVKSEEVKKNVLTQLNRVSHDVAVRVAAAIGLGA
PDADDTYYHNNKTAGVSIVGSGPLPTIKTLRVGILATTSESSALDQAAQL
RTRLEKDGLVVTVVAETLREGVDQTYSTADATGFDGVVVVDGAAALFA
STASSPLFPTGRPLQIFVDAYRWGKPVGVCGGKSSEVLDAADVPEGDG
VYSEESVDMFVEEFKGLATFRFTDRFALDS

APPENDIX L

SEQUENCE ALIGNMENT OF *SCYTALIDIUM THERMOPHILUM* CATPO GENE WITH *PENICILLIUM VITALE* CATALASE GENE

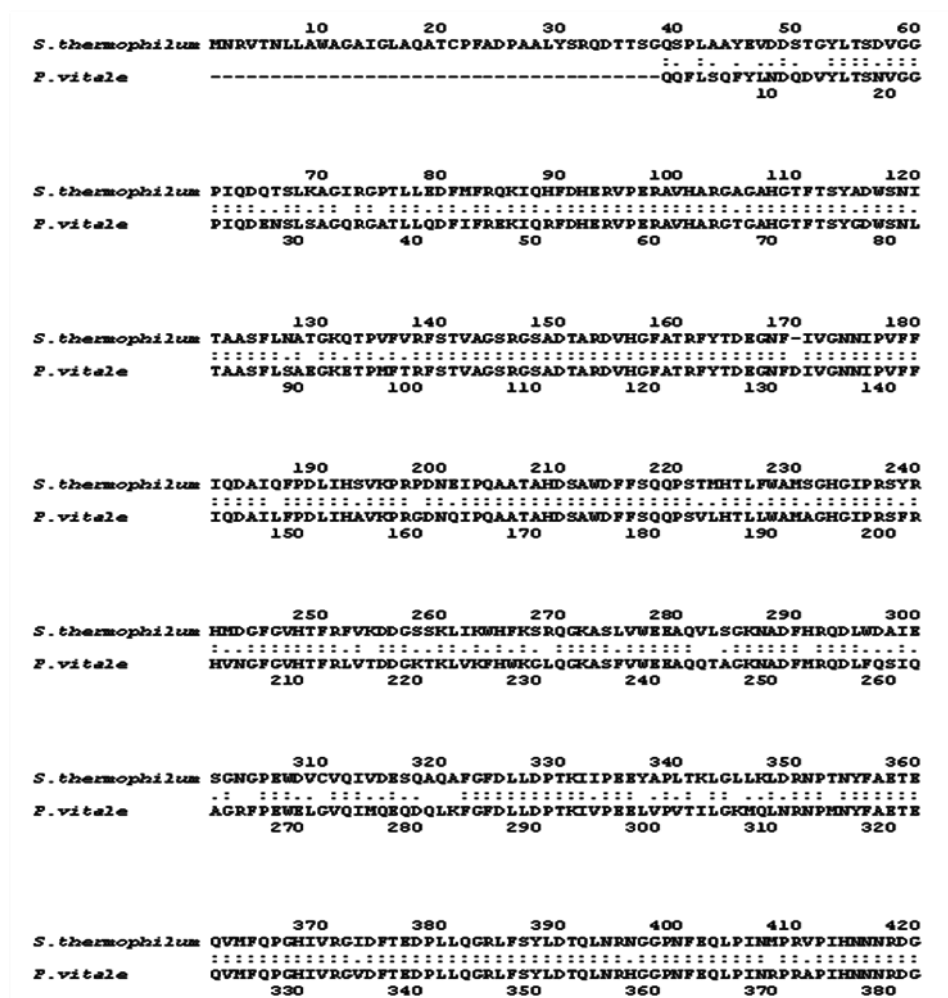


Figure L.1 Multiple sequence alignment of *S. thermophilum* CATPO (United States Patent, No. 5646025) and *P. vitale* catalase (PDB code, 2IUF).

CIRRICULUM VITAE

PERSONAL INFORMATION

Surname, Name: Yüzügüllü, Yonca
Nationality: Turkish (TC)
Date and Place of Birth: 17 October 1980, Eskişehir
Marital Status: Single
Phone: +90 312 287 83 85
email: yyuzugullu@gmail.com

EDUCATION

Degree	Institution	Year of Graduation
BS	Ankara University Biology	2002
High School	Ayrancı High School, Ankara	1997

WORK EXPERIENCE

Year	Place	Enrollment
2002- Present	METU-Biotechnology	Research Assistant

FOREIGN LANGUAGES

Advanced English, Low Spanish

AWARDS

Year	Award	Awarded by
2009	RCSB PDB Poster Prize	25th (ECM) European Crystallographic Meeting

PUBLICATION

- Ögel, Z.B., Yüzügüllü, Y., Mete, S., Bakır, U., Kaptan, Y., Sutay, D., Demir, AS, 2006. "Production, properties and application in biocatalysis of a novel extracellular alkaline phenol oxidase from the thermophilic fungus *Scytalidium thermophilum*", *Applied Microbiology and Biotechnology*, 71(6): 853-862.

CONFERENCES

- 16th National Biotechnology Conference (December 13-16, 2009, Antalya)
- International Symposium on Biotechnology, September 27-30, 2009, Ankara-Turkey
- 25th European Crystallographic Meeting, August 16-21, 2009, Istanbul-Turkey
- BCA Annual Spring Meeting, April 21-23, 2009, Logborough-UK
- XV. Biotechnology Conference, October 28-31, 2007, Antalya-Turkey
- 3rd European Federation of Biotechnology Conference on Physiology of Yeasts and Filamentous Fungi (PYFF3), June 13-16, 2007, Helsinki-Finland
- XIV. Biotechnology Conference (August 31- September 2, 2005, Eskisehir-Turkey)
- XV. National Biology Conference, September 5-9, Ankara-Turkey (Assigned student)

GRANTS

- Grants of State Planning Organization of Turkey; “Crystallisation of bifunctional catalase-phenol oxidase (CATPO) from *Scytalidium thermophilum*” (2008-2009), \$7200
- Tubitak Research Grant, 1001 funding; Production and biocatalytic properties of the bifunctional catalase/catechol oxidase enzyme of the thermophilic fungus *Scytalidium thermophilum* in the presence of phenolic compounds (2007-2009), \$114,424
- Grants of State Planning Organization of Turkey; “Oxidation of functional phenolics by bifunctional enzyme of *S.thermophilum*” (2004-2008), \$22,000